Understanding the Early Events of Human Papillomavirus Lesion Formation

Thesis submitted for

the Degree of Doctor of Philosophy

in accordance with the requirements of the

University College of London, UCL

Emilio Pagliarulo

Student No. 1015472

Division of Virology

MRC National Institute for Medical Research

The Ridgeway, Mill Hill

London

NW7 1AA

Statement of declaration

I, Emilio Pagliarulo, confirm that the work presented in this thesis is my own. Where information has been derived from other sources, I confirm that this has been indicated in the thesis.

Acknowledgments

I would like to thank my supervisor Dr. John Doorbar for his exceptional advice and support throughout my PhD.

I would like to thank the Doorbar lab group for their general support and in particular Dr. Qian Wang for her help and for being always positive and caring.

Above all I wish to thank my girlfriend, Claudia Arbore, and my family for their encouragement and support throughout the course of my studies.

I dedicate this thesis to the loving memory of my father.

Abstract

The events during papillomavirus lesion-formation are not well understood, but are likely to differ between high and low risk HPV types, which have different effects on the infected basal layer. These differences most likely reflect differences in protein function and gene expression patterns that have evolved to support the different biologies of the two virus groups. While high-risk types such asHPV16 or 18 can drive cell proliferation in the basal and suprabasal layers, low-risk types such as HPV 6 and 11 appear not to require this function.

In order to compare the two virus groups we have introduced the different HPV genomes into a genetically identical keratinocyte background and examined their effect on functions required for lesion formation following epithelial trauma. The non-immortal keratinocyte cells have normal differentiation properties, are near-diploid and are sensitive to contact inhibition. They are currently used in the clinic to prepare skin substitutes for burns victims.

In this model, high-risk HPV types increase cell growth (but not migration) rate when cells have space to grow, such as would occur during wound healing. They can also overcome normal cell-cell contact inhibition as the cells pack-up, and this is manifest in organotypic rafts as an increase in basal and parabasal cell division similar to that seen in neoplasia. This growth advantage would allow a single infected cell to outgrow its uninfected neighbours following infection or during lesion expansion after wounding. Interestingly, the low-risk HPV types appear to have negative effect on growth rate, allowing the more rapidly dividing uninfected cells to predominate. This suggests a fundamental difference in the biology of the two HPV groups, and supports the idea that low-risk types may reside in long-lived slow-cycling cell such as stem cell. For the high-risk types this model may not hold true, with lesion-formation being directed actively through functional changes in the infected basal layer

Table of Contents

LIST OF FIGURES 12

LIST OF TABLES 15

LIST OF ABBREVIATIONS 16

CHAPTER 1: INTRODUCTION 20

1.1 Human Papillomavirus and Cancer 21

1.1.1 Incidence of Human Papillomavirus Associated Cancers 21

1.1.2 Development of cervical neoplasia and cancer 24

1.1.3 Physiology of the uterine cervix and HPV infection 25

1.1.4 Classification of cervical intraepithelial lesions 26

1.1.5 Clinical management of HPV caused lesions 29

1.1.6 The prevention of HPV: the prophylactic vaccine 29

1.1.7 Diagnosis of HPV lesions 31

1.1.8 Treatment 33

1.2 Papillomaviruses 33

1.2.1 Classification of papillomaviruses 33

1.2.2 HPV genome organization 35

1.2.3 HPV gene expression 37

1.2.3.1 HPV gene transcription 37

1.2.3.2 Translation in HPV mRNAs 41

1.2.4 The HPV life cycle 41

1.2.4.1 Early events in the HPV16 life cycle: Virion Binding 42

and Internalization

1.2.4.2 Control of viral genome expression in productive infections 43

1.2.4.3. The functions of the viral proteins E1 and E2 46

1.2.4.4 The functions of the viral protein E1^E4 47

1.2.4.5. The functions of the viral protein E8^E2 47

1.2.4.6. The functions of the viral protein E5 48

1.2.4.7. The functions of the viral proteins E6 and E7 49

1.2.4.8. The functions of the viral proteins L1 and L2 53

1.3 Oncogene deregulation in high-risk HPVs 53

1.4 HPV and the Host Immune System 56

1.5 Wound healing process 58

1.5.1 Establishment of HPV Infection During Tissue Injury 59

1.5.2 Growth factors in wound healing 60

1.6 Rational and Aims of this Study 61

CHAPTER 2: MATERIALS AND METHODS 64

2.1 Suppliers of chemicals and reagents 65

2.1.1 Commonly used buffers and reagents 65

2.2 Keratinocyte and fibroblast monolayer cell culture methods **66**

2.2.1 Cell lines 66

2.2.1.1 Normal immortalized Human Keratinocytes (NIKS) 66

2.2.1.2 J2-3T3 mouse fibroblasts 66

2.2.1.3 NIKS HPV16-positive cells 66

2.2.1.4 NIKS HPV11-positive cells 67

2.2.1.5 NIKS GFP positive cells 67

2.2.2 Media and Supplements 67

2.2.3 Maintenance of monolayer cells 68

2.2.3.1 J2 3T3 68

2.2.3.2 NIKS, NIKS HPV16 clones and other NIKS-derived cell populations 69

2.2.4 Cell counts of NIKS, NIKS HPV16 clones and other NIKS-derived cell populations 70

2.2.5 Transfection of NIKS and NIKS HPV11/16-positive cells 70

2.2.6 Electroporation 71

2.3 Growth assays of NIKS, NIKS HPV16 clones and other NIKS-derived cell populations 72

2.4 Short growth assays of NIKS, NIKS HPV16 clones and other NIKS-derived cell populations 72

2.5 Wound healing scratch assay 73

2.5.1 Calculation of the migration rate 73

2.6 Immunocytology and Immunohistochemistry 74

2.6.1 Immunocytology of NIKS, NIKS HPV16 clones and other NIKS-derived cell populations 74

2.6.2 Fixation of coverslips 74

2.6.2.1 Immunocytology and mounting monolayer coverslips 74

2.6.2.2 Primary antibody signal amplification 75

2.6.3 Microscopy and imaging software 77

2.7 Molecular biology techniques 77

2.7.1 Transformation of *E. coli* with DNA 77

2.7.2 Plasmid purification 77

2.7.3 Extraction of total genomic DNA from NIKS and other NIKS- 78

derived cell lines

2.7.4 Quantification of plasmid DNA 78

2.7.5 Restriction enzyme plasmid digestion 78

2.7.6 Vector re-ligation 79

2.7.7 Agarose gel electrophoresis 79

2.8 Quantitative RT-PCR (qPCR) 79

2.8.1 Extraction of total RNA 79

2.8.2 DNase digestion and reverse transcription 80

2.8.3 qPCR primer design and primer sequences 81

2.8.4 qPCR reagent cocktails 81

2.8.5 qPCR plating scheme and cycle parameters 82

2.8.6 Standard curves for primers 83

2.8.7 Copy number determination 84

2.8.8 Analysis of Relative Gene Expression using the ΔΔCt method 84

2.9 Amplification of Papillomavirus Oncogene Transcripts (APOT) 85

analysis

2.10 Protein Analysis 88

2.10.1 Cell lysis for western blot analysis 88

2.10.2 Protein quantification 88

2.10.3 SDS PAGE 88

2.10.3.1 Gel electrophoresis for E7 protein analysis 88

2.10.3.2 Gel electrophoresis for cellular proteins 89

2.10.3.3 Membrane transfer for Western blot 90

2.10.3.4 Blocking, antibody incubations and washing 90

2.10.3.5 Signal detection 92

CHAPTER 3: The analysis of monolayer LSIL-like and HSIL-like HPV16 cell lines

3.1 Introduction 94

3.1.1 The use of NIKS® (Normal Immortal KeratinocyteS) as a host keratinocyte cell line 98

3.2. LSIL-like and HSIL-like monolayer episomal HPV-16 cell lines proliferate faster than NIKS HPV-negative cells 102

3.3. Cellular p53 and pRb expression levels are reduced in both LSIL-like and HSIL-like cell lines cultured in monolayer 106

3.4 The NIKS-HPV16 genome-containing cells, HSIL and LSIL, express their oncogenes from an episomal form of the HPV16 110

3.5 NIKS-HPV16 cells lines cultured in monolayers at 'low-density' resemble the differentiation state of epithelial basal cells. 115

3.6 Cloned NIKS cells have a consistent expression of p53 and pRb expression 121

3.7 Discussion 126

CHAPTER 4: The use of NIKS monolayer system to study wound healing *in vitro*

4.1 Introduction 131

4.2 NIKS cells harboring HPV16 present a higher proliferative ability in an *in vitro* scratch assay 134

4.3 Mitomycin C treatment impede the proliferation of both NIKS and NIKS HPV16 containing cells 139

4.3.1 Mitomycin-C treated monolayers show limited Histone H3 phosphorylation 142

4.4 NIKS-HPV16 cells migrate faster than NIKS HPV negative cells 144

in a wound healing scratch assay

4.5 Comparative analysis of NIKS-HVP 16 and NIKS-HPV 11 genome containing cells during monolayer proliferation *in vitro* 149

4.5.1 NIKS cells containing HPV11 genome have lower growing ability than NIKS-HPV16 and NIKS-HPV negative cells 149

4.5.2 HPV11 genome does not persist in NIKS cells after transfection 152

4.5.3 Comparative analysis of the colonization ability of NIKS-HPV16 cells and NIKS-HPV11 populations 156

4.5.4 NIKS-HPV11 cells expressing GFP are not able to outgrow NIKS-HPV negative cells 160

4.5 Discussion 165

CHAPTER 5: The study of wound healing responses in an *in vitro* model system

5.1 Introduction 170

5.2 Increasing EGF medium concentration results in increased HPV16 viral copy number in monolayer cultures 172

5.2.1 EGF-rich medium treatment increases the HPV16 genome copy number with a long-term effect 178

5.3 EGF treatment increases the HPV11 genome copy number but the effect is not maintained over time 180

5.4 EGF concentration correlates with NIKS-HPV11 and NIKS-HPV16 copy number increase 184

5.5 Increased EGF medium concentration does not produce a proliferative effect in monolayer cultures 187

5.6 NIKS-HPV16 cells exposed to high concentration of EGF present a 190

variation in the splicing pattern of E6/E6* mRNA

5.7 Exogenous EGF treatment affects EGFR expression and its related molecular targets in NIKS-HPV cells 194

5.8 Discussion 201

CHAPTER 6: FINAL DISCUSSION

6.1 General discussion 206

6.2 The further evaluation of the biology of low-risk and high-risk HPV types using a monolayer culture system as laboratory model for comparison 214

Chapter 7: References 215

List of figures

Figure 1.1 Age-standardized incidence rates for cervical cancer. 23

Figure 1.2. Anatomy of the cervix. 26

Figure 1.3. Cervical neoplastic progression and pathological changes in lesions with LSIL and HSIL (adapted from (Branca et al., 2004). 26

Figure 1.4. Schematic representation of the double-stranded circular genome of HPV16. 37

Figure 1.5. Schematic representation of the HPV16 transcript map. 40

Figure 1.6. HPV16 gene expression pattern during productive infection. 45

Figure 1.7 HPV expression patterns during neoplastic progression. 56

Figure 1.8. Immunostaining of HPV11 and HPV16 caused lesions. 62

Figure 2.1 Fluorescence microscopy digital image of NIKS transfection optimization. 71

Figure 2.2 APOT diagram, transcription and amplification 86

Figure 2.3 Schematic representation of the capillary blotting 87

Figure 3.1. Growth characteristics of LSIL and HSIL HPV -16 cell lines 98

Figure 3.2 Pathology of cervical LSIL HPV16 lesion and NIKS-HPV16 raft culture with LSIL-like phenotype. 101

Figure 3.3. Growth characteristics of LSIL and HSIL HPV-16 cell lines. 104

Figure 3.4. Western blot analysis of p53, pRb and E7 proteins in HSIL-like and LSIL-like cells. 109

Figure 3.5. APOT analysis of the viral transcripts from HPV-16 monolayer cell lines. 113

Figure 3.6 Expression of K10 and K13 protein in raft cultures and HPV16-

positive cervical tissue. 118

Figure 3.7a. Differentiation state analysis of keratinocytes cultured in monolayer. 119

Figure 3.7b. Differentiation state analysis of keratinocytes cultured in monolayer. 120

Figure 3.8. The NIKS cloning assay studies variation amongst NIKS cells population prior to HPVs genome transfection. 124

Figure 4.1. Wound healing scratch assay. 137

Figure 4.2. Growth rate analysis +/- Mitomycin C. 140

Figure 4.3 H3P expression in NIKS and NIKS-HPV16 populations. 142

Figure 4.4 Wound healing scratch assay performed with Mitomycin C treated samples. 147

Figure 4.5. NIKS-HPV16/11 and NIKS growth assay. 151

Figure 4.6 Evaluation of HPV11 genome maintenance in NIKS populations. 155

Figure 4.7 GFP expressing cells colonization assay. 158

Figure 4.8. Colonization assays of NIKS, NIKS-HPV16 and NIKS-HPV11 populations. 162

Figure 5.1 Bright-field images of monolayer cultures at 24, 48 and 72 hours post-plating. 176

Figure 5.2. NIKS-HPV16 genome copy number at 72 hours compared to HPV16 genome copy number at plating (0h). 177

Figure 5.3 Evaluation of the copy number change in NIKS-HPV16 populations. 180

Figure 5.4 NIKS-HPV11 copy number variations in monolayer cultures. 184

Figure 5.5. Absolute viral genome copies measured in NIKS-HPV16 and NIKS-HPV11 populations. 186

Figure 5.6. NIKS-HPV11 and NIKS-HPV16 growth assay. 189

Figure 5.7 Analysis of splicing patterns in NIKS-HPV16 cells. 193

Figure 5.8 Expression level of EGFR in NIKS and NIKS-HPV16 clones and populations. 198

Figure 5.9 Quantitative real-time RT-PCR analysis of EGF-modulated molecular target in NIKS-HPV11 populations. 199

Figure 5.10 Quantitative real-time RT-PCR analysis of EGF-modulated molecular target in NIKS-HPV16 populations. 200

Figure 5.11 Quantitative real-time RT-PCR analysis of E6 transcripts inNIKS-HPV16 populations. 201

List of Tables

Table 2.1: Buffers and reagents 65

Table 2.2 Cell Culture and Freeze Media 68

Table 2.3 Primary Antibodies 76

Table 2.4 Secondary Antibodies 76

Table 2.5 Chemical Reagents 76

Table 2.6 Primers used for RT-PCR 80

Table 2.7 Primers used for qPCR 81

Table 2.8 qPCR cocktail 82

Table 2.9a: PCR cycle parameters 82

Table 2.9b: Dissociation parameters 83

Table 2.10: Standard curves for primers used for qPCR 84

Table 2.11: Cycling conditions and primers for the 1st APOT PCR 86

Table 2.12: Cycling conditions and primers for the 2st APOT PCR 86

Table 2.13: H1 and H2 specific probe sequence 87

Table 2.14: Composition of 6, 10 and 15% Tris-glycine SDS-polyacrylamide Resolving gels and 5% Stacking gel 90

Table 2.15. Primary Antibodies for Western Blot 91

Table 2.16 Secondary Antibodies for Western Blot 92

Table 3.1. Image-J analysis of K10 positive cells. Image-j software was used to the number of DAPI (blue) and K10 (red) positive cells present at each time point. 121

Table 4.1 Absolute percentages of H3P positive cells. 143

Table 4.2 Number of colonies counted in the images analysed. 165

List of abbreviations

AKT1	v-akt murine thymoma viral oncogene homolog 1
APC	adenomatous polyposis coli
APS	ammonium persulphate
BPV	bovine papillomavirus
BSA	bovine serum albumin
CDK	cyclin dependent kinase
cDNA	complementary DNA
CIN	cervical intraepithelial lesion
cm	centimetre
CMV	cytomegalovirus
CRPV	cottontail rabbit papillomavirus
Ct	cycle threshold
DAPI	4'-6' diamidino-2-phenylindol
dH2O	distilled water
DMEM	Dulbecco's Modified Eagle's Medium
DMSO	dimethyl sulphoxide
DNA	deoxyribonucleic acid
dNTP	deoxyribonucleic acid triphosphate
DTT	dithiothreitol
E2BS	E2 binding site
E6AP	E6-associated protein
EDTA	ethylenediaminetetraacetic acid
EGF	epidermal growth factor

EGFR	epidermal growth factor receptor
EV	epidermodysplasia verucciformis
FBS	fetal bovine serum
FGF	fibroblast growth factor
g	gram
GAPDH	glyceraldehyde 3-phosphate dehydrogenase
GFP	Green fluorescent protein
hDlg	human homolog of drosophila disc large
HRP	horseradish peroxidase
hScrib	human homolog of drosophila scribble
IFN-1	Type 1 interferon
IGF	Insulin Growth Factor
IgG	immunoglobulin G
Kb	kilobase
kDa	kilo Dalton
KGF	Keratinocyte growth factor
L	litre
LB	lysogenic broth
LCR	long control region
LSIL	low-grade squamous intraepithelial lesion
MAPK	mitogen-activated protein kinase
MCM	minichromosome maintenance
µg	microgram

µl	microliter
µm	micrometre
µM	micro molar
M	molar
mg	milligram
ml	millilitre
mm	millimetre
mRNA	messenger RNA
NIKS	normal immortalized human keratinocytes
ng	nanogram
NGS	normal goat serum
nm	nanometer
nM	nanomolar
NP40	nonyl phenoxylpolyethoxylethanol
ORF	open reading frame
PAGE	polyacrylamide gel electrophoresis
PBS	phosphate buffered saline
PCNA	proliferating cell nuclear antigen
PCR	polymerase chain reaction
PDZ	structural domain acronym of PSD95, Dlg1 and ZO-1
pen/strep	penicillin/streptomycin solution
poly(A)	polyadenylation
PV	papillomavirus
PVDF	polyvinylidene fluoride
qPCR	quantitative PCR

ROPV	rabbit oral papillomavirus
rpm	revolutions per minute
RRP	recurrent respiratory papillomatosis
RT-qPCR	real-time qPCR
SDS	sodium dodecyl sulphate
TAE	tris-acetate EDTA
TBS	tris-buffered saline
TGF	transforming growth factor
v/v	volume/volume
VLP	virus-like particle
w/v	weight/volume

1. Introduction

1.1 Human Papillomavirus and Cancer

1.1.1 Incidence of Human Papillomavirus Associated Cancers

Human variants of Papillomaviruses (HPV) cause various diseases such as visible papillomas, respiratory papillomas, verrucas and even cancer. Papillomas occurring at oral or genital sites can be persistent and often require surgical treatment (Hsueh, 2009). However, approximately one-third of individuals who present for treatment with genital warts will still have their lesions 3 months later, with recurrence after treatment being a significant problem (Lacey et al., 2006). The HPV types that cause such lesions are also implicated in the development of recurrent respiratory papillomatosis (RRP)(Major et al., 2005). RRP is a rare disease as affect 0.004% of children population (Donne and Clarke, 2010; Gerein et al., 2005) but is a serious condition that can only be managed by repeated surgery, and can progress to cancer in a small percentage (approximately 5%) of persistently infected individuals where the infection spreads to the lung (Derkay, 1995).

Other HPV types are known to cause cancer when infect epithelial sites, such as the anus, the endocervix, the penis (Silva et al., 2011; Wikstrom et al., 2012) and the oropharynx (Syrjanen et al., 2011; Szentirmay et al., 2005). The mucosal HPV types that cause infections of the ectocervix and the cervical transformation zone are well studied because of their association with development of cervical cancers (zur Hausen, 2009).

Cervical cancer is the second highest cause of cancer-associated deaths in developing countries and is the third most diagnosed form of cancer in the female population worldwide. There is a significant difference in terms of cancer incidence between developed and developing regions of the world, presumably due to the existence of screening programs established in the developed countries. In 2008, about 530,000 women were diagnosed with cervical cancer resulting in roughly 275,000 deaths worldwide, with the developing world accounting for 85% of this burden (Figure 1.1) (Ferlay et al., 2012). Although the mortality rate among women diagnosed with cervical cancers is consistent throughout the world, the incidence of diagnosed cancer lesions is significantly lower in the developed countries. This lower incidence confirms the importance of active screening programs that should be implemented in all areas of the globe. However, most developing countries cannot afford these screening programs, and therefore there is still an urgent need to develop a specific therapy for this form of cancer.

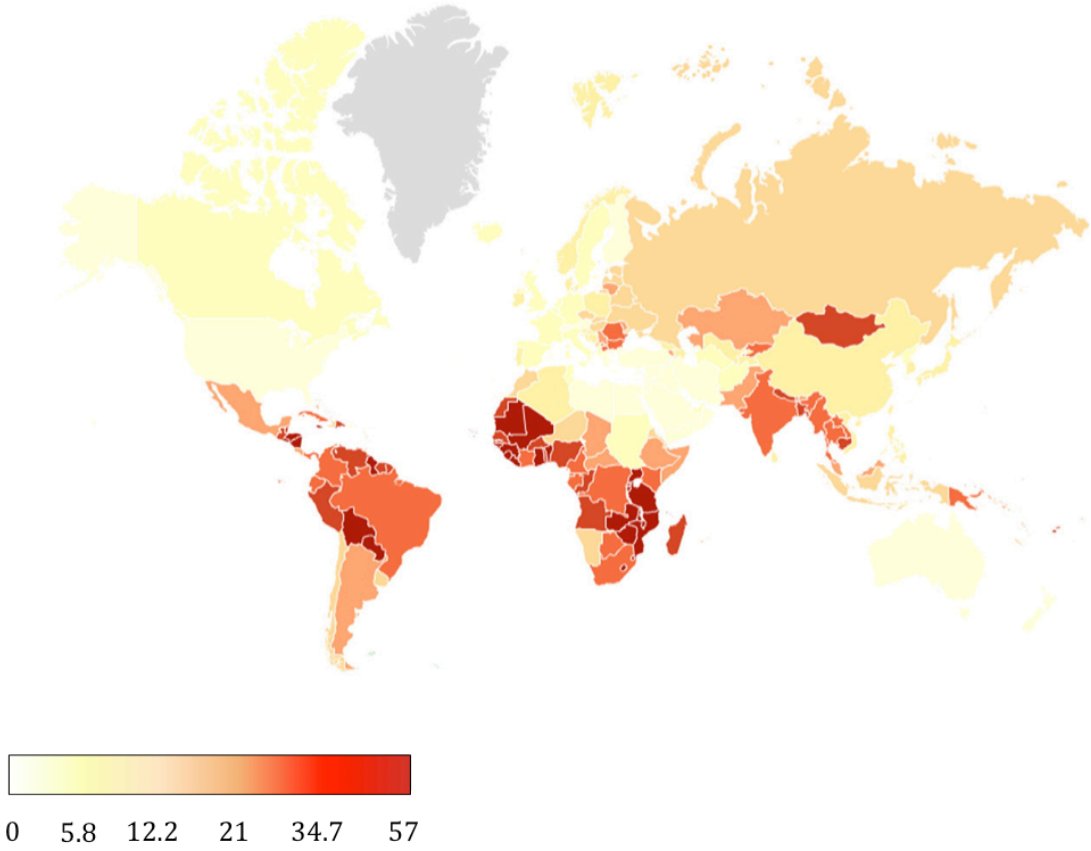

Figure 1.1 Age-standardized incidence rates for cervical cancer. The color scale bar indicates the incidence rates per 100,000 women. Adapted from (Ferlay et al., 2010).

.

1.1.2 Development of cervical neoplasia and cancer

About 85% of cervical cancers diagnosed in both developing and developed countries are squamous cell carcinomas (SCCs). The remaining cancers are equally divided into adenocarcinomas and adenosquamous carcinomas. The neoplastic progression of 'cervical cancer' or 'cervical carcinoma' is a multistep process grading from the mild form of disease, called low-grade squamous intraepithelial lesion (L-SIL), to the more severe and aggressive high-grade squamous intraepithelial lesion (H-SIL), and eventually progressing to the invasive form described as cervical carcinoma (Doorbar et al., 2012).

A number of studies have demonstrated that infection with high-risk Human Papillomaviruses (HR-HPVs) is a prerequisite for the development of cervical lesions in more than 99% of cases (Bosch and Munoz, 2002). Furthermore, infection with a subset of genital HR-HPVs, including mainly HPV16 and HPV18, is largely responsible of the development of cervical lesions, as HR-HPV DNA was found in ~99.75% of cervical carcinomas (Bosch and Munoz, 2002; Stanley, 2001; Walboomers et al., 1999). However, transient infection with HR-HPVs alone is not sufficient to induce carcinogenic cervical lesions; in fact, less than 1% of women that become infected with HR-HPV will develop cervical cancer, as most women will clear the infection within 2 years. Of the women who have a cervical neoplastic lesion resulting from a persistent infection with HR-HPV, a number of risk factors contribute to the progression towards malignancy. The most important risk factor is the deregulation of the HR-HPV oncogenes E6 and E7,

resulting in high and uncontrolled expression of these genes, often caused by integration of HR-HPV genomes into host chromosomes (Stanley, 2001).

1.1.3 Physiology of the uterine cervix and HPV infection

HPVs infect almost every tissue in the female lower genital tract. Usually, infections are asymptomatic and transient, as they are cleared within 1-2 years. The rare infections that progress to cancer usually occur at the cervical tract of the uterus. Understanding of the physiology of the uterus and the cervix is necessary to understand why this particular anatomical site is so susceptible to HPV-associated disease.

Most HPV infections occur at cervix because of its anatomy. A schematic diagram of the female anatomy, highlighting the cervix, is shown in Figure 1.2. The cervix is considered part of the lower uterus, and connects the uterus to the vagina via the internal opening of the cervix (OS) and external OS, respectively. The endocervical canal lies at the centre of the cervix and is comprised of mucus-secreting columnar epithelial cells, which form the endocervical columnar epithelium. The vaginal side of the cervix, called the ectocervix, is comprised of non-keratinising stratified epithelial cells that form the ectocervical squamous epithelium, a tissue with similar characteristics to the vaginal epithelium (Buckley, 1994). This endocervical columnar epithelium meets the ectocervical squamous epithelium at the squamous-columnar junction (SCJ). Hormonal changes caused by puberty, pregnancy, and oral contraceptives can cause cervical ectopy, an elongation of the cervix that exposes the SCJ to the vaginal canal.

During cervical ectopy, the squamous epithelium replaces the columnar epithelium at the 'transformation zone' in a metaplastic process. This 'transformation zone' is particularly susceptible to HPV infection, and it is where the majority of lesions are diagnosed (Arends et al., 1998; Herfs et al., 2012).

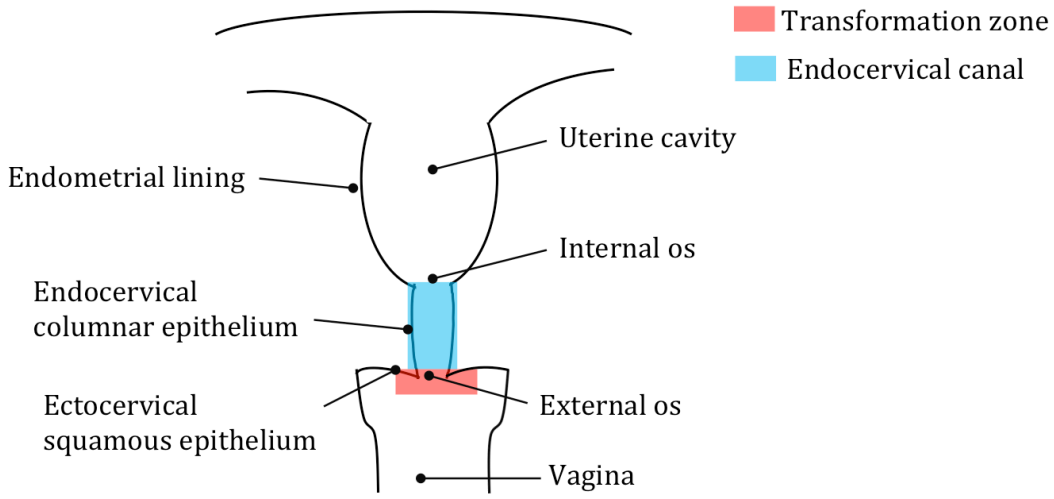

Figure 1.2. Anatomy of the cervix. The diagram shows the location of the transformation zone and the endocervical canal. The other features of the cervix are also detailed (see text for details).

1.1.4 Classification of cervical intraepithelial lesions

In order to understand the physiology of cervical cancer it is necessary to classify cervical lesions so that pathological events are clearly identified. Cervical cancer in fact develops from a pre-malignant neoplastic transformation that presents diverse degrees of severity during its pathological evolution. Two main grading systems, one based on histology and the other based on cytology of cervical

specimens, have been created to define these events and describe the degree of cell atypia (Richart, 1973; Solomon, 1990).

The histology-based system has been used since 1960 and defines cervical intraepithelial neoplasia (CIN) at three different stages (Figure 1.3). By this system, cervical dysplasia is diagnosed according to the proportion of cells in the cervical epithelium displaying dysplastic characteristics or cell atypia, such as multiple enlarged nuclei typical of koilocytes. CIN1 and CIN2 lesions show one-third and two-thirds of the epithelium thickness presenting cell atypia, respectively. Furthermore, squamous maturation occurs only in the middle and upper third of the epithelium, and koilocytes are observed here due to cytopathic virus activity. CIN3 lesions show cell atypia throughout the entire thickness of the epithelium. Because invasive cells are not identified by this method, squamous cell carcinomas are outside this classification range (Doorbar, 2006; Richart, 1973). This histology-based classification system presents some limitations, as the classification does not precisely correlate with the biological behaviour of the lesion. There is also no indication of putative regressing lesions.

In recent years a new methodology to classify lesions based on cytology of cervical specimens, called the Bethesda grading system, has been adapted to overcome these limitations. This system adopts only two grades which indicate the risk of progression to malignancy: the low-grade squamous intra-epithelial lesions (L-SIL corresponding to CIN1) and the high-grade squamous

intraepithelial lesions (H-SIL corresponding to CIN2 and CIN3 of the histology-based classification system) (Solomon, 1990).

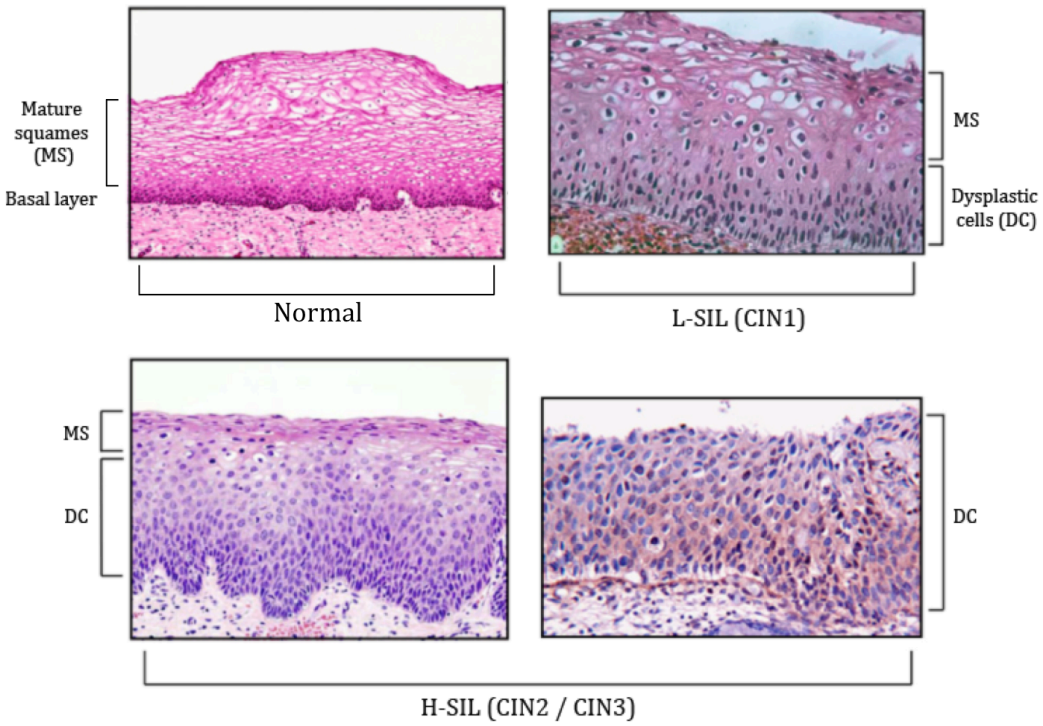

Figure 1.3. Cervical neoplastic progression and pathological changes in lesions with LSIL and HSIL (adapted from (Branca et al., 2004). Top, left panel: In the normal cervix, the basal layer of the epithelium is comprised of small and uniform cells, and squamous maturation occurs in the layers directly above. Top, right panel: An L-SIL lesion (CIN1), however, contains dysplastic cells in about half of the thickness of the epithelium. The dysplastic cells present pleomorphic nuclei and exhibit a loss of polarity. Bottom panels: H-SIL lesions (CIN2 and CIN3) show dysplastic cells in the entire thickness of the epithelium and squamous maturation occurs only in the upper-most layers.

1.1.5 Clinical management of lesions caused by HPV

The pathologies caused by HPV infections have an enormous impact on people's lives in both populations of the developed and developing countries. To date, in order to limit the loss of lives, HPV diseases have been tackled using three major tools: prevention, diagnosis and treatment. In the recent years, the prevention and diagnosis have been considered fundamental to limit the spread of HPV infection and decrease the number of people in need of surgical treatment. Diagnostic and screening programs however, are mainly implemented only in developed countries. Moreover, the recently developed prophylactic vaccine (Hanna and Bachmann, 2006; Szarewski, 2007) is most useful when used in specific categories of people, depending on sex and age group. Although their utility has been demonstrated, the vaccine and the screening programs do not guarantee the maximal efficacy in preventing cervical cancer or in detecting pre-neoplastic lesions. Furthermore the high costs associated with clinical management of the lesions caused by HPV, including screening programs and vaccination limit enormously their use in the developing countries. Therefore, it is necessary to develop cost effective screening tools and to understand the biological mechanisms leading to the formation of HPV associated lesions.

1.1.6 The prevention of HPV: the prophylactic vaccine

Since the discovery that HPV is a necessary cause of cervical cancer, development of a vaccine has been researched. The presence of specific antibodies against the coat proteins of HPV in subjects infected with viruses suggested the possibility

that immunization may be protective against infection. In fact, studies on animal models have demonstrated that antibodies against HPV, produced in infected animals, were able to produce an efficient response when injected in naïve animals (Ghim et al., 2000). The development of a prophylactic vaccine was allowed by the singular feature of the L1 proteins given by their ability to self-assemble and form virus like particles (VLPs) (Galloway, 2003; Salunke et al., 1986). These VLPs were produced by cloning the L1 fragment in competent organisms and the resulting empty shells were used to test their immunogenicity. Clinical trials demonstrated that VLPs containing L1 from HPV16 and HPV18 were able to produce a consistent protection against future infections. This strategy opened the possibility to use such particles in the vaccine production (Stanley et al., 2012).

Since the introduction of licensed products containing VLPs, two vaccines from two companies have been commercialized: Cervarix (GlaxoSmithKline Biologicals) and Gardasil (Merck & Co. Inc.). Both products offer protection against the high-risk HPV16 and HPV18, with an extended protection of Gardasil against two low-risk HPV types (HPV6 and HPV11). Therefore Gardasil has the ability to protect from HPV6 and HPV11 infections causing warts-like lesions. After few years from their release in the market, the efficacy of these vaccines was demonstrated, with Gardasil scoring a remarkable 100% of efficacy (Dyson et al., 1989; Gage et al., 1990). Such vaccines have now been licensed in over 100 countries worldwide.

A vaccination campaign of young women is currently ongoing in the majority of the developed countries. The extension of the vaccination program to the men population is currently debated (Stanley et al., 2012).

Despite the proven efficacy of the recently introduced vaccines, it will still be necessary to sustain an active screening program. In fact, both vaccines cannot be used as therapy for people with current disease. Furthermore, there are a number of HPV types outside the protection range of the two vaccines, which may cause a number of pathologies including cervical cancer. It has been estimated that the protection gained with a vaccination program covering the entire young-women population, would reduce the number of women developing cervical cancer by 70% (Stanley et al., 2012). Moreover, a reduction in the mortality rates from cervical cancer might only be detected after several years because the progression of the HPV infection to cervical cancer is not rapid (Stanley et al., 2012). Thus, the necessity to continue and improve the current screening program for pre-neoplastic lesions is evident.

1.1.7 Diagnosis of HPV lesions

HPVs usually cause benign epithelial lesions known as warts typically located at the ano-genital areas. Some strains produce also verrucas and others are able to cause RRP. Only in rare cases infections from HR-HPVs cause pre-neoplastic lesions that necessarily need treatment.

As discussed earlier, pre-malignant lesions range from LSIL to HSIL according to the severity status of the disease. Such a difference in their grade allows an

efficient management of the pre-cancerous lesions. In fact, LSIL can be monitored whereas HSIL infections can be removed before reaching invasivity.

George Papanicolaou in 1941 introduced a methodology commonly used to detect morphological abnormalities in the cervical cells. The method, known as Pap test or Pap smear, consists of the screening for neoplastic change of cells taken from the cervical surface. The Pap test is not 100% accurate, but it has indeed demonstrated to contribute to the reduction of the fatalities caused by HPV (Vizcaino et al., 2000). A comparative study has shown that the number of women diagnosed with cervical cancer have significantly decreased since the introduction of the screening program in the developed countries. The current cervical cancer incidence in developing countries, where screening programs are not established, is comparable to that of the developed countries before the screening introduction.

As mentioned earlier, the Pap test is not completely efficient (Sasieni et al., 1996). Both specificity and sensitivity of the test are considered low, with Pap test negatives in 86-100% of disease-negative cases, and Pap test positives in 30-87% of disease positive cases (Nanda et al., 2000). The Pap test results depend on a cytopathologists judgement and so it is subjective. Although not completely reliable, the Pap test remains a useful tool in the cervical cancer diagnosis. In addition the test is too expensive to be implemented in developing regions due to the need of a pathologists in performing the test.

In the recent years, many studies have been dedicated to the research of better diagnostic tools, in particular to implement the detection of neoplastic lesions at

the earliest stages, and new methods have been proposed to improve the reliability of the cervical screenings, but not yet implemented (Baldwin et al., 2003). One example is the detection of biomarkers, host genes that become deregulated during cervical neoplastic progression, through a combination of microscope and liquid phase techniques.

1.1.8 Treatment

Cervical cancer can be treated with untargeted cytotoxic therapy, such as radiotherapy, chemotherapy and surgery (Rogers et al., 2012; Stanley et al., 2012). However, such treatments have many unwanted side effects, and might not be successful. Therefore, a targeted therapy for cervical cancer would need to be developed in the future.

1.2 Papillomaviruses

1.2.1 Classification of papillomaviruses

Papillomaviruses (PVs) are a member of the family Papillomaviridae, an ancient family of viruses estimated to date beyond the origin of *Homo sapiens* (Bernard et al., 1994; Ho et al., 1993). PVs are non-enveloped viruses, approximately 55 nm in diameter, containing a double-stranded circular DNA genome of about 7.9kb (Howley, 1982). PVs are highly species and tissue tropic, and have evolved with an estimated mutation rate similar to that of its host germ line (Chan et al., 1997). PVs are known to infect most animal species, as well as reptiles and cetaceans (de Villiers et al., 2004a). Due to the diversity of species with which PVs co-evolved

and their strict species tropism, these viruses have become genetically distinct from one another.

Despite their genetic divergence, PVs share fundamental biological features as they infect exclusively epithelial cells and use the entire epithelium to complete their life cycle. PVs are well adapted to their hosts, as they complete their life cycle and are maintained in the population usually without causing significant harm to their hosts. This characteristic highlights a conserved virus-host interaction that, over time, has lead to a fine balance between virus replication and host immune surveillance (Woolhouse and Gaunt, 2007). It is widely established however that a single PV type can cause a clinical spectrum of disease among individual hosts (Doorbar et al. 2012).

PVs are organized into genera, species, and types based on the nucleotide sequence of their L1 capsid ORF; PVs within a genera share at least 40% L1 sequence identity, species share at least 60%, and types share more than 90% (Barnard and McMillan, 1999; de Villiers et al., 2004b). Most host species are infected by only one PV genera. HPVs represent only a small group of PVs, of which more than 150 types have been completely sequenced to date. HPVs are divided into five genera: Alpha-, Beta-, Gamma-, Mu-, and Nu-papillomaviruses (Doorbar et al., 2012). The most well studied group is the Alpha-PV because of their ability to cause benign genital lesions and cervical, anogenital, and head and neck cancers. The Alpha group is subsequently divided into two sub-groups based on their oncogenic potential: 'low-risk' types (LR-HPVs, including type 6 and 11)

mostly cause benign lesions known as papillomas or warts, and 'high-risk' types (HR-HPVs, such as type 16, 18, 31, 33, 45) cause an array of cancers. Papillomas caused by LR-HPVs frequently require surgical treatment when they occur in genital areas or oral sites. The LR-HPVs are also responsible for the development of respiratory papillomatosis, which requires surgical treatment as well, and in rare cases can progress to cancer (Derkay, 1995; Donne and Clarke, 2010; Major et al., 2005). The variety of epithelial disease caused by HPVs may be related to different transmission strategies as well as their diverse interaction with the host immune system (Doorbar, 2005). This broad range of pathological disease has formed a large basis for the study of different HPV types.

1.2.2 HPV genome organization

As mentioned previously, HPVs are small, non-enveloped viruses containing a circular double-stranded DNA genome of around 7.9kb (Howley, 1982). HPV genomes contain three main domains: the non-coding long control region (LCR), the 'early' region, and the 'late' region (Figure 1.4). The LCR contains the viral origin of replication, which is ~1kb. The names 'early' and 'late' correspond to the position of the ORFs in the genome and the kinetics of expression during vegetative viral replication, and the numbers indicate the relative size of the corresponding ORF (Duensing and Munger, 2004). The early region is ~4kb and contains the non-structural genes. These are E6 and E7, which are involved in host cell immortalization, and E1, E2, E8^E6, E1^E4, and E5, which are primarily involved in virus replication and regulation of viral gene transcription. The late

region is ~3kb and contains the structural genes, L1 and L2, which encode the major and minor capsid proteins, respectively.

The two major promoters that regulate the viral gene expression in the epithelium are the 'early' p97 promoter and the 'late' p670 differentiation-dependent promoter. The p97 promoter controls the expression of early genes E6 and E7, and the p670 promoter, located within the E7 ORF, controls the expression of several early genes including E1, E2, E4 and E5 as well as late genes L1 and L2 (Grassmann et al., 1996; Smotkin and Wettstein, 1986). Transcription from the late promoter must bypass the early polyadenylation site (early poly-A) to allow gene expression from the late region (Zheng and Baker, 2006).

The long control region (LCR) is located immediately upstream of the E6 ORF in proximity of the p97 promoter. This region contains *cis*-acting regulatory promoter sequences, which are fundamental for virus replication and viral transcription.

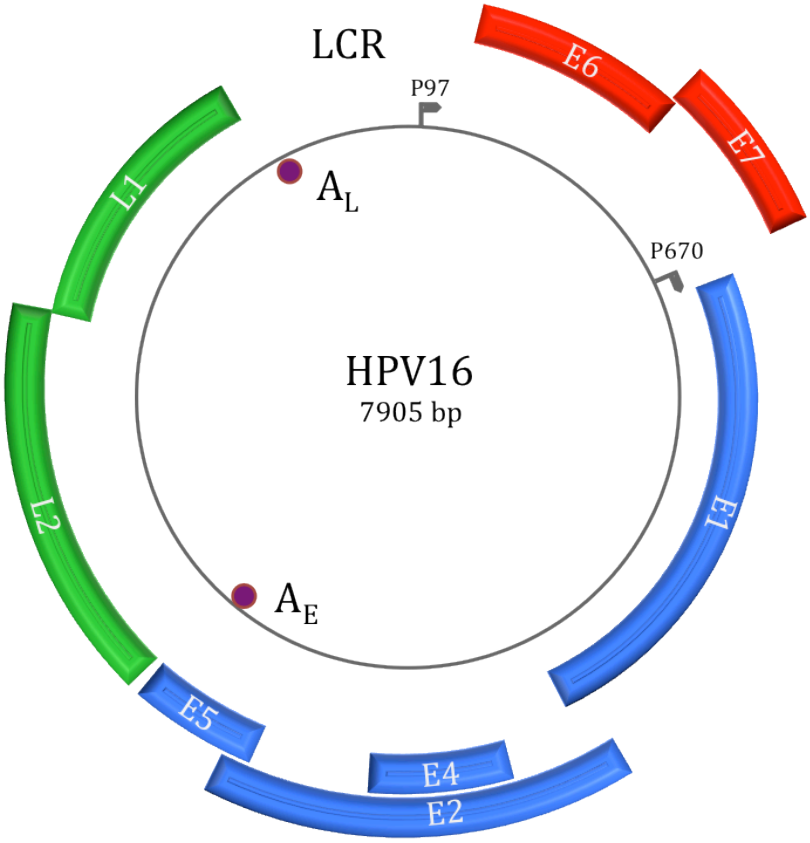

Figure 1.4. Schematic representation of the double-stranded circular genome of HPV16. The early (E) and late (L) genes as well as the long control region (LCR) are shown. The early and late polyadenylation sites are indicated as A_E and A_L. P97 and P670 indicate the position of the early and late promoters.

1.2.3 HPV gene expression

1.2.3.1 HPV gene transcription

HPV gene transcription has been characterised studying mainly the HPV16 type. The HPV16 early promoter, p97, is responsible for early gene expression whereas the late genes are transcribed from the late promoter, p670. However several other promoters have been identified within the LCR and within the E4 ORF

(Doorbar et al., 1990; Milligan et al., 2007). Binding of specific cellular transcription factors such as Sp-1, AP-1, Oct-1 and YY1 within the LCR can have both positive and negative effects on viral transcription (Lace et al., 2009). Furthermore, the LCR contains sites responsive to glucocorticoid binding (Todaro and Green, 1963), which enhance virus replication (Piccini et al., 1997). Interestingly, the HPV16 E2 protein is a known regulator of early transcription, as the HPV16 LCR also contains four binding sites for the E2 protein (E2BS (1-4)) that are located in the proximity of the cellular transcription factor sites (Androphy et al., 1987). Binding of E2 to E2BS-2 and -4 sites within the LCR impedes access to cellular transcription factors, thereby repressing p97 promoter activity (Sousa et al., 1990).

The transcription starting points within HPV genomes is variable and strictly HPV type-dependent. Interestingly, transcription occurs only from one of the viral DNA strands in clockwise direction as shown in Figure 1.5. During many years of evolution, PVs have made extraordinary use of alternative splicing mechanisms to diversify the proteins encoded by the viral genome. Transcription of the virus genome produces a number of polycistronic mRNAs from both the early and late promoters that undergo a series of post-transcriptional splicing and are polyadenylated at either an early (A_E) or late (A_L) poly-A site (Zheng and Baker, 2006). Splicing is intricately regulated by both viral *cis*-elements and cellular splicing factors (Zheng and Baker, 2006). The splice transcripts produced from the early promoter include many combinations of E1, E2, E4, E5, E6 and E7 poly- and bi-cistronic mRNAs (Figure 1.5) (Doorbar et al., 1990).

Referring to HPV E6/E7 splicing, selection of the first 5'-alternative splice site gives rise to a new ORF termed E6* (which has so far only been described for high-risk but not for low-risk HPVs (Schneider-Gadicke and Schwarz, 1986). Alternative splicing of HPV16 E6 and E7 oncogenes, which are mainly transcribed by the p97 promoter, result in multiple products which are functionally distinct. The E6 mRNA contains one intron, which when spliced at 3' site, produces three transcripts: E6*I, E6*II and E6^E7 (Figure 1.5) (Doorbar et al., 1990; Zheng and Baker, 2006). E6*I is the most abundant E6 transcript detected in cervical cancer cell lines and may have functional importance in the virus life cycle (Cornelissen et al., 1990). Interestingly, splicing of E6 is thought to promote E7 translation (Tang et al., 2006). However, it is important to mention that full-length E6 is always transcribed alongside full-length E7. The mRNA products derived from the differentiation-dependent late promoter, p670, include a combination of E1, E2, E5, E1^E4, and the structural genes L1 and L2 (Milligan et al., 2007). E1^E4 and L1 transcripts were originally identified in the suprabasal differentiating cells (Doorbar, 2005; Doorbar et al., 1997; Middleton et al., 2003), however non-functional L1 transcripts lacking a poly-A tail have recently been found in undifferentiated cells also (Milligan et al., 2007). This demonstrates that transcription of late genes can occur during early stages of the virus life cycle, however the post-transcriptional modifications necessary to produce functional transcripts occur in a differentiation-dependent manner.

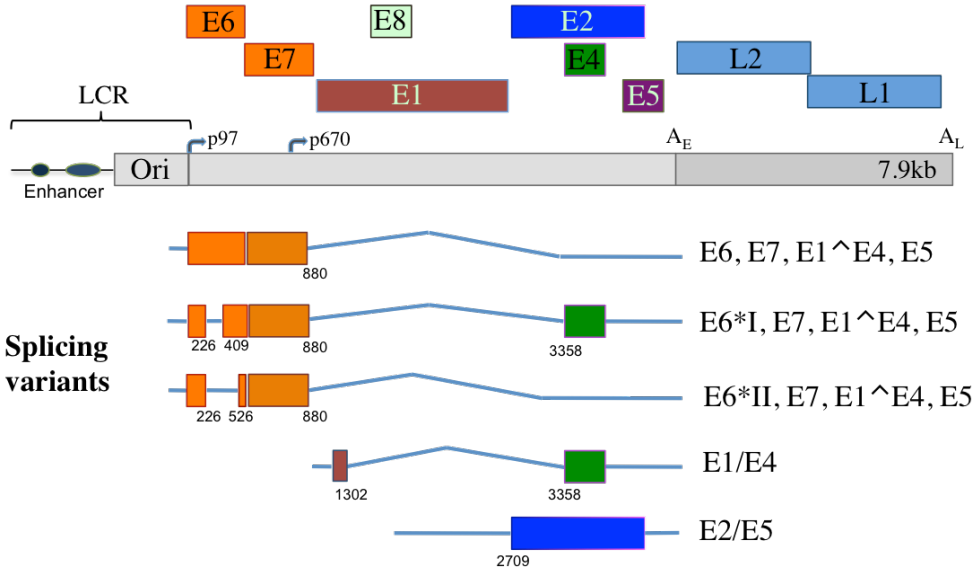

Figure 1.5. Schematic representation of the HPV16 transcript map. The boxes indicate the HPV16 genome ORFs situated on three levels representing the coding frames. The position of the early (P97) and late (P670) promoters is shown underneath the boxes, the arrows indicate the direction of transcription. The early (A_E) and late (A_L) polyadenylation sites are identified at nucleotides 4215 and 7321, respectively. The mRNA species are indicated as splicing variants.

1.2.3.2 Translation in HPV mRNAs

Translation of HPV transcripts generally occurs with low efficiency relative to translation of host cellular transcripts, which occurs constitutively (Zheng and Baker, 2006). Furthermore, HPV transcripts are bi- and poly-cistronic, while cellular transcripts are typically monocistronic (Firth and Brierley, 2012). One explanation for the observed slow translation rate of viral transcripts is the requirement for rare codons used for translation of HPV mRNAs (Zhao and Chen, 2011). Instability of viral mRNAs and complex translation initiation control may also be contributing factors to the low translation efficiency of HPV transcripts (Zheng and Baker, 2006). Translation initiation control mechanisms, such as through translation re-initiation, leaky scanning, ribosome jumping and internal ribosome entry not only explain the low translation efficiency but also how downstream ORFs in a polycistronic transcript are translated (Remm et al., 1999; Stacey et al., 2000; Tang et al., 2006). All the above mechanisms have limited experiment evidence except for the internal ribosome entry as the HPV16 has no internal ribosome entry sites (IRES) (Stacey et al., 2000).

1.2.4 The HPV life cycle

During transient infections, the HPV life cycle is controlled to limit the host immune response, and does not increase proliferation of the infected cells. However, persistent infection with HR-HPVs results in an abortive viral life cycle, which can cause the infected cells to progress to malignancy.

1.2.4.1 Early events in the HPV16 life cycle: Virion Binding and Internalization

The initial events of HPV infection are thought to happen in the basal cells of the stratified squamous epithelium. In the normal epithelium, the undifferentiated basal keratinocytes are the only cells, which are proliferating and thus undergoing mitosis, a necessary feature to support the establishment of the viral infection *in vivo* (Pyeon et al., 2009; Stanley et al., 2007). Recent studies carried out using animal models showed that HPV infection requires gentle abrasion of the genital epithelium (Roberts et al., 2007). Further investigations demonstrated that these abrasions exposed the basement membrane of the epithelium, where initial attachment of virions occurs. The binding of virions to the basement membrane is followed by binding and internalization of the virions in the basal keratinocytes, as these cells continuously move towards the site of the abrasion in order to repair the damaged epithelium (Roberts et al., 2007). Therefore, abrasion of the epithelium allowing virion binding to basement membrane ensures access to the basal cells, which are permissive to HPV infection. Moreover, wound-healing responses promote proliferation of the basal keratinocytes, thereby further contributing to the establishment of virus infection (Pyeon et al., 2009; Schiller et al., 2010). Wound-healing stimulated cell divisions are, in fact, necessary for viral entry into nucleus and thus productive HPV infection (Pyeon et al., 2009).

The initial binding of the major capsid protein, L1, to the basement membrane is mediated through interactions with heparin sulphate proteoglycans exposed by injury to the epithelium (Johnson et al., 2009). Binding to the basement

membrane triggers a conformational change in L1, which allows for furin cleavage of the L2 minor capsid protein at the N-terminus, thereby exposing a portion of the L1 that was previously hidden. Exposure of this hidden epitope of L1 by furin cleavage of L2 is required for binding to the basal keratinocytes (Schiller et al., 2010). Internalization of virions of many HPV types including HPV16 was originally suggested to occur through clathrin-dependent endocytosis (Schiller et al., 2010). However, more recent data suggests that HPV16 internalization is clathrin-independent and instead requires tetraspanin-enriched microdomains (Spoden et al., 2008). Furthermore, internalization mechanisms among HPV types does not appear to be conserved, as HPV31 virions have been shown to enter via caveolin-dependent endocytosis (Smith et al., 2008). All HPV types, however, require transit through low-pH compartments such as late endosomes and lysosomes, where uncoating occurs prior to transport of the viral genome to the nucleus via microtubules (Kamper et al., 2006).

1.2.4.2 Control of viral genome expression in productive infections

Upon successful entry, the L1 capsid protein remains in late endosomal/ lysosomal compartments and the L2/DNA complex enters the host cell's nucleus, a process which requires mitosis (Day et al., 2003; Pyeon et al., 2009). The viral genome is then established as an episome in the host nucleus (Schiller et al., 2010). As discussed above, the HPV life cycle is tightly linked to the differentiation state of the host cells, whereby infection of basal keratinocytes is followed by timely controlled expression of viral genes throughout the thickness of the epithelium (Figure 1.6). During the initial phase of infection, the viral

genome is replicated to around 200 copies (De Geest et al., 1993; Doorbar et al., 2012). Expression of E1 and E2 from the early promoter facilitates the initial replication of the virus. The E1 protein serves as a viral helicase and is loaded onto the origin of replication by the E2 protein (Masterson et al., 1998). E2 also attaches viral episomes to mitotic chromosomes, leading to correct viral genome segregation during mitosis (You et al., 2004).

In the uninfected epithelium, basal cells proliferate actively pushing daughter cells upwards to the suprabasal layers. Upon reaching the differentiating strata, these cells exit the cell cycle and initiate terminal differentiation. In a productive HPV infection, viral gene expression is tightly regulated and low copies of viral DNA are produced alongside the host DNA during basal cell divisions. Following the movement of the proliferating basal and suprabasal cells to the differentiating strata, viral gene expression from the early P97 promoter is up-regulated (Stanley et al., 2007). Importantly, expression of the two viral oncogenes E6 and E7 from the early P97 promoter extends the S-phase of the cycling cells thereby prolonging cell cycle arrest and terminal differentiation (Cheng et al., 1995; Middleton et al., 2003). Once the infected cells reach the upper layer of the epithelium, the late P670 promoter is up-regulated and the cells undergo differentiation. The up-regulation of the late P670 promoter allows expression of structural viral genes L1 and L2 as well as further amplification of the viral genome to around 1000 copies per cell (Hebner and Laimins, 2006; Stanley et al., 2007). The viruses are packaged with the newly formed capsid proteins in the upper layer of the differentiating epithelium, which naturally sloughs off, releasing fully functional virions without cytolysis.

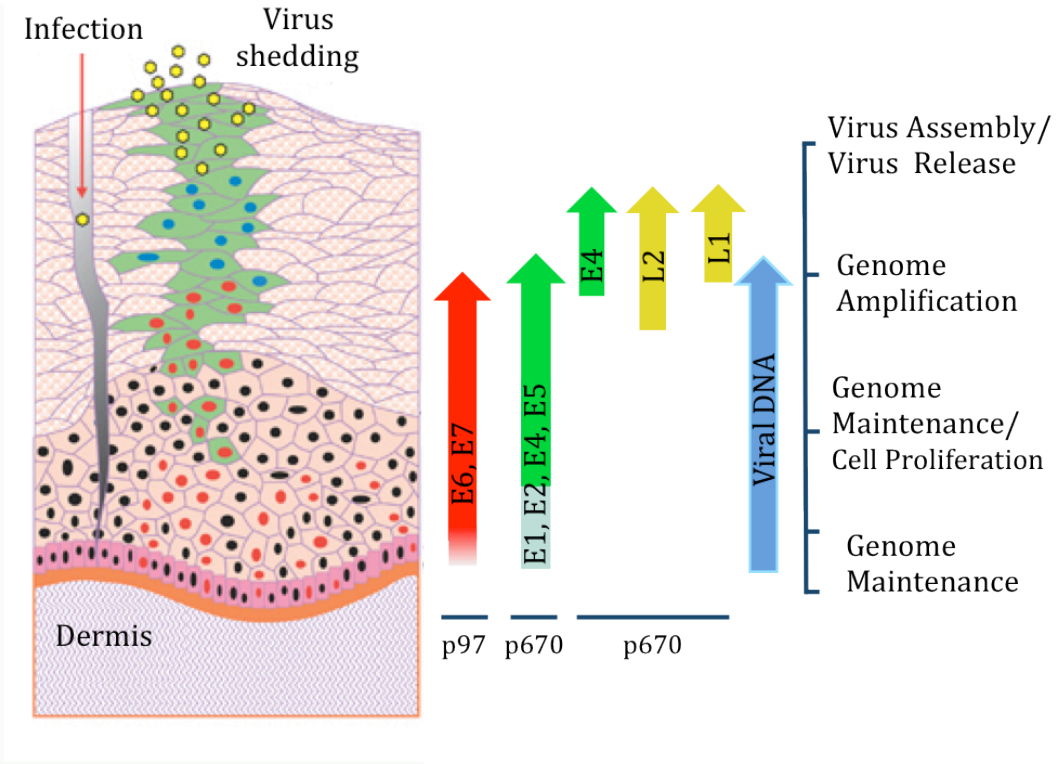

Figure 1.6. HPV16 gene expression pattern during productive infection. (Adapted from Doorbar 2006). Viruses gain access to the basal layer of the epithelium through a micro-wound. As the HPV infected cells divide they are pushed up into the suprabasal layers where the terminal differentiation program begins The HPV-16 p97 early promoter activation results in the expression of the E1 and E2 replication proteins as well as the E6 and E7 oncogenes (cells with red nuclei/arrow). The E7 oncogene is necessary for S-phase entry. In addition to E1 and E2, E6 and E7 are necessary for episomal replication. As the keratinocytes differentiate, the (late) promoter p670 is upregulated. This leads to increased levels of E1, E2, E5 and E4 (green cells/arrows). The start of late gene expression also coincides with a brief overlap of early genes and late genes. Cells that contain both (early) E7 and (late) E4 are thought to be the site of viral DNA amplification (blue nuclei). In the upper-layer cells the early genes are no longer expressed and high levels of E4 are expressed from the late promoter. A large number of E4 positive cells also contain amplified genomes (green cells with blue nuclei) and later L1/L2 capsid proteins (green cells with yellow dots). Mature capsids that contain amplified genomes (yellow dots) are released as cells are shed from the top layers.

1.2.4.3. The functions of the viral proteins E1 and E2

The major role of E1 and E2 proteins is in HPV genome replication and transcription. In particular, E2 facilitates the docking of viral episomes to mitotic chromosomes, ensuring stable maintenance of viral copies in replicating cells. E1, an ATP-dependent helicase, and E2 act together to assemble the viral replication complex with host replication machinery at the origin of replication (Boyer et al., 1996; Cripe et al., 1987; Hebner and Laimins, 2006).

E2 also acts as a transcription factor as well as a repressor, as it binds to specific palindromic sequences ($ACCN_6GGT$) within the viral genome and regulates HPV gene transcription. In HR-HPVs, three E2 binding sites are located near the origin of replication in the LCR, and a fourth is situated in the proximity of the L1 ORF (Hebner and Laimins, 2006). E2 binding at these sites has either a repressive or a stimulative effect on viral gene transcription depending on the HR-HPV type and E2 concentration. This is caused by the misplacement of two transcription factors, SP1 and TFIID (Bechtold et al., 2003; Hamid et al., 2009). Recent evidence suggests that E2 might have a role in enhancing the viral transcription of late genes by inhibiting early polyadenylation (Johansson et al., 2012). Importantly, E2 regulates the transcription of host cancer-associated genes hTERT and p21 (Lee et al., 2002b; Steger et al., 2002). Because of these characteristics, the roles of E2 are considered critical in regulating viral gene expression and neoplastic progression.

HPV16 E2 promotes virus replication, as it recruits the helicase protein E1 (Berg and Stenlund, 1997). E1 serves as the viral helicase, which is transferred to the

origin of replication by the E2 protein (Hughes and Romanos, 1993; Masterson et al., 1998).

1.2.4.4 The functions of the viral protein E1^E4

The E1^E4 protein, commonly referred as E4 protein, is the most abundant HPV protein expressed in the normal HPV life cycle. E1^E4 gene expression is limited in the undifferentiated basal cells and increases as cells differentiate. The main role of E1^E4 is to facilitate virion release through interference with cytokeratin networks (Khan et al., 2011; McIntosh et al., 2010). Another function of E1^E4 is to induce G2 arrest, which may collaborate with E7 to allow for more efficient viral replication before the cells enter the M phase (Chow et al., 2009; Davy et al., 2002).

1.2.4.5. The functions of the viral protein E8^E2

The E8^E2 protein is produced from splicing of the E8 transcript to the E2 transcript. Presently, only HPV16 and HPV31 are known to transcribe this protein. E8^E2 is important for viral episome maintenance in HPV31 and it has repressive effects on viral transcription and replication in both HPV16 and HPV31 (Lace et al., 2008; Stubenrauch et al., 2000). Interestingly, E8^E2 transcription is unique, as it does not require activation of the early P97 promoter. Rather, E8^E2 transcription is regulated by conserved *cis* elements in the LCR (Lace et al., 2008).

1.2.4.6. The functions of the viral protein E5

The HR-HPV E5 protein primarily functions as a mild oncogene. E5 can contribute to cellular transformation, modulate the levels of growth factor receptors and alter the immune response in the proximity of infected cells (Venuti et al., 2011). As the E5 gene is frequently deleted upon HPV genome integration during late progression to malignant disease, it is thought to play a role only in the early stages of carcinogenesis (Kim et al., 2010). Recent data, however, indicates E5 expression during cervical neoplastic progression is more common and may contribute to cervical carcinogenesis (Chang et al., 2001; Lorenzon et al., 2011).

Due to its hydrophobic characteristics, the E5 protein associates with cellular membranes, including the Golgi, endoplasmic reticulum (ER), and endosome membranes (Hu and Ceresa, 2009). It performs its transforming effect mainly through interaction with the Epidermal Growth Factor Receptor (EGFR) signaling pathway (Genther Williams et al., 2005; Straight et al., 1993). Activation of EGFR regulates host gene transcription and modulates several biological processes such as cell proliferation, apoptosis, angiogenesis, tumour invasion and metastasis through the Ras-Raf-Map kinase pathway and the PI3-Akt pathway (Crusius et al., 2000). E5 increases the number of EGFR molecules present on the cell surface through binding and inhibition of vacuolar ATPase, which is necessary for EGFR degradation (DiMaio and Mattoon, 2001). Plasma membrane-associated E5 proteins exhibit weak oncogenic properties by further increasing the number of EGFR molecules on the cell surface and by inhibiting the expression of Major Histocompatibility Complex class I and II (MHC-I and MHC-II) (Venuti et al., 2011;

zur Hausen, 2002). A number of E5 functions can be related to the specific membrane locations: ER-localised E5 inhibits endosomal acidification (Disbrow et al., 2005) and possibly is involved in altering the trafficking of growth factor receptors as well as molecules involved in immune control (Venuti et al., 2011). HPV16 E5 has recently been described as an oligomeric channel-forming protein with viro-porin functions *in vitro,* which makes it a potential target for future drug treatments (Wetherill et al., 2012). Lastly, E5 has recently been shown to cause cell-cell fusion and to inhibit the induction of apoptosis *in vitro* (Lagunas-Martinez et al., 2010).

1.2.4.7. The functions of the viral proteins E6 and E7

The E6 and E7 proteins of HR-HPV types have major roles in immortalization of human keratinocytes *in vitro* and are required for carcinogenesis *in vivo* (Doorbar, 2006). Deregulated expression of E6 and E7 oncogenes in basal and parabasal cells initiates transformation, and in fact, immunization of mice with recombinant E7 proteins results in regression of HPV16-associated neoplastic lesions through generation of E7 antibodies (Gerard et al., 2001). High-risk E6 and E7 proteins drive proliferation of infected non-cycling cells primarily through inactivation of p53 and retinoblastoma (pRb) tumour suppressors, respectively, thereby interfering with cell-cycle checkpoints and cell death signals. The E6 and E7 proteins together are critical for the viral life cycle as they force the infected cells to remain in a replication-competent state, and control cell-death pathways to favour viral persistence. However, when high-risk E6 and E7 gene expression

is not controlled, their dramatic effects on cellular homeostasis often lead to deleterious transformation events (Doorbar et al., 2012).

The main difference in transforming capacity between low- and high-risk HPV types lies in the features of E6 and E7. For example, one important way E6 contributes to transformation is through interaction with proteins containing PDZ-binding motifs. While high-risk E6 proteins bind PDZ motifs very efficiently, the low-risk E6 proteins have only a weak affinity for the PDZ motifs, and thus do not have a significant effect on the proteins containing them. In the case of E7, high-risk E7 proteins have a high affinity for Rb pocket proteins, and binding to these proteins results in activation of E2F-driven gene expression and cell proliferation. The low-risk E7 proteins, however, have a much lower affinity for pocket proteins and therefore do not significantly induce expression of E2F-driven genes and cell proliferation (Oh et al., 2004).

The High-risk E6 protein weighs 18kDa and contains two zinc finger-like motifs (Cole and Danos, 1987). Specific mass spectrometry-based studies have been used to identify the interactions between human papillomavirus and host cellular proteins. These studies reported 153 cellular proteins, including several previously reported HPV E6 interactors such as p53, E6AP, MAML1, and p300/CBP and proteins containing PDZ domains (White et al., 2012).

Thus, E6 interacts with a wide range of host proteins that are involved in 1) transcription and DNA replication; 2) apoptosis and immune evasion; 3)

epithelial organization and differentiation; 4) cell-cell adhesion, polarity and proliferation control; and 5) DNA repair.

Many of these interactions occur through PDZ-binding motifs within the host proteins, of which high-risk E6 proteins efficiently bind. One of the most important functions of high-risk E6 in cellular transformation is its ability to interfere with the tumour suppressor p53 in order to prevent cell cycle arrest and apoptosis. High-risk E6 interferes with p53 in several different ways. First, it forms a complex with the cellular ubiquitin ligase E6AP to target p53 for proteasomal degradation (Tomaic et al., 2009). However, E6 also mediates p53 degradation via a ubiquitin-independent mechanism (Camus et al., 2007). Furthermore, E6 acts as a repressor of p53 transcription through inactivation of the transcriptional coactivator hADA3 (Kumar et al., 2002). Aside from interfering with p53, another important function of high-risk E6 proteins is to induce telomerase activity by inducing hTERT expression (Yugawa and Kiyono, 2009). It does this through ubiquitination of the hTERT repressor NFX1-91 (Xu et al., 2008), and transactivation of the hTERT promoter in an E6, E6AP and c-myc complex (Katzenellenbogen et al., 2009; Liu et al., 2005; Veldman et al., 2003).

The high-risk E7 protein has a molecular weight of approximately 19kDa, and consists of three regions: CR1, CR2 and CR3 (Barbosa et al., 1990; Dyson et al., 1992). The primary function of E7 is to drive cells into S-phase in order to enable viral DNA replication and transcription. While E7 interferes with several host proteins involved in cell cycle regulation, one of its most important functions is to interfere with the pRB tumour suppressor. pRB is a pocket protein which

interacts with and sequesters E2F transcription factors, thereby inhibiting E2F-driven genes, of which many have important roles in cell cycle progression and proliferation (Zerfass et al., 1995). Similar to E6's multifaceted approach to interfere with p53, E7 interferes with pRB in multiple ways. First, the CR1 and CR2 regions of E7 bind directly to pRB resulting in release of E2F and subsequent activation of E2F-driven gene transcription. Interaction of the CR1 domain with pRB also results in proteasome-dependent degradation of pRB (Hebner and Laimins, 2006). Finally, it has been suggested that E7 interacts with cyclins to promote cyclin A and cyclin E complex formation with Cyclin-dependent kinase-2 (CDK2), which facilitate phosphorylation and subsequent degradation of pRB (He et al., 2003).

Aside from interfering with pRB, E7 also binds the other pocket proteins, p107 and p130, and targets them for degradation. Similar to pRB, these proteins sequester and thus inhibit E2F transcription factors, however they are also inhibitors of CDK2/cyclin A and CDK2/cyclin E complex formation. Therefore, by interfering with pocket proteins p107 and p130, E2F-driven gene expression is further induced by release from p107 and p130, as well as by release from pRB upon cyclin-dependent phosphorylation and degradation (Barrow-Laing et al., 2010). E7's ability to interfere with pRB function both directly and indirectly results in release of E2F transcription factors, thereby driving cell cycle progression through the S-phase.

The low-risk E7 has lower affinity for p105 and p107 but can interact with p130 in the supra-basal layers of the epithelia sustaining cell cycle maintenance and creating the condition for viral genome amplification (Klingelhutz and Roman, 2012).

1.2.4.8. The functions of the viral proteins L1 and L2

The viral life cycle is completed in the upper layers of the epithelium where the structural proteins L1 and L2 are uniquely expressed (Ozbun and Meyers, 1997). L1 and L2 proteins form the shell of the new virions by self-assembling into an icosahedral capsid comprised of 72-capsomeres of five L1 molecules per one L2 molecule (Belnap et al., 1996; Chen et al., 2000). The assembled mature capsids are incredibly stable and resistant to proteolysis (Buck et al., 2005). Newly formed virions are released from the uppermost layers of the epithelium as cells naturally exfoliate.

1.3 Oncogene deregulation in high-risk HPVs

As mentioned in sections 1.1.3 and 1.2.4.1, high-risk HPV infections can cause lesions ranging from low- to high-grade neoplasia, also classified as LSIL and HSIL (Figure 1.6). The main reason for progression to high-grade neoplasia is the continue persistence of high-risk HPVs that are not cleared by the immune system. Low-risk HPVs, instead, cause essentially benign lesions, and, except in rare cases, are not associated with invasive tumours. As discussed earlier, the main reason relies on the different effects that the early proteins E6 and E7 exert

on infected cells: with high-risk E6 and E7 featuring the greater transforming capacity (Figure 1.7) (Pim and Banks, 2010).

In tissues infected by HR-HPVs the mechanism that leads to cancer starts with the deregulation of the E6 and E7 expression. The deregulation of the early oncogenes causes the maintenance of the cell cycling state that in the HSIL classified lesions involves the whole thickness of the epithelium. When infections are not cleared by the immune system, the increased cell cycling activity leads to a continuous auto-selective competitive state, where infected keratinocytes actively select their polyclonal populations. The keratinocyte outgrowth mechanism of selection selects for clones with specific characteristics resulting in a monoclonal cancerous population (Dall et al., 2008; Doorbar et al., 2012; Isaacson Wechsler et al., 2012). The deregulated expression of E6 and E7 is thought to play a critical role in the malignant progression; it was in fact shown that their expression quantitatively increases in the compartment addressed to a more invasive cell phenotype both *in vivo* (Durst et al., 1992; Stoler et al., 1992) and i*n vitro* (Gray et al., 2010; Isaacson Wechsler et al., 2012). Thus, deregulated expression of early oncogenes in HR-HPVs infections are of considerable interest in the study of the mechanisms for infections management and control.

To date, the events that lead to a deregulated expression of E6 and E7 are not fully understood. HR-HPVs early gene deregulation can follow two main routes. The most common of the two potential mechanisms relies on the integration of the LCR, E6 and E7 parts of the viral genome in the host DNA, which is estimated to occur in 85% of cervical cancers (Choo et al., 1987; Klaes et al., 1999). E6 and

E7 expression from integrated genome, however, can be repressed by E2 expressed from episomes. However, until the episomes are completely lost the effects of integrated E6 an E7 are not at their best. Thus, episome loss, E6 and E7 integration confer advantageous growth characteristics to the infected cells (Dall et al., 2008).

Another mechanism by which E6 and E7 can be deregulated is by maintaining the integrity of the physical state of the viral episomal genome. In fact, it is estimated that at least 15% of the cervical cancers still retain viral genomes as episomes (Klaes et al., 1999). Furthermore, it was shown that episomal HPVs were able to cause serious disease, such as head and neck cell squamous cancers (HNSCCs), underlining the possibility that E6 and E7 deregulation can happen in regions of the infected epithelium not containing integrants (Joseph and D'Souza, 2012; Theelen et al., 2010). The exact mechanism behind the deregulation of E6 and E7 has not been completely elucidated. It is suggested that changes in acetylation status of the viral chromatin may cause expression instability and oncogene deregulation. Furthermore, *in vitro* studies have shown that differential expression of E6 and E7 oncogenes causes a broad range of cell phenotypes, ranging from LSIL to HSIL, in HR-HPVs episome-containing cell lines (Isaacson Wechsler et al., 2012).

The maintenance of the episomal physical state requires immune system escape. As stated earlier E6 and E7 oncogenes are able to interfere with the interferon (INF) pathway, which is sustained by evidence from studies on episome-contained neoplastic progression model systems (Gray et al., 2010).

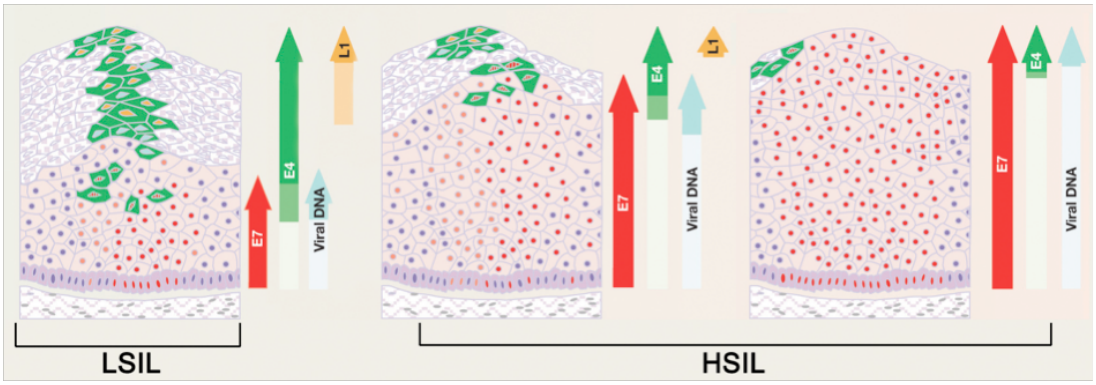

Figure 1.7 HPV expression patterns during neoplastic progression. The E6 and E7 oncogenes are expressed in the suprabasal and upper layers of the epithelium during neoplastic progression. Lesions classified as low-grade present expression of early oncogenes limited at basal-suprabasal layers of the infected epithelium. High-grade squamous intraepithelial lesion (HSIL) present oncogene expression throughout the thickness of the epithelium. In HSIL lesions the keratinocytes are maintained in S-Phase state by the action of oncogenes E6 and E7 instead of differentiating. Misregulation of oncogene expression causes lesions to persist for a long time and in some cases to progress to cancer (adapted from (Doorbar, 2005).

1.4 HPV and the Host Immune System

There is no evidence of an immune response during HPV DNA amplification, as the virus is only poorly visible to the host immune system, replicating with the host DNA and not causing any cytopathology in the host cells (Stanley, 2004). Furthermore, during HPV infections, there is very little release of pro-inflammatory cytokines that are important for Antigen-Presenting Cell (APC) activation and migration towards the sites of infection, resulting in a lack of immune recognition response (Stanley et al., 2007). HPV, like other viruses, have

developed mechanisms to interfere with the production of certain cytokines that are necessary for immune defense (Stanley et al., 2012). In particular, the E6 and E7 proteins from HR-HPVs interact directly with components of the interferon (IFN)–signalling pathway (Barnard and McMillan, 1999; Lace et al., 2009).

To date, it is not clear whether persistent HPV infections with chronically reappearing lesions are due to exposure to new exogenous HPVs or due to reactivation of undetected latent viruses. HPV latency is not well understood, but there is evidence that lesions tend to reappear in treated areas, and reactivation of previous infections in immunosuppressed patients is very common (Penn, 1986; Sillman et al., 1984). Furthermore, it has been suggested that the viral episome may persist for a long time in slow-cycling epithelial cells without causing apparent disease (Maglennon and Doorbar, 2012). These observations suggest that the host immune system is unable to fully clear HPV virions, which could explain recurrent lesions.

Paradoxically, establishment of HPV infections requires wounding of the epithelium in order for virions to physically reach the basement membrane, yet any potential inflammatory response invoked during wound healing does not clear these infections. It is yet unclear whether wound healing does not induce a strong inflammatory response or whether HPV has evolved a mechanism to evade this response. Thus, elucidation of the phases of wound healing is necessary to understand the mechanism of lesion formation following HPV infection.

1.5 Wound healing process

In order to understand the environmental conditions in which HPV infections occur, it is useful to characterize the phases of the wound healing process. The primary purposes of the healing process is to fill the gap created by tissue destruction and restore the structural continuity of the injured parts. Wound healing is commonly divided into three phases: the inflammatory phase, the proliferative phase, and the remodeling phase. The inflammatory stage primarily serves to remove the injury-causing agent and prepare the wounded environment for healing (Eming et al., 2007). During this stage there is a release of growth factors and cytokines, which attract surrounding fibroblasts, including basic fibroblast growth factors (bFGF), interleukin-6 (IL-6), and transforming growth factor beta-1 (TGFβ-1).

The arrival of fibroblasts marks the beginning of a second phase of wound healing, the proliferative phase. The purpose of the proliferative phase is to build new tissue to fill the wound space. The recruited fibroblasts, which are connective tissue cells, synthesize and secrete collagen. They also secrete growth factors that induce the growth of blood vessels in a process called angiogenesis, which then promotes endothelial cell proliferation and migration. The fibroblasts and endothelial cells together form granulation tissue that serves as a foundation for scar tissue development. The final process of the proliferative stage is epithelialization, which involves regeneration, migration, proliferation and differentiation of epithelial cells at the wound's edge in order to form a new surface area similar to that destroyed by the injury. By the end of the proliferative

phase, white blood cells leave the wound site and the newly formed small blood vessels eventually degenerate.

The third phase of wound healing is the remodeling phase, which begins at variable times, typically weeks after the injury, continues for six months or longer. During this final stage, scar tissue is formed by simultaneous synthesis and lysis of collagen. At this stage the scar tissue becomes avascular and may achieve 70-80% of tensile strength after three months (Clark et al., 1996; Werner et al., 2007).

1.5.1 Establishment of HPV Infection During Tissue Injury

HPVs require wounding of the epithelium in order to expose basal cells for virus entry. Generally, a micro-trauma exfoliates the primary layer of the epithelium, exposing the basal cells and basement membrane without causing a strong inflammatory or immune response (Kines et al., 2009). Thus, it is plausible that HPV infection and viral genome replication occur during the early phase of wound healing known as the proliferative phase. To date, it is unclear whether the increased cell proliferation observed during early HPV infections is caused by viral oncogene expression or by the proliferative responses in the would healing environment. The phases of wound healing in the context of an HPV infection can be studied *in vitro* using keratinocytes cultured in monolayer.

1.5.2 Growth factors in wound healing

It was recently documented that wound healing might increase the efficiency with which the HPV DNA becomes established as a nuclear plasmid in basal cells, because the basal cells are then in a hyperproliferative state (Pyeon et al., 2009; Werner et al., 2007). The hyperproliferative state of basal cells is due to the augmented concentration of growth factors during wound healing (Shirakata, 2010).

Growth factors and cytokines are produced from a variety of epithelial and immune cells during wound healing. They are important during the proliferative phase to attract surrounding cells to fill in the damaged area and to induce cellular proliferation and/or differentiation in the recruited cells. Growth factors in particular are secreted by keratinocytes and fibroblasts and bind to receptors on the cell surface to produce new epithelia. Many of these growth factors are quite versatile, stimulating cellular division in numerous different cell types, whereas others are more specific, imparting their functions in only one particular cell type. The main keratinocyte-derived growth factors are: Epidermal Growth Factor (EGF), Transforming Growth Factor - α (TGF-α), Platelet Derived Growth Factor (PDGF), Transforming Growth Factor – β (TGF-β), and Keratinocyte Growth Factor (KGF). Fibroblasts also produce growth factors to induce cellular proliferation, and the most important are the 18 members of Fibroblast Growth Factor family (FGF-1 - FGF-18), and TGF-β (Goodsell, 2003).

The role of EGF has been extensively investigated in normal and pathological wound healing. Since the discovery of EGF, the first growth factor to be isolated,

over 50 years ago, growth factor therapy has progressed into clinical practice in the treatment of wounds (Weltman, 1987).

EGF, like all growth factors, binds to specific high-affinity, low-capacity receptors on the surface of responsive cells to induce signal transduction cascades resulting primarily in DNA synthesis and proliferation. Binding of EGF to the EGF receptor (EGFR) stimulates its intrinsic tyrosine kinase activity, which then results in autophosphorylation and subsequent binding to proteins containing SH2 domains. EGF has proliferative effects on cells of both mesodermal and ectodermal origin, and particularly on keratinocytes and fibroblasts. Growth-related responses to EGF include the induction of MAPK, Akt, and JNK pathways and nuclear proto-oncogene expression, such as *fos*, *jun* and *myc* (Carpenter, 2000).

1.6 Rational and Aims of this Study

The general aim of my thesis study is to further the understanding of the early phases of HPV lesion formation.

The formation of a lesion is a complex and not yet well-understood process that implicates several protagonists. Current hypotheses suggest that in many cases HPV infection of the basal layer happens through an epithelial micro-wound (Kines et al., 2009). Recent work also suggests that a wound healing environment and the presence of growth factors can facilitate infection of basal cells (Surviladze et al., 2012). According to clinical biopsy studies, the HPV genome expression in the basal layer can vary between HPV types (Fig. 1.8). For example, low risk HPV do not produce an increase in cell proliferation markers in basal

cells, whereas high risk HPV have the ability to drive basal cell proliferation, possibly because of the expression of the early oncogenes E6 and E7. To date it remains unclear why the phenotypic differences between the two groups have evolved, and how low- and high-risk viruses produce such lesions.

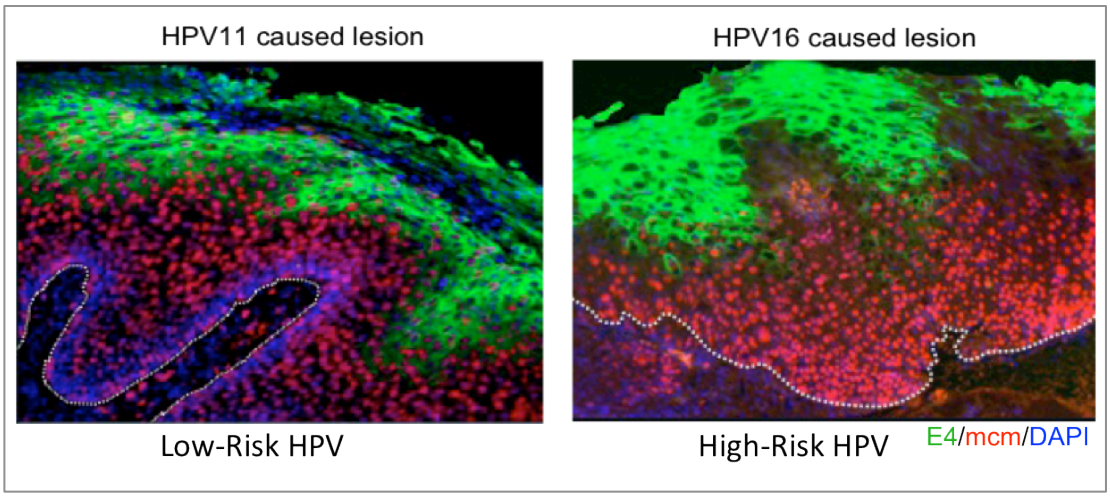

Figure 1.8. Immunostaining of HPV11 and HPV16 caused lesions. Sections of human lesions caused by low-risk and high-risk HPVs were stained using a cell proliferation marker (mcm, in red) and E4 (in green) antibodies. Dapi staining (blue) was used to visualize cell nuclei. The white dots indicate the position of the basal layer (Adapted from Doorbar et al., 2012).

Hypotheses:

1. We hypothesize that during infection with high-risk HPV, wound-healing responses lead to up-regulation of viral E6/E7 expression. This in turn leads to increased cell growth, with infected cells out-growing their uninfected neighbours.

2. We hypothesize that low-risk viruses also elevate their E6/E7 expression in response to wound healing but that the low-risk E6/E7 proteins are not capable of increasing growth of the infected cells.
3. We hypothesize that the wound healing response facilitates establishment of HPV genomes.

Objectives:

1. Develop an *in vitro* model system that recreates the conditions of wound healing.
2. Study the effects of the presence of growth factors on viral genome expression in 'infected' cells.
3. Compare the effect of wound healing responses between low- and high- risk HPV types.
4. Investigate the differences between low- and high-risk types in terms of cell proliferation *in vitro.*

2. Materials and Methods

2.1 Suppliers of chemicals and reagents

The chemicals used, unless otherwise stated, were purchased from Sigma-Aldrich (Boukamp et al.), BDH Laboratory Supplies (Boukamp et al.), Fisher Scientific (Boukamp et al.) or VWR International Ltd. (Boukamp et al.).

2.1.1 Commonly used buffers and reagents

Table 2.1 shows the commonly used buffers and reagents. The buffers listed were prepared by the NIMR media facility.

Table 2.1: Buffers and reagents

Name	**Components**
Penicillin/Streptomycin (for cell culture)	0.6 % (v/v) penicillin, 1 % (v/v) streptomycin
Trypsin-versene (for cell culture)	0.8 % NaCl, 0.02 % KCl, 0.12 % Na_2HPO_4, 0.02 % KH_2PO_4, 0.01 % EDTA, 0.13 % trypsin, 0.001 % phenol red
1X Phosphate buffered Saline (PBS)	1 % NaCl, 0.025 % KCl, 0.14 % Na_2HPO, 0.025 % KH_2PO_4
1X Tris-buffered saline (TBS)	2.42 g Tris base, 8 g NaCl; pH 7.6 (for 1L)
Luria-Bertani (LB) medium	1 % Tryptone, 0.5 % yeast extract, 1 % NaCl
LB agar	LB medium plus 2 % Bacto agar
50X Tris acetate EDTA (TAE)	242 g Tris base, 57.1 ml glacial acetic acid, 18.6 g EDTA (for 1L)
SDS electrophoresis buffer	25 mM Tris base, 200 mM glycine, 0.1 % sodium dodecyl sulphate (SDS); pH 8.3
Transfer buffers	(Western blots) 25 mM Tris-HCl, 200 mM glycine, 20 % (v/v) methanol; pH 8.3; (Southern blots) Saline-sodium citrate 20x

2.2 Keratinocyte and fibroblast monolayer cell culture method

2.2.1 Cell lines

2.2.1.1 Normal immortalized Human Keratinocytes (NIKS)

NIKS, a cutaneous foreskin keratinocyte cell line, were used as host cell and as negative control with all HPV16 and HPV11 experiments. NIKS are a spontaneously immortalized HPV-negative human foreskin keratinocyte cell line. These cells arose originally from their parental BC-1-Ep cell line, isolated from neonatal foreskin, through serial passaging (Allen-Hoffmann et al., 2000).

2.2.1.2 J2-3T3 mouse fibroblasts

J2-3T3 are an immortalized fibroblast cell line that was originally isolated from Swiss albino mouse embryos (Todaro and Green, 1963). J2-3T3 cells were γ-irradiated and used as 'feeder layer' to support the growth of NIKS cells.

2.2.1.3 NIKS HPV16-positive cells

HPV16 clonal cell lines were established from two independent transfections (made by Kenneth Raj; NIMR, London, UK and Qian Wang; NIMR, London, UK). NIKS were co-transfected with re-circularized replication competent HPV16 wild type (WI2) genomes and a pcDNA6 vector containing a Blasticidin resistance gene. Clonal cell lines were recovered after selection with 6 μg/ml of Blasticidin. After individual colonies became visible, cells were first cultured in single wells of 60 mm 6-well plates (Thermo Scientific; 140675) and subsequently expanded to make cell stock.

2.2.1.4 NIKS HPV11-positive cells

NIKS-HPV11 cell populations were prepared co-transfecting NIKS with re-circularized replication competent HPV11 wild type (Hershey) genomes and a pcDNA6 vector containing a Blasticidin resistance gene. Cell populations were recovered after short selection with 6 μg/ml of Blasticidin. The cell population were separated and kept growing in single wells of 60 mm 6-well plates (Thermo Scientific; 140675). After Blasticidin selection the NIKS-HPV11 populations were assessed for the presence of HPV11 genome.

2.2.1.5 NIKS GFP positive cells

NIKS-GFP positive cells were produced transfecting NIKS cells with the ZsGreen1 Fluorescent Protein transforming vectors (#632473; Clontech Laboratories, Inc. USA). The bright green fluorescent protein-encoding gene derived from a *Zoanthus* sp. reef coral. We find that the protein is stable and non-toxic in NIKS, and can be easily visualized in living and fixed specimen.

2.2.2 Media and Supplements

The following media were used for culturing the cell lines as well as for freezing of cells for long-term storage are described in Table 2.2. The supplements used in the FI medium for NIKS were prepared either as 100 or 1000X stock, filter sterilized using a 0.2 μM membrane filter unit (Sartorius; 16534). All supplements were stored as 5 ml aliquots at -20 °C.

Table 2.2 Cell Culture and Freeze Media		
Cell type	**Medium type**	**Medium components**
NIKS, HPV16, clones and and other NIKS-derived cell populations	F-Medium Incomplete (FI)	500 ml F Medium (3 part F12-Hams + 1 part high glucose DMEM) (PAA; T15-355), 5 % (v/v) FBS (Biosera; S1900-500), 24 µg/ml adenine (Sigma-Aldrich; A2786), 8.4 ng/ml cholera toxin (Sigma-Aldrich; C8052), 0.4 µg/ml hydrocortisone (Calbiochem; CAS 50-23-7), 5 µg/ml insulin (Sigma-Aldrich; I4011) and 1 % (v/v) pen/strep
NIKS, HPV16 clones and other NIKS-derived cell populations	F-Medium Complete (FC)	FI medium with Epidermal Growth Factor (EGF) added prior to use at a concentration of 10 ng/ml (R&D Systems; 236-EG)
NIKS, HPV16 clones and other NIKS-derived cell populations	NIKS freezing Medium	90 % (v/v) FBS, 10 % (v/v) DMSO (Sigma-Aldrich; D2650)
J2-3T3	DMEM complete	500 ml high glucose DMEM (Sigma-Aldrich; D6429), 10 % (v/v) FBS and 1 % (v/v)
J2-3T3	J2-3T3 Freezing Medium	95 % (v/v) FBS, 5 % (v/v) DMSO

2.2.3 Maintenance of monolayer cells

2.2.3.1 J2 3T3

J2-3T3 fibroblasts cells were cultured in 10 ml of DMEM complete medium in T75 flasks (Fisher Scientific; TKV-123-013L) at 37 °C and 5 % CO2. The fibroblasts were grown until they were 80% confluent and were then split between 1:10 and 1:40 as required. To harvest, cells were washed with 5-10 ml of PBS and then incubated with 1 ml of trypsin-versene for 2 minutes at 37 °C. Thereafter, 9-12 ml

of DMEM Complete Medium were added to the fibroblasts flask. A small aliquot of the suspended cells was then added to anew flask for further culturing. Cells were given fresh medium every 3-4 days. For long-term storage, a confluent flask of low passage cells was harvested, spun down at 1500 rpm using a MSE Mistral 1000 centrifuge for 5 minutes, re-suspended in 2 ml of J2-3T3 freezing medium, transferred to 2 Cryovials (Thermo Scientific; 5000-1012) and froze down at -80° C or in liquid nitrogen. J2 3T3 cells above passage 20 were not used for experimental purposes.

2.2.3.2 NIKS, NIKS HPV16 clones and other NIKS-derived cell populations

NIKS, and NIKS-HPVs cells, were cultured on a layer of γ-irradiated J2-3T3 cells. J2-3T3 cells were irradiated at a dosage of 60 Gy using a Caesium source. Approximately $1.8x10^6$ feeders were seeded in a T75 flask in 10 ml of FI medium and left to attach for 1.5- 2 hours prior to plating NIKS cells. NIKS were cultured to a maximum of 80% confluence and split approximately once a week between 1:5 and 1:30, depending on the growth rate of the cells. NIKS cells above passage 15 were not used for experimental purposes. To harvest the NIKS, the cells were washed with 8-10 ml of PBS and then incubated with 1 ml of trypsin-versene for 2-4 minutes at 37 °C, in order to remove the fibroblast layer. After tapping the flask few times to completely dislocate the fibroblasts, trypsin was aspirated, and cells washed with 8-10 ml of PBS. Keratinocytes were then incubated in 2 ml of fresh trypsin-versene at 37 °C for about 10-15 minutes. When all cells had dislodged from the flask, 8 ml of FI medium was added, cells were collected into a single cell suspension and transferred to a flask of γ-irradiated fibroblast for

further culturing. Cells were provided with fresh FI or FC medium every second day. For long-term storage, a flask of low passage cells was harvested, spun down at 1500 rpm for 5 minutes. Approximately 2-3x106 cells were re-suspended in 1 ml of NIKS freezing medium, transferred to a cryovial and stored at -80 °C.

2.2.4 Cell counts of NIKS, NIKS HPV16 clones and other NIKS-derived cell populations

For all experiments involving NIKS, cells were counted using a Z1Coulter® Particle Counter (Beckman Coulter; UK). After cell harvest, as described earlier, 0.5 ml of the cell suspension was re-suspended in 9.5 ml of Isoton II diluent (Beckman Coulter; 8546733) in a coulter counter cuvette (VWR International Ltd.; 720-0812). The coulter counter was optimized to NIKS cells size. As previously established the majority of cells fell within a peak range of 11-20 μm in size (Erin Isaacson; NIMR, London, UK). In order to account for cells that are slightly larger, the coulter counter parameters were set to count all cells above the lower limit tL=11 μm.

2.2.5 Transfection of NIKS and NIKS HPV11/16-positive cells

For transfections, NIKS and varieties thereof, were harvested and plated on 60 mm 6-well plates at a density of 5x105 cells per well on a layer of 1x105 feeders and left to grow overnight in FC medium. Transfections were carried out using the Effectene® Transfection Reagent Kit (Qiagen; 301425) following the manufacturer's instructions. Cells were transfected with up to a total of 1 μg of

circular or linearized DNA, which was purified from bacterial cultures. Six hours after transfection cells were given fresh FC medium.

2.2.6 Electroporation

Alternatively to Effectene® transfection reagent we have performed the transfection of the NIKS and NIKS-derived cells by electroporation.

NIKS, NIKS-derived cells were harvested, washed twice with PBS, counted and divided into aliquots of $2.0x10^6$ cells in individual micro centrifuge tubes. Cells were electroporated using the 4D Nucleofector® X Unit from Lonza (Boukamp et al.) and the Amaxa™ SE Cell Line 4D-Nucleofector™ X Kit L (Lonza; V4XC-1024), according to the manufacturer's instructions. The specific program used was previously optimized for NIKS cells according to manufacturer's instructions (Figure 2.1). Subsequently cells were seeded into 6-well plates on top of $1x10^5$ feeder cells in FC medium and given fresh FC medium after 24 hours.

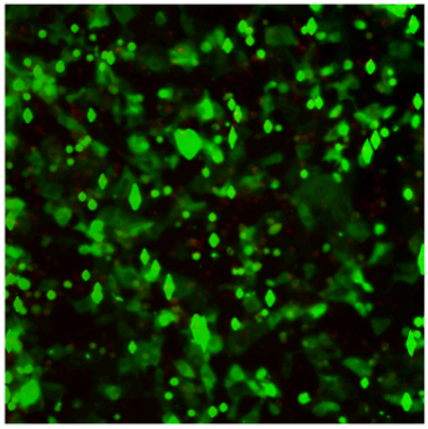

Figure 2.1 Fluorescence microscopy digital image of NIKS transfection optimization. GFP expressing plasmid was used to optimize the electroporation protocol for NIKS transfection. 48 hours post transfection 60-70% of NIKS cells were GFP positive.

2.3 Growth assays of NIKS, NIKS HPV16 clones and other NIKS-derived cell populations

To determine the proliferation patterns of NIKS, NIKS-HPV clones and NIKS-HPV populations, $1x10^5$ keratinocytes were seeded on top of a layer of $0.8\text{-}1x10^5$ γ-irradiated J2-3T3 fibroblasts per well of a 6-well plate. Triplicate wells were set-up for each cell type and time-point. The day of seeding was denoted as day 0. The seeded cells were left to grow overnight in 3 ml of FI medium. On the following day (day 1) cells were counted to determine the seeding efficiency. For most experiments cells were grown for a total of 7 days and counted at days 1, 3, 5, and 7. On day 1 and every other day thereafter (days 3, 5, and 7) cells were fed with 3 ml of FC medium. For harvesting, cells were washed with 3 ml of PBS and then incubated for 2-4 minutes with 1 ml of trypsin-versene at 37 °C to dislodge the fibroblasts. After tapping the plate few times to completely separate the fibroblasts, trypsin was aspirated. To remove the keratinocytes, 1 ml of trypsin-versene was added to each well and cells were incubated at 37 °C for about 10 minutes. When all cells had detached from the bottom of the wells, 4 ml of FI medium was added, cells collected into a single cell suspension and 0.5 ml of the mix used for counting. Cells remaining from counting at each time-point were collected in cell pellets and stored at -80 °C for protein and/or transcript analysis.

2.4 Short growth assays of NIKS, NIKS HPV16 clones and other NIKS-derived cell populations

This growth assay format was developed to assess the proliferation patterns of NIKS and NIKS-HPV16 clones during a shorter time frame. $1.0x10^5$ keratinocytes were seeded on top of a layer of $1x10^5$ feeders per well of a 6-well plate in FI

medium. Triplicate wells were set-up for each cell type and time-point. The day of seeding was denoted as day 0. On the following day (day 1) cells were given fresh FI medium and counted as described in Section 2.3 to assess the seeding efficiency of cells. On the following 12, 24, 36, and 72 hours, cells were counted and all remaining cells fed with 3 ml of FC medium. The cells remaining from counting at each time-point were pelleted and frozen at -80 °C.

2.5 Wound healing scratch assay

In both migration and invasion assay, 100µl of NIKS or NIKS derived cell lines (10^6 cells per ml) in FI Medium were seeded onto a γ-irradiated fibroblast layer in 35 mm Glass Bottom Dishes (P35GC-1.5-14-C; MatTek Co., USA). The dishes were incubated at 37˚C and 24 hours after seeding the Medium was changed with 3ml of fresh FC Medium. The cells were grown to confluence and scratch wounds then created using a pipet tip. The wound site was photographed digitally at two-hours intervals. Image-J® software was then used to calculate the cell-free area, and the cell migration rate was calculated using the changes in this area. A reproducibility test showed that repeated annotation of the same image area produced an average difference of 1.4% of the total image area between replicates and that the difference never exceeded 4.2%.

2.5.1 Calculation of the migration rate

The cell migration rate was calculated as the area conquered in the free-cell area by the cells over time. The measurement were taken using the Image-J® software and using the free cell area measured at the specified time-point we have

calculated the area cover by the movement of the two fronts in the vertical direction. Results were obtained from at least three independent experiments with using different sets of NIKS and NISK-derived cell lines. Data collected were presented as means ± Standard Deviations (SDs) of triplicates from a representative experiment.

2.6 Immunocytology and Immunohistochemistry

2.6.1 Immunocytology of NIKS, NIKS HPV16 clones and other NIKS-derived cell populations

To harvest monolayer keratinocytes for immunocytology, round coverslips (VWR International Ltd.; 631-0713) were sterilized using 70 % ethanol and placed into 60 mm 6-well plates. Irradiated fibroblasts and keratinocytes were seeded on top as described in Section 2.3.

2.6.2 Fixation of coverslips

The cells on coverslips were fixed with 5% paraformaldehyde for 5 minutes at room temperature. To do this, growth medium was aspirated from the wells and the coverslips washed twice with 1x PBS. After the incubation period, cells were washed twice with PBS and stored in 0.01% sodium azide in PBS at 4 °C.

2.6.2.1 Immunocytology and mounting monolayer coverslips

The PBS/azide solution in each well with the coverslips was aspirated. The cells were blocked in 5 % normal goat serum (NGS) (Cell Signaling Technology; 5425) in PBS for 1 hour at room temperature. After blocking, the primary antibody (Cell

Signaling Technology; 9733) was made up in 5 % NGS in PBS at a 1:200 dilution, applied to the coverslips and left for 1 hour at room temperature. Thereafter, 5 quick rinses of the coverslips (within the wells) were done using PBS. Next, the secondary antibody was applied as a secondary antibody in 5 % NGS in PBS and left for 1 hour at room temperature. DAPI was added as a nuclear counterstain alongside the secondary antibody at a 1:1000 dilution. Subsequently, the coverslips (within the wells) were rinsed 5 times using PBS. Coverslips were rinsed once in dH2O, lifted out of the wells carefully and dried gently. Then 10-20 µl of Citifluor® reagent was dropped onto a Superfrost-plus slide and the coverslip inverted on top, taking great care to ensure no air bubbles were trapped underneath. Slides were stored in a folder at 4 °C.

2.6.2.2 Primary antibody signal amplification

In cases where an amplified signal of the primary antibody was needed, secondary biotinylated antibodies were applied to the raft sections, according to Table 2.5. Approximately 30 minutes through this incubation, Strep A/B (avidin/biotin) complexes were assembled using the ABC (peroxidase) kit according to Table 2.6 and the manufacturer's instructions. The complexes were removed using the same PBS-Tween 0.05 % wash regimen. In order to quench endogenous human peroxidases, 3 % hydrogen peroxide/PBS (v/v) was applied to the section for 15 min. at RT, following the removal of ABC complexes. The hydrogen peroxide was removed by rinsing the sections several times in PBS. To complete the amplification process, the fluorochrome labeled Tyramide (rhodamine) was applied to the sections according to Table 2.6 and the

manufacturer's instructions. The rhodamine was removed using the same PBS-Tween 0.05 % wash regimen.

Table 2.3 Primary Antibodies

Target	**Species**	**Clone**	**Dilution**	**Incubation**	**Supplier**
K10	Mouse	DE-K10	1:200	1 hr. RT	Neomarkers
H3P	Rabbit	LYS-27	1:250	1 hr. RT	Cell Signaling

Table 2.4 Secondary Antibodies

Target	**Species raised**	**Conjugate**	**Dilution**	**Incubation**	**Supplier**
Mouse IgG	Goat	Alexa-594/ Biotinylated	1:150	1 hr. RT	Invitrogen
Rabbit IgG	Goat	Alexa-488	1:200	1 hr. RT	Life Technologies

Table 2.5 Chemical Reagents

Reagent	**Dilution/Diluent**	**Incubation**	**Supplier**
DAPI	1:1000 / 5% NGS	1 hr.	
Strep A/B (avidin/biotin) (peroxidase) complex	1:400 50mM Tris/HCL pH 7.6	30 min.	Vector Labs
Tyramide (rhodamine)	1:100 Amplification diluent	8 min.	NEN Life Science

2.6.3 Microscopy and imaging software

All fluorescently stained cells were viewed on a Zeiss A1 microscope equipped with fluorescent filters. Fluorescent images were captured using a Carl Zeiss Microscopy AxioCam MRm camera and images viewed using Axiovision software.

2.7 Molecular biology techniques

2.7.1 Transformation of *E. coli* with DNA

Plasmid DNA was mixed with 50 µl of competent XL10-Gold® Ultracompetent cells (Stratagene; 200314) and incubated on ice for 30 minutes. The mix was heat-pulsed in a water bath at 42 °C for 30 seconds and then cooled on ice for 2 minutes. Subsequently, 800 µl of SOC medium (Life Technologies; 15544-034) was added and cells were incubated at 37 °C for 45 minutes at constant shaking (220 rpm). Cells were plated on LB agar plates containing ampicillin (Sigma Aldrich; A5454) at 100 µg/ml. All plates were left incubate at 37 °C overnight.

2.7.2 Plasmid purification

To extract plasmid DNA from bacteria, three commercial kits were used depending on the amount and purity of plasmid required. The QIAprep® Spin Miniprep Kit (Qiagen; 27106) was used for small-scale preps, from 2-5 ml overnight bacterial cultures. The QIAGEN® Plasmid Midi Kit (QIAGEN; 12143) and the QIAGEN® Plasmid Maxi Kit (QIAGEN; 12162) were used for larger-scale preps, from 100 ml up to 500 ml cultures, respectively. The purification was carried out following the manufacturer's instructions.

2.7.3 Extraction of total genomic DNA from NIKS and other NIKS-derived cell lines

Prior to extracting the DNA, the cells were washed with PBS and pelleted at a low speed (3000rpm) in a microcentrifuge for 5 minutes. The cells were immediately put on ice and the pellets were prepared for the removal of RNA. In order to remove RNA from the cells, the pellet was resuspended in 140 µl of PBS and 40 µl of (10mg/mL) RNase A (Invitrogen; UK). The cells were incubated in a 37ºC water bath for 20 minutes and the DNA extraction protocol immediately followed. The extraction of total genomic DNA, including HPV genomic DNA, from NIKS or HPV-16 cell lines was performed using the QIAamp® DNA Blood Mini kit (protocol for small volumes of blood) (Qiagen; UK). The complete set of buffers and reagents required to extract the DNA were contained in the Qiagen kit.

2.7.4 Quantification of plasmid DNA

Plasmid DNA was quantified using a Nanodrop® ND-1000 Spectrophotometer.

2.7.5 Restriction enzyme plasmid digestion

To allow for the transfection of cells with linearized DNA (as outlined in Section 2.2.5), wt-HPV11 (Hershey), wt-HPV16 (W12) and pcDNA6 vectors were digested using restriction enzymes BamH1 (New England Biolabs; R0136). A total of 20 µg of plasmid DNA was used in the reaction for each of the vectors and digested with 20 units of the enzyme.

2.7.6 Vector re-ligation

Vector re-ligation was carried out using T4-Ligase kit (New England Biolabs, UK) according to manufacture's instructions.

2.7.7 Agarose gel electrophoresis

To assess the presence and quality of plasmid DNA or for subsequent gel extraction, DNA was separated on a 1 % (w/v) agarose (NBS Biologicals, UK) gel in 1x TAE containing 0.5 µg/ml Ethidium Bromide (Bio-Rad; 161-0433) at 120 V for up to 45 minutes.

2.8 Quantitative RT-PCR (qPCR)

Quantitative real-time (RT) polymerase chain reaction (PCR) was carried out using cDNA as a template. Forward and reverse primers (Table 2.7) were used to assess the levels of HPV16 E6, p21, EGFR, Akt, Cyclin D1, p53, Caspase 3 and GAPDH transcripts in NIKS-HPV11 and NIKS-HPV16 cell populations. GAPDH primers were used as endogenous controls.

2.8.1 Extraction of total RNA

To perform the extraction of the total RNA, cells were harvested, washed with PBS and then placed on ice. Total RNA extraction was carried out using the RNeasy® Mini Kit (Qiagen; 74104) and QIAshredder® kit (QIAGEN; 79654) according to the manufacturer's protocol. RNA was stored at -80 °C. If RNA extraction was not carried out immediately after harvest of cells, pellets were

resuspended in RNAprotect® Cell Reagent (QIAGEN; 76526) following the manufacturer's instructions and stored at -80 °C indefinitely.

2.8.2 DNase digestion and reverse transcription

Prior to making cDNA, genomic DNA was removed from 2 µg of total RNA using the DNA-*free*™ kit (Ambion; AM1906) according to the manufacturer's protocol. The reverse transcription was done using the SuperScript™ III First-Strand Synthesis Kit (Life Technologies; 18080-051). A volume of 16 µl (approximately 0.5 µg) of clean RNA was added to a tube along with 2 µl oligo $(dT)_{20}$ primers and 2 µl dNTPs. The mixture was incubated at 65 °C for 5 minutes and then placed on ice for at least 1 minute. Subsequently 4 µl of 10X RT Buffer, 8 µl of $MgCl_2$, 4 µl of DTT, 2 µl RNase OUT™ and 2 µl SuperScript™ III reverse transcriptase was added to each tube before incubating at 50 °C for 1 hour. To stop the reaction, tubes were placed at 85 °C for 5 minutes. Thereafter, cDNA was stored at -80 °C or used for qPCR. An additional tube was prepared using 2 µl of nuclease-free H_2O (Life Technologies; AM9935) instead of the enzyme. The reaction without enzyme was used as control. The cDNA was generally diluted 40- fold with nuclease-free H_2O prior to doing qPCR.

Table 2.6 Primers used for RT-PCR

E6/E6* primers	Forward: 5'-TCAGGACACAGTGGCTTTT-3'
	Reverse: 5'- ACTGCAATGTTTCAGGACCCA-3'
GAPDH primers	Forward: 5'-TGGATATTGTTGCCATCAATGACC-3'
	Reverse: 5'-GATGGCATGGACTGTGGTCATG-3'

2.8.3 qPCR primer design and primer sequences

Caspase 3, Akt-1, Cyclin D1, p21, p53, EGFR, HPV11 E4, HPV16 E6 and GAPDH primers were designed using Primer Select software and ordered from Sigma Aldrich (Boukamp et al.). A list of the primers and their sequences is shown in Table 2.7

Table 2.7 Primers used for qPCR

p21 primers	Forward: 5'-CTCTCCAATTCCCTCCTTCC-3'
	Reverse: 5'-AGAAGCACCTGGAGCACCTA-3'
p53 primers	Forward: 5'-GCTGGCTTCCATGAGACTTC-3'
	Reverse: 5'-AGGGTGTGATGGGATGGATA-3'
Cyclin D1 primers	Forward: 5'-TCGCTGGAGCCCGTGAAA-3'
	Reverse: 5'-GCGTGTGAGGCGGTAGTAGTAGGA-3'
EGFR primers	Forward: 5'-ATGCCCG-CATTAGCTCTTAG-3'
	Reverse: 5'-GCAACTTCCCAAAATGTGCC-3'
HPV16 E6 primers	Forward: 5'-TGTTTCAGGACCCACAGGAGC-3'
	Reverse: 5'-CGCAGTAACTGTTGCTTGCAG-3'
GAPDH primers	Forward: 5'-CCTCCCGCTTCGCTCTCT-3'
	Reverse: 5'-CTGGCGACGCAAAAGAAGA-3'
Caspase 3 primers	Forward: 5'-TTTTTCAGAGGGGATCGTTG-3'
	Reverse: 5'-TCAAGCTTGTCGGCATACTG-3'
Akt-1 primers	Forward: 5'-GGCAGCGGCAGCGTGT-3'
	Reverse: 5'-GGCCCACACACTCACCGAGAA-3'
HPV11 E4 primers	Forward: 5'-ACATTAGATCCGTGGACAGTACAATC-3'
	Reverse: 5'-TTCCTTCTTTGGTGCTTGTTGTAA-3'

2.8.4 qPCR reagent cocktails

Power SYBR® Green PCR Master-Mix (Applied Biosystems; 4367659) was used to amplify and detect cDNA in 96-well PCR plates (Thermo Scientific; TUL-962-

011N) using an ABI -7500 Real-Time PCR System. A fresh master mix of reagents was prepared for each primer set (see Table 2.7) immediately prior to loading the plate. The final volume in each well was 25 µl.

Table 2.8 qPCR cocktail

	Cocktail Mix (µl) per reaction (well)
***Primer Forward**	1.75 µl
***Primer Reverse**	1.75 µl
SYBR Green	12.5 µl
H_2O	8 µl
	x number of reactions

2.8.5 qPCR plating scheme and cycle parameters

Samples were run in triplicate wells (for each primer set). To set up the reaction, 19-22 µl of the master mix was pipetted into each well, followed by 3-6 µl of cDNA pipetted separately. Table 2.9a outlines the qPCR cycle parameters. They include a dissociation curve at the end of the amplification steps. This was included because SYBR Green can bind to unspecific double stranded DNA, such as primer-dimers, which can interfere with results. The dissociation curve shows whether a single or multiple PCR products have been amplified. Table 2.9b outlines the parameters for the dissociation program.

Table 2.9a: PCR cycle parameters

Step	**Number of cycles**	**Time per cycle**	**Temperature**
1	1	2 minutes	50 °C
2	1	15 minutes	95 °C
3	40	15 seconds	95 °C

4	1	1 minute	60 °C
Table 2.9b: Dissociation parameters			
Step	**Number of cycles**	**Time per cycle**	**Temperature**
1	1	15 seconds	95 °C
2	1	20 seconds	60 °C
3	1	95 seconds	95 °C

2.8.6 Standard curves for primers

A standard curve and linear equation was generated for each primer set used in order to establish their efficiency and sensitivity. To generate the standard curve, a DNA plasmid containing the sequence that is amplified by the primers was chosen as a template. To establish a linear relationship, six 10-fold serial dilutions of the template were prepared which corresponded to a known number of copies of the template, from 1 to $1x10^6$, and served as a template for the qPCR reaction. To generate the standard equation, the logarithms of the values of the known copy numbers in each dilution (either 1, 10, 100, 1000, 10000 or 1000000) were plotted on a graph along the x-axis against the Ct (cycle threshold) value given by the qPCR machine for each dilution along the y-axis, and an equation was obtained in the form of $y = mx + c$. The slope (m) refers to the efficiency of the primer pairs, where a slope of -3.33 shows a perfect linear relationship between DNA copy number and Ct value and corresponds to an increase of 3.33 Cts for every 10-fold dilution of sample. The y-value in this equation is the Ct value that the qPCR measures, which refers to the number of cycles, needed to amplify one

copy of DNA. The following table shows the standard curve equation for HPV16-E6, HPV11-E4 and GAPDH.

Table 2.10: Standard curves for primers used for qPCR

Standard curve equation HPV16-E6:	y = -3.362x + 34.18
Standard curve equation HPV11-E4:	y = -3.395x + 38.16
Standard curve equation GAPDH:	y = -3.316x + 36.23

2.8.7 Copy number determination

The standard curves for the primer sets were used to calculate the copy numbers of the transcripts of interest in each sample. Each triplicate set of Ct values per sample and primer set was averaged. To account for pipetting error the software calculated the standard deviation for each set, with those above 0.5 indicating excessive variation. Reactions were repeated if standard deviations exceeded 0.5. Acceptable Ct averages were used to calculate copy number. To do so, the standard curve equation was solved for *x*. The number of copies is the inverse log of *x* i.e. 10x. When transcript numbers had been established for all primer pairs, the values of HPV16-E6 and HPV11-E4 were divided by the values of GAPDH to normalize the results. In order to establish the total number of cells in each reaction, the GAPDH copy numbers were divided by four. This was due to the fact that previous work with these GAPDH primers had identified two additional GAPDH pseudogene sequences within the NIKS genome. To complete the HPV copy number/cell calculation for each cell line, the total number of HPV copies were divided by the total number of cells.

2.8.8 Analysis of Relative Gene Expression using the ΔΔCt method

The Ct values provided from real-time qPCR were imported into a spreadsheet program such as Microsoft Excel®. The relative variation between samples was established following the protocol as described in (Livak and Schmittgen, 2001). The GAPDH primers were used to assess the calibrator gene GAPDH.

2.9 Amplification of Papillomavirus Oncogene Transcripts (APOT) analysis

$2x10^6$ sub-confluent NIKS-HPV16 cell lines were first harvested for total RNA extraction. Total RNA extraction was carried out using the Qiagen RNeasy kit (Qiagen; UK). APOT analysis of HPV-16 extracted RNA was carried out using the exact primers and protocol as described in (Klaes et al., 1999). The basic principles of the APOT assay for the integrated and episomal transcripts are shown in Figure 2.2. The reserve transcription reaction is performed using an adaptor linked oligo dT primer (dT P3). Subsequently, two PCR reaction steps are performed using oligo dT or Adaptor primers and HPV E7 specific primers. The amplification products are hybridized to HPV E7 and HPV E4 specific probes to discriminate episomal from integrated-derived transcripts (Figure 2.2). The cycling conditions and the primers sequences are listed in Table 2.12 and Table 2.13.

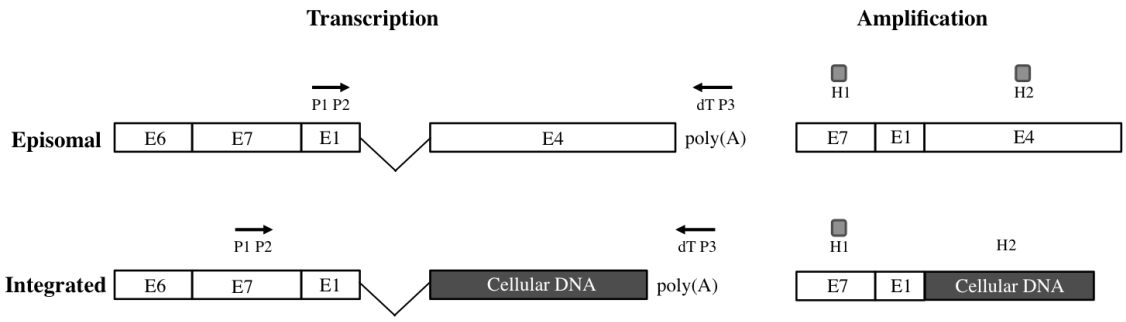

Figure 2.2 APOT diagram, transcription and amplification. The arrows show the primer binding sites. P1 and P2 are HPV specific forward primers for 1st and 2nd PCR. dT-P3 is a Oligo dT primer. H1 and H2 are the probes designed to bind at E7 and E4 respectively. Transcript schemes are shown on the left side. The corresponding amplification products are depicted on the right side.

Table 2.11: Cycling conditions and primers for the 1st APOT PCR

30 Cycles	HPV16
Initial denaturation	94 ° C 3 min
Denaturation	94 ° C 45 sec
Annealing	59 ° C 30 sec
Extension	72 ° C 4 min
Final Extension	94 ° C 7 min
P1- sequence	5'- CGGACAGAGCCCATTACAAT -3'
P3 - sequence	5'- GACTCGAGTCGACATCG -3'

Table 2.12: Cycling conditions and primers for the 2st APOT PCR

30 Cycles	HPV16
Initial denaturation	94 ° C 3 min
Denaturation	94 ° C 40 sec
Annealing	67 ° C 30 sec
Extension	72 ° C 4 min
Final Extension	94 ° C 7 min
P2- sequence	5'- CCTTTTGTTGCAAGTGTGACTCTACG-3'
(dT)17-P3 - sequence	5'- GACTCGAGTCGACATCGATTTTTTTTTTTTTTTT-3'

The PCR products are electrophoresed in 1.0% agarose gels, blotted on nylon membranes (Hybond N+, Amersham Life Science, Buckinghamshire, England) as shown in Figure 2.3. The membrane is then hybridized with an E7-specific probe (H1, Table 2.13) at 55 ˚C. A second membrane is hybridized with the E4-specific probe (H2, Table 2.13) at 55 ˚C. The labeling and detection of the probe was performed using the ECL oligo-labeling and detection kit (GE Healthcare, USA) following manufacture's instructions. The amplified products that did not hybridize with the E4-specific probe were suspected to be derived from integrated HPV genomes.

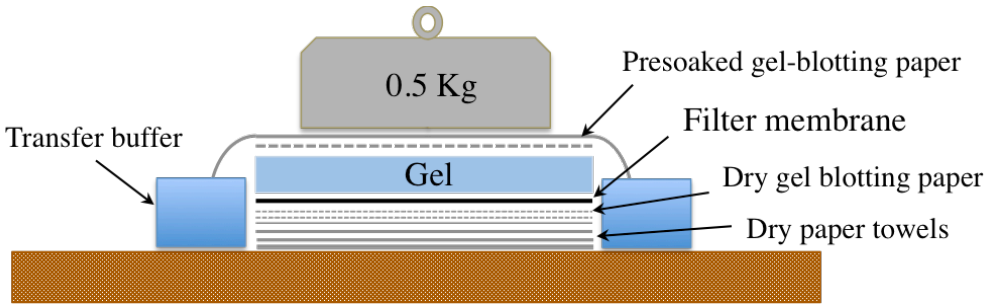

Figure 2.3 Schematic representation of the capillary blotting. Transfer buffer is drawn up the wick, through the gel and membrane, and into the dry stack of towels. The flow of buffer elutes the nucleic acid molecules from the gel onto the membrane, preserving the band pattern.

Table 2.13: H1 and H2 specific probe sequence

H1 E7-specific probe	5'- TCGTACTTTGGAAGACCTGTTAATG -3'
H2 E4-specific probe	5'- GAAGAAACACAGACGACTATATCCAG -3'

2.10 Protein Analysis

2.10.1 Cell lysis for western blot analysis

Monolayer HPV-16 cell lines were grown in 60cm dishes. Approximately $2x10^6$ NIKS or HPV-16 cell lines were harvested and pelleted for lysis. Pellets were washed with 1 X PBS and were then were resuspended in 100-200 µl lysis buffer (50 mM Tris [pH 7.4], 150 ml NaCl, 1 mM EDTA + 4µl of 1x complete protease inhibitor solution (Roche; UK)), The lysates were held on ice for 30 minutes and then were spun at 14000 rpm for 30 minutes. The soluble supernatant was removed and stored separately at -70 °C until further analysis. The insoluble pellet was then resuspended in 100 µl 3x Laemmli Sample buffer (New England Biolabs; UK) and was spun at 14000 rpm for 15 minutes at room temperature.

2.10.2 Protein quantification

The protein quantification of soluble lysates was carried out using the Bio-Rad RCDC kit (Bio-Rad; UK). Quantification was carried out according to the manufacturers instructions. BSA standards, prepared in 0.5 mg/ml increments ranging from 0 mg/ml to up to 10 mg/ml, were used to create a standard absorbance curve.

2.10.3 SDS PAGE

2.10.3.1 Gel electrophoresis for E7 protein analysis

The separation of E7 proteins was carried out using 15 % Tris/ Glycine polyacrylamide gels. Table 2.14 contains the gel composition for both the stack and resolving gel. 7.5 mL of the resolving gel mixture was first poured and set at

room temperature for 30 minutes. 2 mL of the stack gel was overlaid on top of the resolving gel and was left to polymerize for 30 minutes. 20-40 µg of soluble lysate was loaded into each well. Each gel was submerged in 500 mL of SDS Running buffer (25mM Tris pH 8.3, 200mM glycine, 0.1% SDS) in Bio-Rad gel tanks. The separation of E7 proteins was carried out at 80 V for 30 minutes and then at 160 V for 1 hour.

2.10.3.2 Gel electrophoresis for cellular proteins

The separation of various cellular proteins was carried out using 8 % or 10% Tris-Glycine polyacrylamide gels. Proteins greater than 80 kDa were separated on an 8% gel. Table 2.14 contains the gel composition for both the stack and resolving gel. 7.5 mL of the resolving gel mixture was first poured and set at room temperature for 30 minutes. 2 mL of the stack gel was overlaid on top of the resolving gel and was left to polymerize for 30 minutes. 15-30 µg of soluble lysate was loaded into each well. Each gel was submerged in 500 mL of SDS running buffer in Bio-Rad gel tanks. The separation of cellular proteins was carried out at 80 V for 30 minutes and then at 160 V for 40 minutes to 1 hour depending on the protein size.

Table 2.14: Composition of 6, 10 and 15% Tris-glycine SDS-polyacrylamide Resolving gels and 5% Stacking gel			
Resolving gel (for 10 ml)			
Reagent	**6 %**	**10 %**	**15 %**
dH_20	5.3 ml	4 ml	2.3 ml
30 % acrylamide mix	2 ml	3.3 ml	5 ml
1.5 M Tris (pH 8.8)	2.5 ml	2.5 ml	2.5 ml
10 % SDS	0.1 ml	0.1 ml	0.1 ml
10% ammonium persulphate	0.1 ml	0.1 ml	0.1 ml
TEMED	8 µl	4 µl	4 µl
Stacking gel (2 ml)			
dH_20	1.4 ml		
30 % acrylamide mix	0.33 ml		
1 M Tris (pH 6.8)	0.25 ml		
10 % SDS	20 µl		
10 % ammonium persulphate	20 µl		
TEMED	2 µl		

2.10.3.3 Membrane transfer for Western blot

The 15% gels were transferred onto 0.2 µm Immuno-Blot PVDF membranes (Bio-Rad; 162-0176). All other gels were transferred onto 0.45 µm PVDF membranes (Millipore; IPVH00010). Before use, membranes were submerged in methanol, and left to soak in transfer buffer until mounting on the protein-transfer equipment. All transfers were done using 500 ml of Transfer buffer per Bio-Rad Mini Trans-Blot® Cell tank (containing up to 2 gels) at 4 °C overnight at 50V.

2.10.3.4 Blocking, antibody incubations and washing

Following protein transfer, the membranes were incubated under light shaking in 0.1 % PBS/Tween containing 5% of milk powder (Oxoid; LP0031) for 1 hour at

room temperature or overnight at 4 °C. Subsequently, the membranes were incubated with primary antibody for 1-2 hours at room temperature or overnight at 4 °C. Commonly, the membranes were cut into several smaller strips before applying antibody to allow incubation with several different antibodies at once. The antibodies were diluted in 5 ml of 5 % milk in 0.1 % PBS/Tween. Table 2.15 lists all the primary antibodies used for protein analysis and their respective dilutions. Following the incubation with the primary antibody, all membrane pieces were washed in 0.1 % PBS/Tween at room temperature for 30 minutes to up to 1 hour with a change in wash buffer every 10-15 minutes. The membranes were then incubated with secondary antibody, listed in Table 2.16, in 5 ml of 5 % milk in 0.1 % PBS/ Tween for 1 hour at room temperature. The incubation with secondary antibody was followed by a second round of washing with 0.1 % PBS/Tween at room temperature, lasting up to 2 hours with a change in wash buffer every 20-30 minutes

Table 2.15. Primary Antibodies for Western Blot

Antibody	Clone	Dilution	Supplier
E7*	ED17 and 8C9	1:500 / 1:500	Santa Cruz/ Invitrogen (Zymed)
EGFR	Sc-71034	1:1000	Santa Cruz
GAPDH	MAB374	1:4000	Chemicon
Rb	G3-245	1:1000	Pharmingen
P53	D0-1	1:1000	Santa Cruz

* The E7 antibodies were together used as cocktail

Table 2.16 Secondary Antibodies for Western Blot

Antibody	Clone	Dilution	Supplier
Anti-Mouse IgG-HRP	NA931V	1:10000	GE Healthcare

2.10.3.5 Signal detection

The proteins on membranes were detected using 2 different kits, partly depending on the level of sensitivity needed. The Amersham™ ECL Western Blotting Detection kit (GE Healthcare; RPN2106) was used for highly abundant proteins while the Amersham™ ECL Advance kit (GE Healthcare; RPN2135) was used to detect low level proteins.

3. The analysis of monolayer LSIL-like and HSIL-like HPV16 cell lines

3.1 Introduction

As demonstrated in previous studies, the viral gene expression patterns and pathological features of HSIL-like raft cultures are similar to those of high-grade cervical lesions (Isaacson Wechsler et al., 2012). This discovery has been important in the development of a HPV-16 raft model system that reflects the LSIL and HSIL phenotypes seen *in vivo*, and to further study the viral molecular basis of HPV-associated neoplasia.

Our understanding of the viral mechanisms that lead to HPV-induced neoplasia and HPV-related cancers proposed in the past is primary based on the E6 and E7 oncogenes (Duensing et al., 2000). In fact, both E6 and E7 have been demonstrated to have transforming capabilities for the cell (Galloway and McDougall, 1996). The integration of E6 and E7 genes into a host chromosome often correlate with precancerous high-grade neoplasia and cancer (Klaes et al., 1999). Although previous investigations suggested that both E6 and E7 transcripts are more expressed following viral integration, presumably due to the loss of viral negative regulatory elements during integration, it has been more recently shown that 85% of precancerous high-grade lesions and 15% of HPV related cancers contain only viral episomes (Hafner et al., 2008; Klaes et al., 1999). For this reason, considering that integration is likely to occur during the final stages of neoplastic progression and less frequently in the precancerous stages of neoplasia, E6 and E7 expressed essentially from episomes might be important during the phases of lesion formation. This would therefore suggest that a deregulation of E6 and E7 expression could occur from intact viral

episomes and that their expression might be an important driving force for the formation of the HR-HPV lesions.

Several studies using E6 and E7 transgenic mouse models have shown that persistent E6 and E7 expression is important for the development of neoplasia and cancer (Griep et al., 1993). However, although this was seen in models where E6 and E7 were expressed, this was not seen in systems that express endogenous levels of E6 and E7 from a full intact HPV-16 genome (Brake and Lambert, 2005; Shai et al., 2007). Other studies showed that E6 and E7 from HR-HPVs are able to enhance cell proliferation of wounded epithelia when expressed in mice models (Davies et al., 1993). Furthermore, it has been suggested from studies on clinical material that early oncogene expression might drive cell proliferation at basal sites (Zhonglin Wu, NIMR). However, there is not evidence that correlates the expression of E6 and E7 genes with the very early stages of the lesion formation process.

Other interesting questions are how gene expression differs between HPV types and whether the environment in which basal cells proliferate after wounding might influence their proliferation after HPV infection.

Here we hypothesize that early genes from HR-HPVs are able to drive cell proliferation and are important in early stages of lesion formation. LR-HPVs may, however, not have evolved this feature and possibly have developed a different strategy to form a lesion, perhaps exploiting the local microenvironment of the epithelia.

A well-known role of high-risk E7 is its ability to bind Rb, p107 and p130, and target them for proteasomal degradation (Boyer et al., 1996; Davies et al., 1993; Dyson et al., 1989).

E7 from low-risk viruses can also bind to Rb, but with a lower affinity than high-risk E7. This may explain the inability of low-risk E7 to induce transformation (Gage et al., 1990). However, low-risk E7 can cause hyper-proliferation in the suprabasal layers of the epithelium(Heck et al., 1992). Another difference between low- and high-risk E7 proteins relies in the ability to degrade RB, p107 and p130. Low-risk E7 can in fact only degrade p130 (Zhang et al., 2006). Both p107 and p130 share the role of Rb to modulate E2F levels. The degradation of Rb by E7 is commonly efficient in basal and suprabasal cells, while p130 degradation has been found mainly in differentiating cells (Collins et al., 2005; Klingelhutz and Roman, 2012). This suggests that an inefficient Rb degradation in favor of p130 destabilization may contribute to the lack of transformation potential of low-risk E7.

The E6 protein from low-risk and high-risk HPV types also present different functions (Klingelhutz and Roman, 2012). In particular E6 from low-risk types lack the ability to bind and degrade p53 (Doorbar, 2006). Contrary to high-risk E6 the low-risk E6 lack binding to PDZ-domain proteins and have weak inhibition of interferon responses. Furthermore, it is important to notice that high- and low-risk HPV types have significant differences in promoter positioning and promoter regulation, as well as in patterns of mRNA splicing, which affect expression of E6 and E7 genes (Doorbar, 2003, 2006, Roman). Current hypotheses suggest that the differential expression of viral genes and the differences in the protein functions

in the various compartments of the epithelium play a major role in determining disease phenotype following infection.

In this Chapter we aim to characterize a monolayer culture system NIKS to perform experiments oriented to further the understanding in the biology of the high- and low-HPV types, and in particular to consider the behaviour of the NIKS-HPVs cells in a wound healing like environment. We address important issues relating to the development of a suitable wound-healing model system used subsequently to study the episomal NIKS-HPV16 cell lines. Early passage monolayer cultures were used for these experiments, as they approximate the pre-differentiated basal layer of raft cultures where early viral events (e.g. viral replication and viral oncogene expression) are likely to begin. Using monolayer LSIL-like and HSIL-like cultures, we investigated the early E6 and E7 oncogene expression and cellular growth characteristics. In addition, we investigated whether the E7 oncogene expression in HPV-16 cell lines was mainly derived from episomal forms of the viral genome. Furthermore, as NIKS cells were used regularly throughout the various phases of the project, we checked that no appreciable differences in the cell background were present in parental NIKS clones. The evaluation of the keratinocyte differentiation state in our monolayer system was also considered.

In this study, we support the hypothesis that early viral episomal establishment in the basal layer can lead to phenotypic differences in terms of cell proliferation, which are not however significant at early stages of cell proliferation in monolayer. LSIL-like and HSIL-like phenotypes are instead always manifest when cells are cultured for an extensive length of time (Figure 3.1).

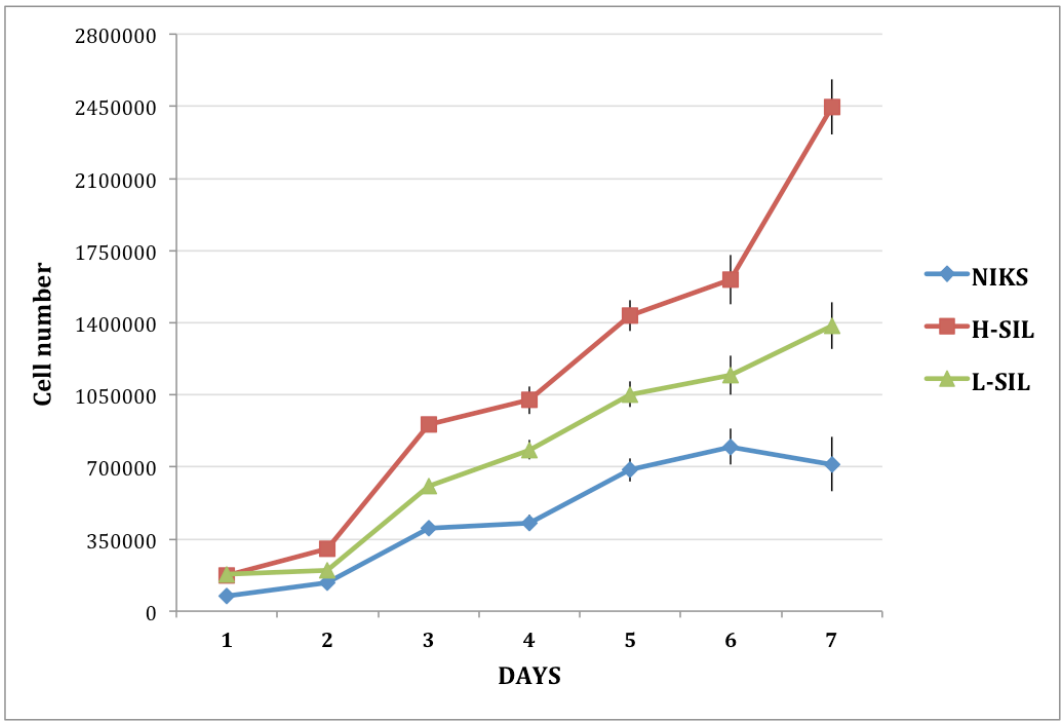

Figure 3.1 Growth characteristics of LSIL-like and HSIL-like NIKS-HPV16 cell lines. Monolayer culture of NIKS and LSIL and HSIL NIKS-HPV16 cell lines were counted in triplicate over seven days time period. The average cell number from triplicate counts for each cell line was plotted against days of growth. The error bars represent the standard deviation of the triplicate counts.

3.1.1 The use of NIKS® (Normal Immortal KeratinocyteS) as a host keratinocyte cell line

To develop a model system I have established NIKS clonal cell lines and populations that maintain episomal forms of the HPV-16 and HPV-11 genomes.

We specifically chose the high-risk type HPV-16 and the low-risk type HPV-11 as models with an interest in evaluating the biology of both HPV groups. HPV-16 and HPV-11 present substantial genetic differences and have very different oncogenic potentials. HPV-16 alone has been shown to cause over 50% of total cervical cancers, whereas HPV11 commonly associates with benign lesions.

The experiments describe the establishment of a monolayer model system useful for the study of the effects that wound healing responses might have on a productive HPV16 or HPV11 infection.

Normal Immortalized Human Keratinocytes (NIKS) were chosen as a host cell line for our model system due to their known ability to successfully maintain HPV viral episomes (Nicolaides et al., 2011). NIKS raft cultures (which are used extensively in our laboratory as a system to support the life cycle of several HPV types) were preferred over the use of primary foreskin keratinocytes. Primary Normal Human Epidermal Keratinocytes (NHEK), in fact, are generally available from single or from pooled donors isolated from the epidermis of juvenile foreskin or adult skin from different locations like the face, the breasts, the abdomen, and the thighs. NIKS cells however, result from expansion of a single colony (Allen-Hoffmann et al., 2000). In addition to the clonal characteristics, NIKS are also immortalized cell lines, whereas primary cell lines typically contain an assortment of stem cells and transit amplifying cells. Therefore, in order to make a HPV cell line or population we chose a clonal recipient instead of a heterogeneous population of cells.

The NIKS cells were isolated and characterized as a spontaneously immortalized human keratinocyte cell line, and were derived from a normal human neonatal foreskin keratinocytes strain, BC-1-Ep. However, the NIKS population presented a specific abnormality following karyotyping studies (Allen-Hoffmann et al., 2000). In fact, all of the NIKS had acquired an additional copy of chromosome 8. This

abnormality did not compromise their ability to be employed as HPV recipient and to produce a fully differentiated epithelium. Further investigation confirmed that NIKS cells were free from HPV as no detectable level of viral DNA was found. NIKS maintained normal growth characteristics compared to the parental cell line The studies on the autocrine expression levels of the growth factors and markers such as the Transforming growth factor (TGF), TGF-ß1 (a keratinocyte growth inhibitor), the Epidermal growth factor (EGF), the oncogene c-myc and keratin K14, showed no differences with the original population (Allen-Hoffmann et al., 2000). Moreover, NIKS have been shown to be non-tumorigenic when injected into mice, which indicates that they are not a transformed line.

Our studies show that, NIKS cells grow, differentiate, and develop into skin tissue in a similar manner to the normal human keratinocytes, exhibiting characteristic physical, chemical, and histological properties of the skin (Figure 3.2) (Boukamp et al., 1988; GIbson, 2007; Isaacson Wechsler et al., 2012; Middleton et al., 2003).

We also further developed the analysis on NIKS background to make sure that no genetic variations were present in transfected NIKS cells that may alter the HPV cell lines produced.

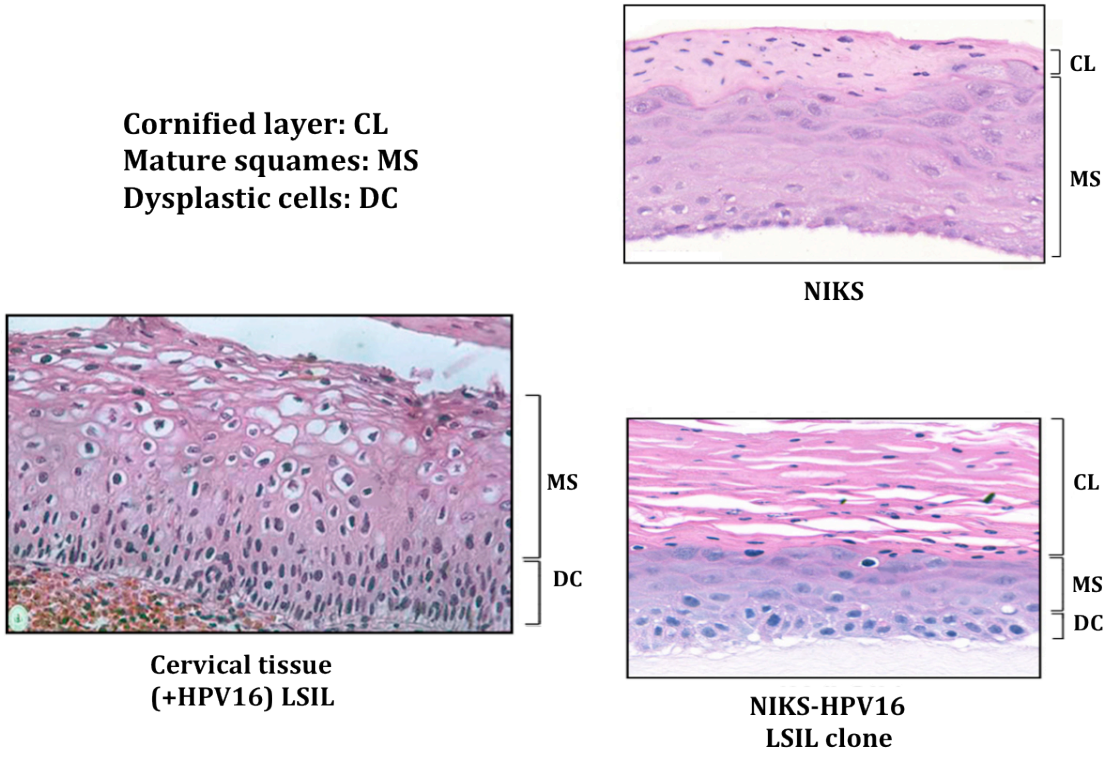

Figure 3.2 Pathology of cervical LSIL HPV16 lesion and NIKS-HPV16 raft culture with LSIL-like phenotype. Haematoxylin and eosin (H&E) were applied to raft culture sections of NIKS (HPV-negative) and NIKS-HPV16 LSIL-like clone. The anatomy of the tissue was compared with H&E stained cervical sections of HPV16 LSIL grade lesion. The anatomy of the raft culture obtained from NIKS cells shows normal characteristics with small size nuclei in the basal and suprabasal strata (MS). Normal stratification and cytoplasmic maturation is evident at upper layers of the section. A thin cornified layer (CL) is present in the uppermost region. In both NIKS-HPV16 LSIL raft and HPV16 LSIL cervical lesion the cells at basal compartment present a mild dysplasia (Doorbar et al.). Normal stratification and cellular maturation occur in the middle and final-third of the epithelium. NIKS-HPV16 raft culture present a cornfied layer (CL) in the uppermost region of the section.

3.2. LSIL-like and HSIL-like monolayer episomal HPV-16 cell lines proliferate faster than NIKS HPV-negative cells.

Isaacson et al. (Isaacson Wechsler et al., 2012) showed in raft culture that the HSIL-like cell lines maintained proliferating cells throughout the majority of the epithelium, and that this coincided with a delay in cellular differentiation and late viral gene expression. Such proliferating cells were only detected in the first few layers of raft epithelium formed by NIKS-HPV16 LSIL, which coincided with a more normal onset of cellular terminal differentiation and an earlier onset of late viral gene expression. It was reported that the HSIL and LSIL related characteristics were consistent phenotypes deriving from NIKS-HPV16 clonal cells and this was exclusively supported by my experience with these cell lines (Figure 3.1; 3.3A). In addition, it was demonstrated that these cell lines retained these characteristics in monolayer culture as well. In fact, HSIL-like cells cultured in monolayer dishes were able to overcome the cell-to-cell contact inhibition stimuli and proliferated beyond the confluence point. The LSIL-like cell lines, however, were not able to grow well beyond the usual confluence point, and generated a low number of cells than HSIL cells grown for the same time.

In this study the phenotypical characteristics of the HSIL-like and LSIL-like cells were investigated (in particular at the early phases of cell proliferation in monolayer) as in this phase the cells have space to proliferate as would occur during the proliferative phase of wound healing.

In order to understand the dynamics of infected cells during wound healing, we considered low-density monolayer culture as a model to measure the proliferation rate of cells that have limited contact with their neighbouring cells.

These conditions are similar to those expected during the proliferative phase of wound healing.

We considered the 72 hour time frame following cell plating to be important to understand whether the HPV16 genome contained in the NIKS cells is able to give infected cells a proliferative advantage in comparison with NIKS HPV-negative cells.

We aimed to evaluate if LSIL-like and HSIL-like cell lines have a higher growth potential than NIKS HPV-negative cells. In order to compare the growth potentials of LSIL-like, HSIL-like and NIKS cell lines, we seeded the NIKS, the LSIL-like and the HSIL-like cell lines at 1 x 10^5 cells per well in 6-well plates. Each cell line was harvested and counted in triplicate over a 72 hour time course in which the cells maintain a sub-confluent growth density (Figure 3.3B). Both LSIL-like and HSIL-like cell lines maintained a growth advantage over the HPV-negative NIKS. This was expected since the viral oncogenes lead to higher levels of proliferation. At the end of the 72 hours LSIL-like and HSIL-like cell lines reached a similar cell numbers. We reported no significant difference in the growth rate between the two NIKS-HPV16 cell lines in the 72 hours following cell plating. This is interesting because, in absence of cell-to-cell contact, the proliferation rate of LSIL-like and HSIL-like cells was consistently comparable (Figure 3.3B).

Furthermore, we considered the possibility that the presence of the HPV16 genome enhanced the cell cycling pace, often referred to as doubling time.

The study of the doubling time, which considers the number of replicating cells during the 24 hours post-seeding, demonstrated that cells containing the viral

genome were cycling considerably faster than NIKS HPV-negative cells (Figure 3.3C).

Interestingly we noticed that, although the LSIL-like cells presented an enhanced cycling speed during the initial 24 hours, proliferating at a similar rate to the HSIL-like cells, they retained their characteristic phenotype (growth beyond confluence point) at later stages of proliferation.

We further speculate that this might be the case for the low-risk HPV infection, as it is thought that the early E6 and E7 genes from these HPV types do not confer growth advantages to the infected cells (Roman, 2006).

The analysis of the genome copy number maintenance and the putative influence that growth factors have on viral oncogenes expression will be considered in the following chapters.

Figure 3.3. Growth characteristics of LSIL and HSIL HPV-16 cell lines. (A) Monolayer cultures of LSIL and HSIL cell lines were counted in triplicate over seven day time frame. The mean total cell numbers from triplicate counts for each cell line were plotted against days of growth. (B) Monolayer cultures of LSIL and HSIL cell lines were counted in triplicate over 72 hour time frame. The mean total cell numbers from triplicate counts for each cell line were plotted against the time points of growth. The error bars represent the standard deviation of the triplicate counts. (C) The doubling time was estimated in hour units for each cell line during the 24 hours following cell plating. Six measurements were taken for each cell lines from two independent experiments and the results were averaged. The absolute mean, maximum, and minimum values are shown in the table below the chart. The error bars represent the standard deviation of the triplicate counts. There was significant difference between NIKS-HPV16 (H-SIL and L-SIL) and NIKS ($p < 0.05$). The experiment was repeated three times.

A

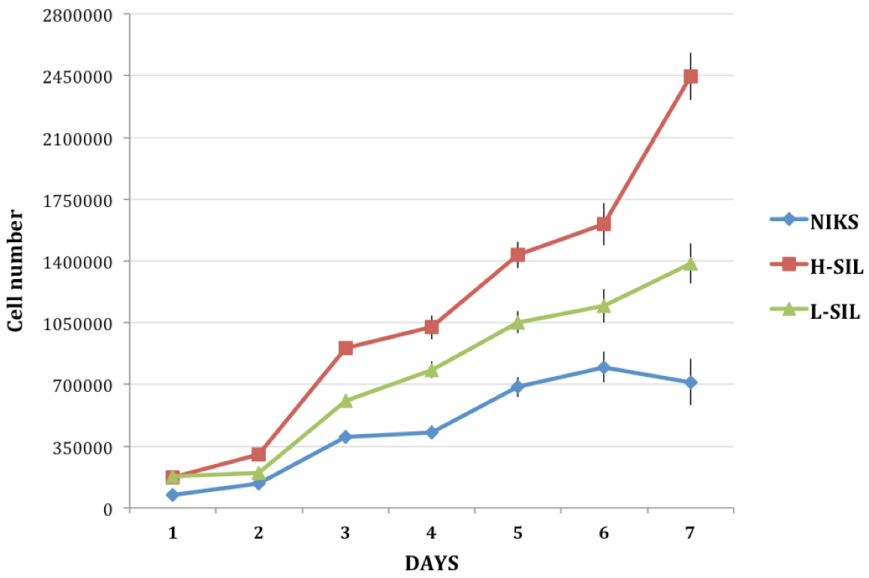

B

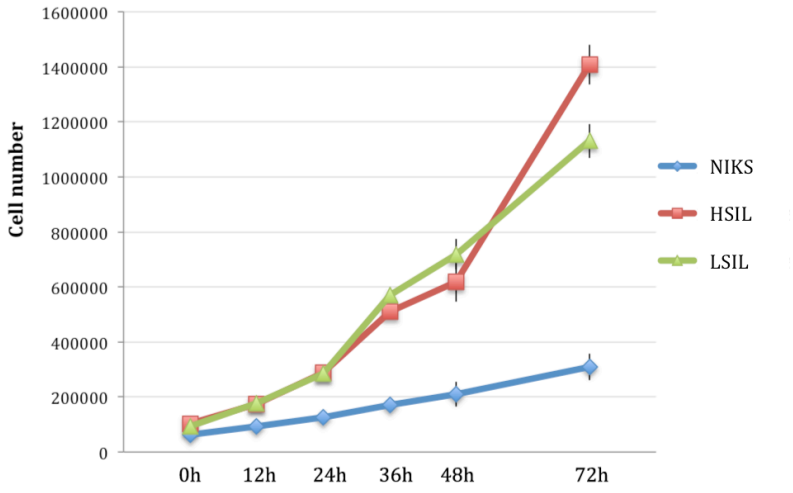

C

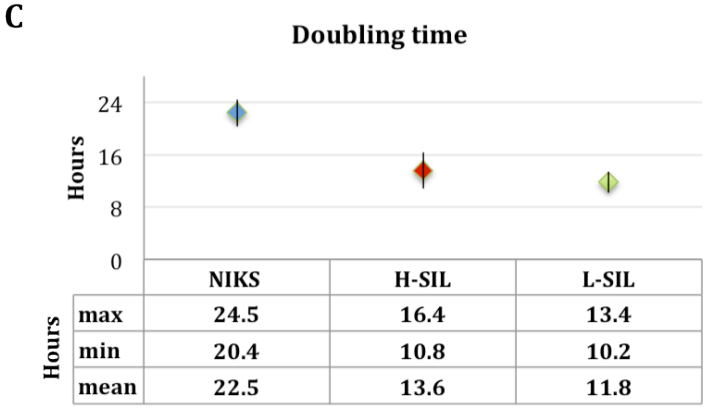

Hours	NIKS	H-SIL	L-SIL
max	24.5	16.4	13.4
min	20.4	10.8	10.2
mean	22.5	13.6	11.8

3.3. Cellular p53 and pRb expression levels are reduced in both LSIL-like and HSIL-like cell lines cultured in monolayer

So far I have shown that the LSIL-like and the HSIL-like cell lines have increased proliferation rates compared to NIKS HPV-negative cells. A molecular explanation for this phenomenon is that the E6 and E7 proteins expressed in these NIKS HPV16 clones act on cellular pathways. The main E6 and E7 cellular targets are the p53 and the pRb proteins respectively. E7 can bind to Rb protein and induce its degradation (Gonzalez et al., 2001; Munger et al., 1989). Such process is important as the Rb protein allows for the transcription factor E2F to remain in an active state as the binding of Rb to the E2F-2 peptide conceals several conserved residues that are crucial for transcription activation of E2F (Lee et al., 2002a). This promotes entry into S-phase from G1. It is thought that that E7 expression can lead to Rb protein degradation, activation of E2F, which then increases cellular proteins such as MCM-7, which are involved in cell proliferation.

Another cellular protein marker that is altered after HPV infection is the tumour suppressor protein p53. In fact, the continuous Rb protein degradation and MCM-7 induction by viral E7 in cells expressing only E7 results in the up-regulation of p53 levels (Demers et al., 1994; Laurson et al., 2010).

The main role of p53 is to play as a G1 to S-phase checkpoint protein (Agarwal et al., 1995). This prevents the cell from proceeding through S-phase. In a separate pathway, p53 can also encourage cellular apoptosis (Demers et al., 1994; Ozaki and Nakagawara, 2011). Furthermore, activation of p53-mediated transcription is a critical cellular response to DNA damage (Lakin and Jackson, 1999). p53

stability and site-specific DNA-binding activity and, therefore, transcriptional activity, are modulated by post-translational modifications including phosphorylation and acetylation (Sakaguchi K. et al., 1998) .

HR-HPVs have evolved to exploit these pathways and to counteract the p53 functions. These viruses have, in fact, developed a way to degrade p53 by the action of protein E6. This happens through the ubiquitination and proteosomal degradation of p53 (Scheffner et al., 1993).

According to the described biological functions, p53 and Rb loss have been used as surrogate markers for E6 and E7, respectively. However, due to their interdependent relationship, it is not certain whether the levels of the p53 protein and pRb degradation exactly correlate with the levels of the E6 and E7 proteins. Taking this into consideration, we anticipate that NIKS-HPV16 cells, actively expressing E6 and E7 proteins, have reduced expression levels compared to p53 and pRb seen in the parental NIKS line. Such a relationship was also supported in my previous studies using the NIKS-HPV16 systems (Isaacson Wechsler et al., 2012).

In order to evaluate whether the LSIL and HSIL cell lines express viral oncogenes from the very early stages following cell plating, a western blot analysis of p53, pRb and GAPDH was performed on lysates obtained from cells harvested on day: one, three, five, six and seven, from cells cultured in monolayer (Figure 3.4A).

Furthermore, we used anti HPV16-E7 specific antibodies on the same cell lysates in order to compare the levels of expression of pRb to the levels of E7 protein (figure 3.4B).

The western blot analysis showed that in both LSIL and HSIL cell lines p53 and pRb were undetectable indicating their effective degradation for all the time points analysed (Figure 3.4A). NIKS HPV-negative cells were used alongside as positive controls, and presented visible bands at all stages. The expression levels of the p53 and pRb proteins in NIKS HPV-negative cells were considered physiological and the differences in expression found in the NIKS-HPV16 transfected cells were then implicated in the expression of the oncogenes E6 and E7. Specific antibodies against GAPDH were used as loading control (Figure 3.4A). E7 expression was investigated using HPV16-E7 specific antibodies and it was found to be persistent in all lysates (Figure 3.4B). The analysis of the early phases of cell proliferation (day 1 to 3) showed an increase in the expression level of the E7 protein in both LSIL-like and HSIL-like cell lines. However, as the expression levels of the Rb protein was drastically reduced in the analysed cell lysates, we concluded that the E7 expression level could not be correlated precisely with the expression of pRb.

Although previous investigations employed successfully E6 antibodies on NIKS-HPV16 cell extracts (Isaacson Wechsler et al., 2012), in the recent time the levels of E6 expression could not be further investigated as effective anti HPV-16 E6 antibodies showed irregular reliability. Nonetheless, we conclude that the drastically reduced p53 levels in LSIL-like and HSIL-like cell lines were likely caused by the action of the viral E6 protein.

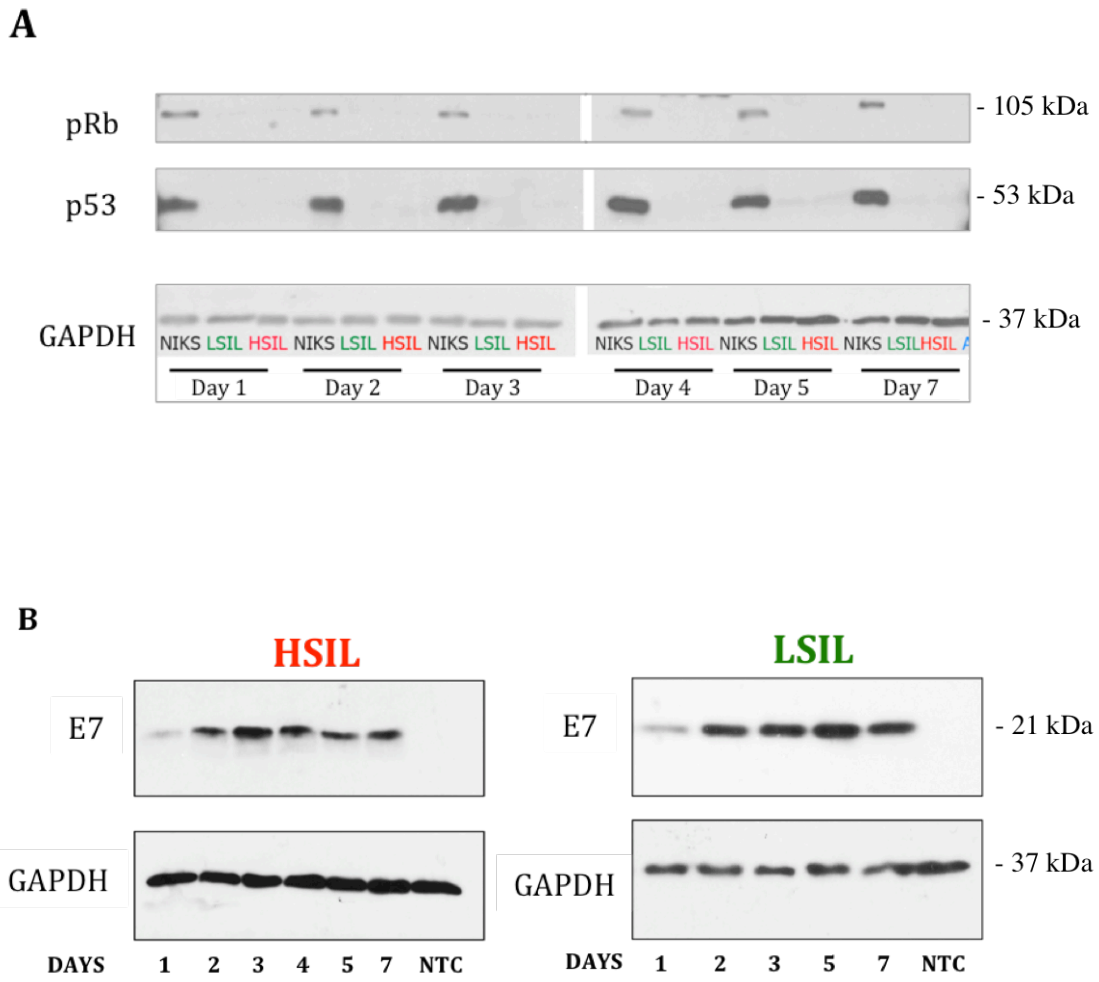

Figure 3.4. Western blot analysis of p53, pRb and E7 proteins in HSIL-like and LSIL-like cells. (A) Cell Lysates of NIKS and NIKS-HPV16 cell lines (HSIL and LSIL) were collected at day 1, 2, 3, 5 and 7 after plating and the levels of p53 and pRb proteins determined by western blotting. The expression levels of p53 and pRb in NIKS lysates were used as comparative control. GAPDH was used as loading control. (B) Cell lysates of HSIL-like and LSIL-like cells were also used to determine the expression levels of the E7 protein. NIKS lysates were used as negative control and GAPDH as protein loading control.

In summary, the data suggest that the continuous expression of E6 and E7 allowed the reduction of both p53 and pRb proteins in both cell lines. The result of the expression of viral oncogenes, contributed to the phenotypic change and to the consequential increase of the observed proliferation rate (Untersperger C. PhD Thesis, 2013). The expression of these genes might thus confer to the HR HPVs infected cell an obvious growth advantage in a competitive environment immediately post infection. My aim is to further understand these characteristics by artificially recreating competitive-like conditions, such as occurs in the wound healing-like proliferative environment. Additional aim was to investigate whether exogenous growth factors contribute to the proliferation rate of infected cells facilitating the formation of HPVs caused lesions.

3.4 The NIKS-HPV16 genome-containing cells, HSIL and LSIL, express their oncogenes from an episomal form of the HPV16.

E6 and E7 viral integrants versus intact 8kb episome have been detected in the majority of HPV-related cancers and also in about 15% of pre-cancerous HPV-induced high-grade lesions (Klaes et al., 1999). In addition, the expression of E6 and E7, following integration, can lead to chromosomal abnormalities, pushing cells towards transformation. Thus, in order to simulate a post-infection/basal-like environment we preferred to perform the experiments exclusively using cells that did not contain viral integrant.

A specific molecular assay, the Amplification of Papillomavirus Oncogene Transcripts (APOT), was used to determine whether our cells contained episomal genomes or oncogene integrants.

This method has been successfully used in the past to understand if E7 transcripts were produced from episomal or integrated forms of the viral genome (Klaes et al., 1999). Results from studies using the APOT method surprisingly show that the majority of HPV-induced high-grade lesions contain E7 transcripts that are produced only from the episomal form of the virus (Klaes et al., 1999; Wentzensen et al., 2002).

The viral integration within the host genome is thought to happen in later stages of neoplastic progression and there is little evidence that integrants are present in the early stages of lesion formation. A recent study using the APOT method, in fact, identified that in 85% of HSIL classified lesions, E7 transcripts were produced from episomal virus forms only (Klaes et al., 1999). In contrast, E7 transcripts were produced predominantly from integrated viral genomes in the majority of in-*situ* carcinomas. Therefore it is recognized that the integration of E6 and E7 is likely to be a later event in the pathological process, and even more importantly in the final stages of cancer development.

Previous investigations in our laboratory using NIKS cells transfected with the HPV16 genome showed that they contained predominantly episomal forms of the HPV16 virus. However, to confirm the validity of our model system it was necessary to show that these episomal lines maintain their integrity when passaged in culture. We performed the APOT assay to understand whether the E7 expression came from episomal or integrated forms of the virus.

The APOT method specifically involves RT-PCR analysis of two primer sets, which are specific for the E7 ORF and the early viral poly-A region, which lies

downstream of E7. In this method, if E7 transcripts are created from a non-disrupted episomal form of the HPV-16 genome, these primers will amplify a single 1.1 kb cDNA fragment, which contains part of the E4 ORF. However, if E7 transcripts are created from integrated transcripts, the E4 ORF fragment is typically deleted, and a series of assorted E7 fragments are generated (Klaes et al., 1999).

To perform the APOT experiment we used RNA extracts from sub-confluent cultures of each NIKS-HPV16 cell line. The APOT procedure resulted in the generation of a single 1.1 Kb band for all three LSIL and HSIL clones (Figure 3.5A). We used a NIKS-HPV16 clone (Int.) as positive 'integrant' control sample of which APOT products were compared alongside the NIKS-HPV16 cell lines. The integrant NIKS-HPV16 clone was prepared by culturing the cells for over thirty passages. NIKS-HPV16 negative cells were also used as APOT negative control. Southern blot using specific oligo-primers to detect E4 and E7 were used to confirm that the sequences amplified contained both genes, when amplification occurred from episomal genomes (Figure 3.5B). In contrast, the lack of E4 in the integrant sample confirmed the validity of the method.

These results confirm that E7 transcripts are produced from episomal forms of the HPV-16 genome in both LSIL-like and HSIL-like cell lines. This also suggests that differences in promoter activity, early viral gene expression and differences in episomal copy number, rather than E6 and E7 integration, may be important to determine the cell phenotype in later stages of neoplastic progression.

Figure 3.5. APOT analysis of the viral transcripts from HPV-16 monolayer cell lines (A) The agarose gel shows single amplified 1.1 kb PCR products containing E7 and partially E4, in all LSIL and HSIL cell lines, which indicates that E7 transcripts have come from an intact episome. For the DNA marker (M) the size of two bands is shown. Amplified cDNA obtained from mRNA extracted from cells containing integrated sequences of HPV16 genome was used as internal 'positive' control. This integrated control (Int.) contains several amplified bands, which represent E7 transcripts that are produced from several E7 integration sites in the host genome. HPV-negative NIKS (N-) were used as a negative control. All tested HPV-16 cell lines show only the 1.1kb amplification product indicative of episomal forms of the viral genome. (B) Agarose gel of PCR amplified products was blotted against specific oligo-probes for E7 and E4. The Southern blot analysis showed that all amplified sequences were positive to E7 probes, but evidenced the presence of E4 transcripts in the 1.1 kb PCR product only. E7 transcripts generated from integrants (Int.) were negative for E4 confirming that the E4 gene was deleted upon integration.

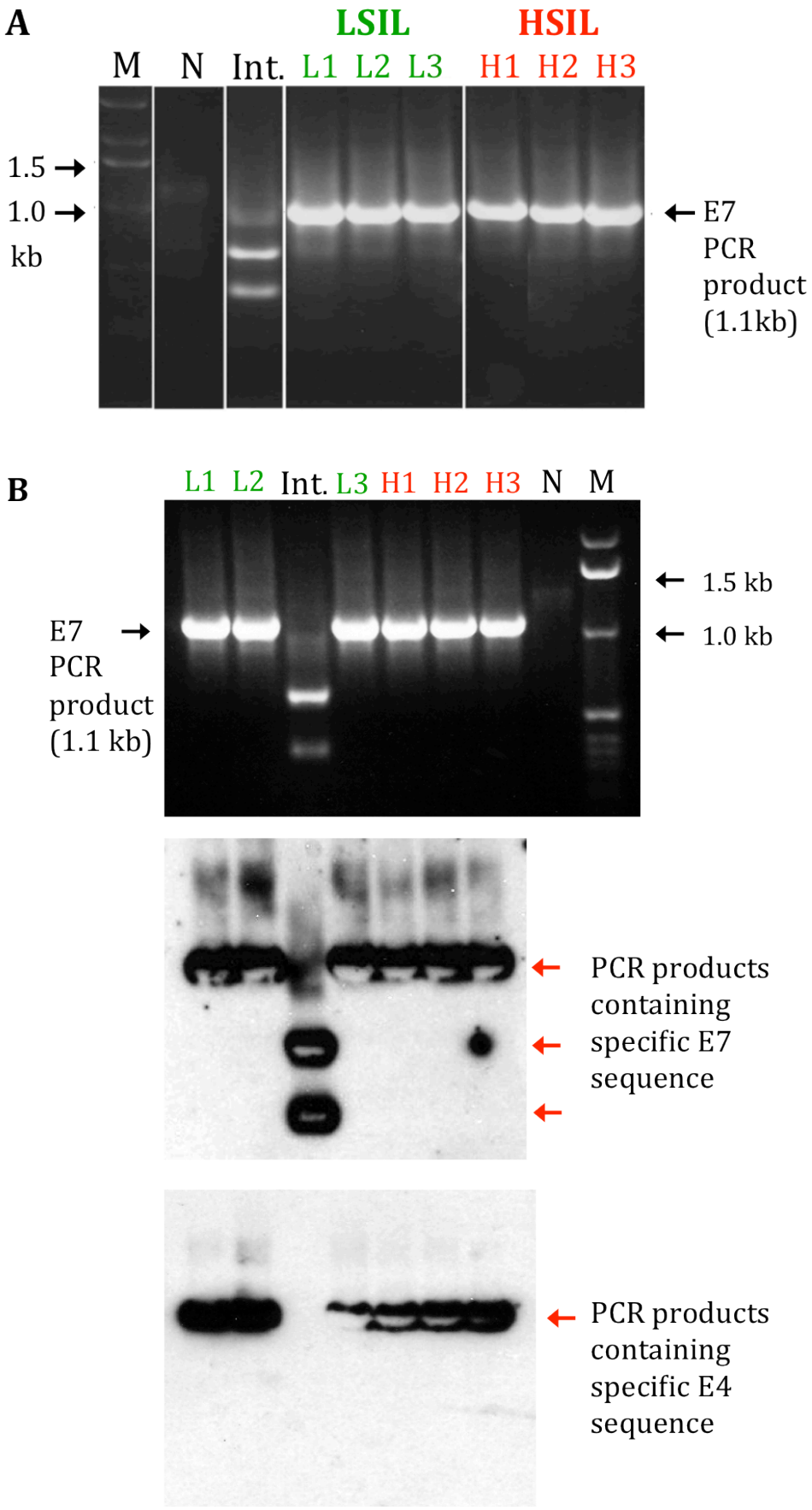
A
LSIL
HSIL
M
N
Int.
L1
L2
L3
H1
H2
H3
1.5
1.0
kb
E7
PCR
product
(1.1kb)
B
L1
L2
Int.
L3
H1
H2
H3
N
M
E7
PCR
product
(1.1 kb)
1.5 kb
1.0 kb
PCR products
containing
specific E7
sequence
PCR products
containing
specific E4
sequence

3.5 NIKS-HPV16 cells lines cultured in monolayers at 'low-density' resemble the differentiation state of epithelial basal cells.

The wound healing like environment that I aim to recreate *in vitro* depends on the presence of monolayer cells that have the characteristics of basal cells upon plating, including the possibility to proliferate and migrate as happens during the wound healing process. In order to recreate such conditions, the NIKS cells used must be able to grow and be maintained in an undifferentiated steady state, at least until the space between cells has been filled.

As mentioned earlier, NIKS-HPV16 cell lines were used to recreate *in vitro* a system able to support a productive HPV infection, similar to the cervical/mucosal epithelium during infection. In fact, as the activation of the viral late promoter is linked to the terminal differentiation program, it was important to show that our cutaneous NIKS model could follow a differentiation program that was similar to the one of cervical/mucosal epithelium. Although some architectural differences exist in cutaneous and mucosal epithelium, the overall process of terminal differentiation is a highly conserved process between these tissue types (Fuchs, 1990), and similar patterns were reproduced in NIKS cells (Isaacson Wechsler et al., 2012; Middleton et al., 2003). Our scope was to confirm that NIKS-HPV16 cells cultured in monolayer show only limited differentiation, which is comparable with what is seen in the basal compartment of the normal epithelium.

Two main strategies exist that can be useful for the study of the differentiation-dependent life cycle of HPV using *in vitro* cultures of NIKS cells. The first method,

known as organotypic raft culture (Figure 3.2) (Isaacson Wechsler et al., 2012; Middleton et al., 2003), is used to induce terminal differentiation of keratinocytes epithelium and involves the production of a three-dimensional epidermis. Such organotypic raft can support the entire life cycle of several viruses (Lambert et al., 2005; Nakahara et al., 2005; Wilson and Laimins, 2005). The other method is a modification of the standard monolayer culture approach. The differentiation of cells cultured in monolayer can be triggered by cell-to-cell contact signals, for example when the cell density is too high and the cells remain confluent for a significant period of time (Studzinski, 2007).

In order to examine the extent to which monolayer cells have characteristics of the basal epithelium, we used specific antibodies targeted against proteins expressed during early keratinocyte differentiation, including Keratin-10 (K10), which is the first keratin to be produced at initial stages of terminal differentiation in cutaneous epithelia (Eckert et al., 1997). In normal cutaneous tissue, K10 is first detected in cells immediately above the basal layer (i.e. parabasal and. spinous layer). Although K10 is actively expressed only in the parabasal and spinous layers, it can still be detected in its cross-linked forms throughout the granular and cornified layers.

Previous studies using raft systems showed that basal-like cells did not stain for K10 antibodies, as expected given the undifferentiated status (Isaacson Wechsler et al., 2012; Middleton et al., 2003) (Figure 3.6).

In cultured keratinocytes K10 antibodies were used to establish extent of differentiation (Figure 3.7a; 3.7b).

The experiment was carried out using glass cover-slips onto which fibroblasts had been previously seeded. Once the fibroblasts were completely attached to the wells, NIKS-HPV16 LSIL and HSIL cells were plated at very low density in order to allow the cells to proliferate for few days prior to reaching a confluent state. The glass cover-slips were removed and fixed at seeding point (Day 0), and at Day 1, 2, 3, 5 and 7. Immuno-staining with specific antibodies showed that, in both cells lines, the percentage of K10 positive cells was consistently below 5% from Day 1 to Day 5 (Figure 3.7a; 3.7b). Interestingly, on Day 0, 7.4% of the keratinocytes on the HSIL cover slips and 5.1% of the keratinocytes on the LSIL cover slips were found to be positive for K10, which may be the result of differentiated cells being carried over from the previous culture passage.

Consequently, we conclude that cells cultured in monolayer show limited differentiation under the conditions used here, and in this respect resemble the basal cells of normal and infected epithelium.

The comparison between the two cell lines showed that there were no significant differences in K10 expression at any of the time points considered (Table 3).

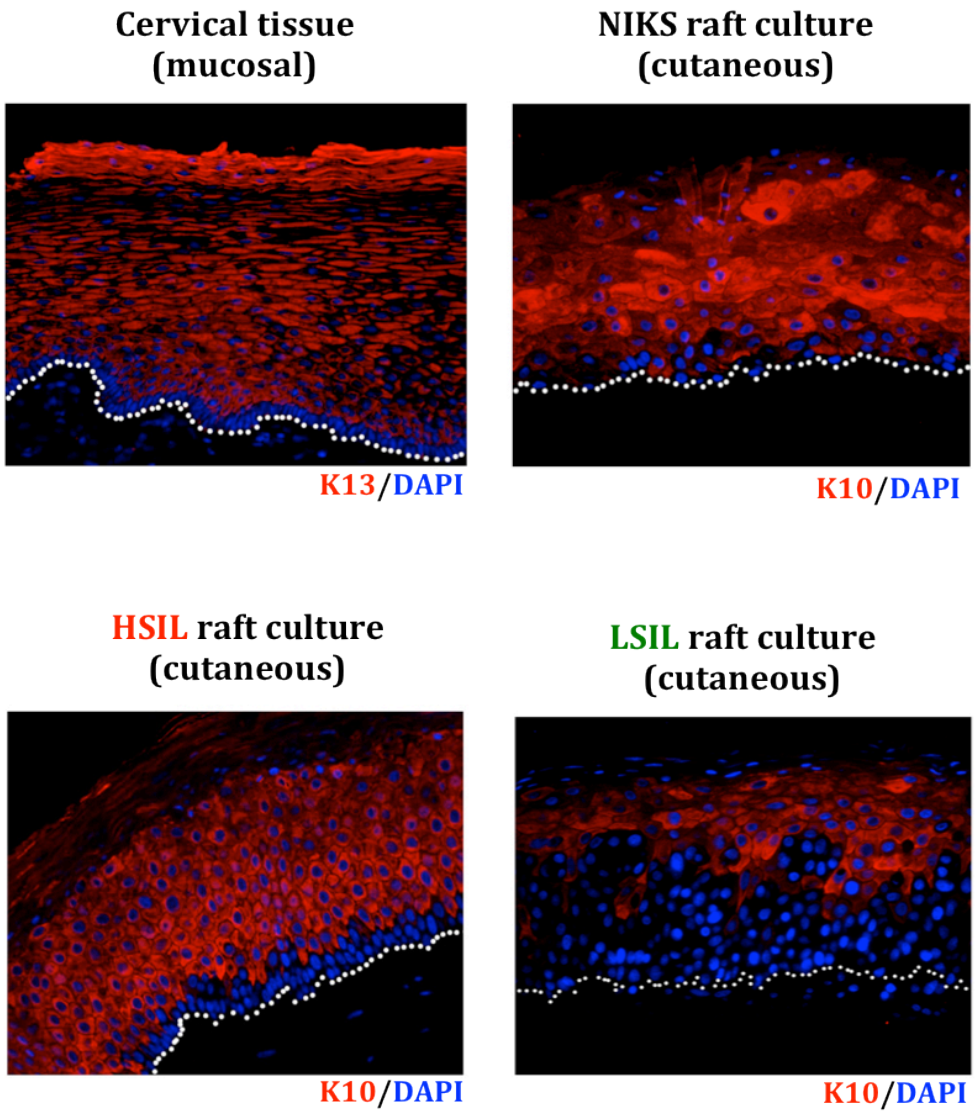

Figure 3.6 Expression of K10 and K13 protein in raft cultures and HPV16-positive cervical tissue. Raft culture obtained from NIKS, NIKS-HPV16 HSIL and LSIL clones were stained using K10 (Red) antibodies to show the extent of the cell early differentiation. A section of HPV16 positive cervical tissue was stained with the differentiation marker K13 (Red) antibody and used for comparison. All sections were counterstained with DAPI (Blue) and images were acquired digitally at x20 magnification. The dotted lines indicate the location of the basement membrane. The immoistochemistry of the cervical tissue and raft cultures were carried out by Kate Middleton and Erin Isaacson (NIMR, London) respectively and used with permission.

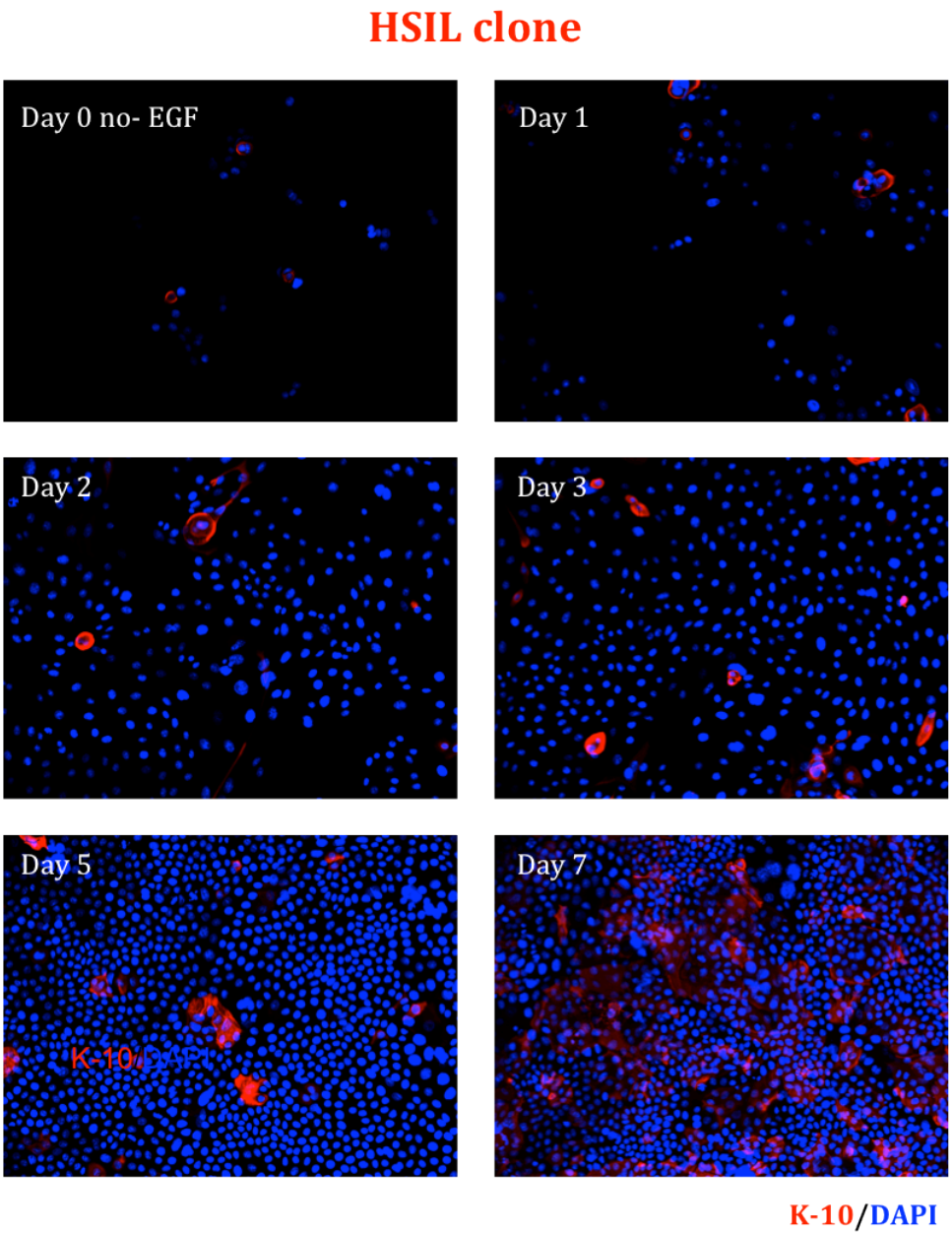

Figure 3.7a. Differentiation state analysis of keratinocytes cultured in monolayer. NIKS-HPV16 HSIL and LSIL cell lines were seeded at low density in on cover slips, cultured in standard medium for up to seven days and stained at each time point with anti-keratin 10 specific antibodies (red). DAPI staining (blue) was used to help localize cell nuclei. Fluorescent light images were acquired digitally at 10x magnification.

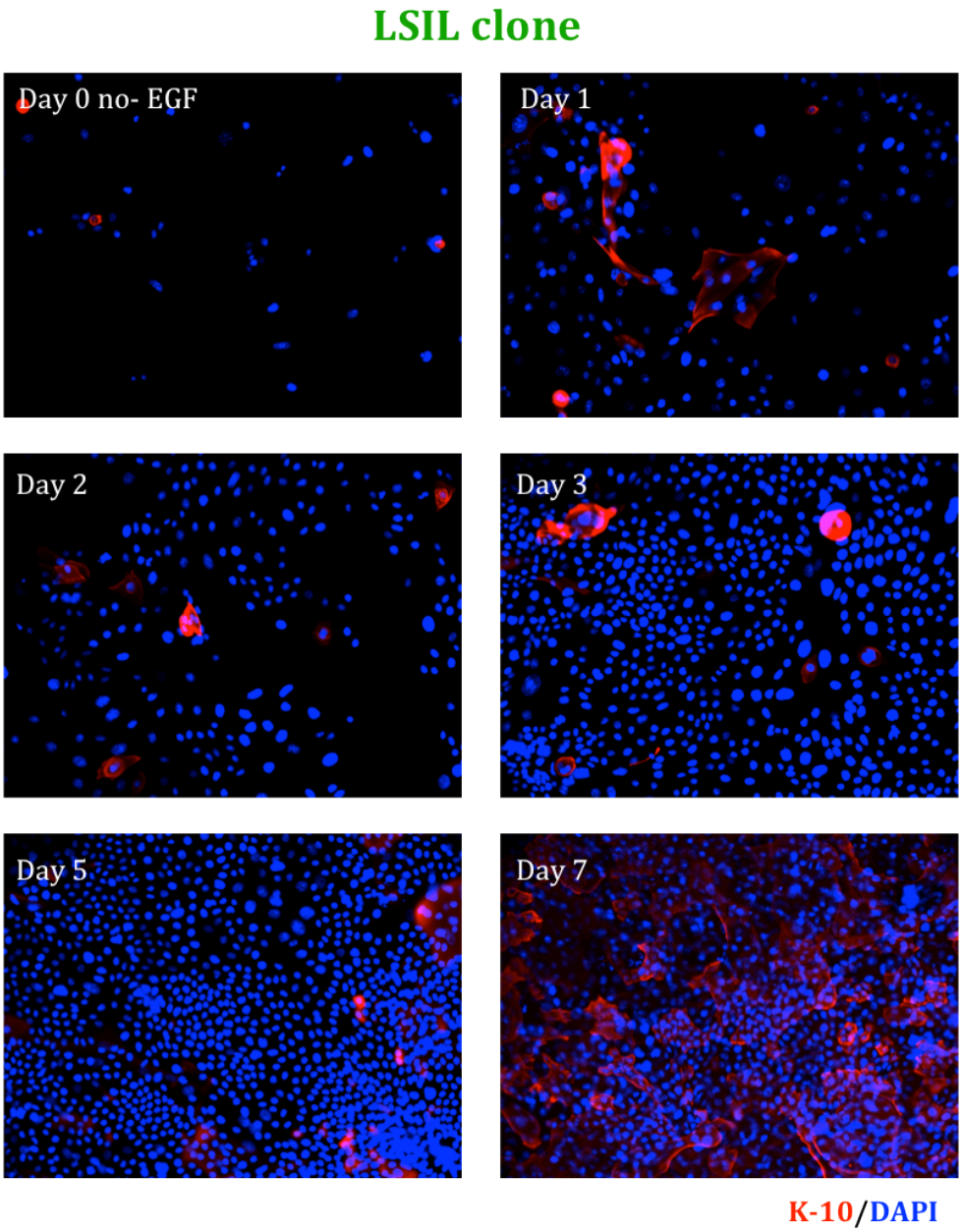

Figure 3.7b. Differentiation state analysis of keratinocytes cultured in monolayer. NIKS-HPV16 HSIL and LSIL cell lines were seeded at low density on cover-slips, cultured in standard medium for up to seven days and and stained at each time point with anti-keratin 10 specific antibodies (red). DAPI staining (blue) was used to help localize cell nuclei. Fluorescent light images were acquired digitally at 10x magnification.

Table 3.1. Image-J analysis of K10 positive cells. Image-j software was used to count the number of DAPI (blue) and K10 (red) positive cells present at each time point. The number of K10 positive cells is represented as percentage of the total number of keratinocytes staining positive for DAPI. Counting has been performed from three independent cover slips for each time point considered. The experiment was repeated three times.

	Day 0	Day 1	Day 2	Day 3	Day 5	Day 7
LSIL	6/117 (5.1%)	14/451 (3.1%)	17/654 (2.6%)	24/1827 (1.3%)	78/2568 (3.0%)	n.a./4944 (≥10%)
HSIL	9/121 (7.4%)	12/276 (4.3%)	24/822 (2.9%)	37/1347 (2.7%)	84/3198 (2.6%)	n.a./5475 (≥10%)

3.6 Cloned NIKS cells have a consistent expression of p53 and pRb expression.

Previous studies have indicated that NIKS are genetically stable and have a uniform genetic background. This was important for our experiments, as we wanted to avoid genetic variation in the cell population within our HPV cell lines. Moreover, in order to investigate the effects that exogenous growth factors have on transfected cells, it was fundamental to confirm that NIKS have no variation within their populations. NIKS are near-diploid human keratinocytes containing a stable isochromosome, 8q, which it is not known to affect the expression of p53 and pRb (Allen-Hoffmann et al., 2000). The NIKS used in our experiments were produced from a parental neonatal foreskin cell line that, after 59 culture

passages, immortalized spontaneously (Allen-Hoffmann et al., 2000). Despite the fact that foreskin keratinocytes can be a natural host cell for HPV viruses, the authors confirmed there were no detectable levels of HPV DNA. They also confirmed that the growth characteristics of NIKS cells were consistent between each passage. To further investigate this, the authors measured the mRNA levels of autocrine growth factors and markers such as Transforming growth factor (TGF), TGF-ß1 (a keratinocyte growth inhibitor), Epidermal growth factor (EGF), the oncogene c-myc and keratin K14. Their results confirmed that there were no differences in the expression levels of these growth factors and markers when compared to the parental cell line (Allen-Hoffmann et al., 2000). NIKS have also been shown to be non-tumorigenic when injected into mice, which suggests that they are not a transformed cell line. More recently, NIKS cells have been used as dermo-epidermal skin substitutes in subjects affected by serious burns (GIbson, 2007; Schurr et al., 2009).

The analysis of NIKS clones aimed to verify that any fluctuation between NIKS-HPV16 clones in the way they affect the expression of p53 and pRb expression was associated primarily to HPV16 E6 and E7 and not dependent by the NIKS cell background.

Preliminary studies on HPV16-LSIL and HPV16-HSIL clones protein extract have demonstrated that p53 and pRb levels may vary between clones (Figure 3.8A). Upon several culture passages, however, these differences appear less evident as shown previously in Figure 3.4. We hypothesise that the selective pressure on cells in culture might be the cause of the loss of p53 and pRb expression over time.

Thus, in order to determine that NIKS expressed similar levels of p53 and pRb, which are the main targets of the viral oncogenes E6 and E7, we developed a specific cloning assay. To do this fifty NIKS clones were isolated from the NIKS population. NIKS cells were plated at low density so that the colonies generated from single cells were able to outgrow and be harvested as soon as they became visible. Clones obtained using this method were then transferred to independent plates and grown five days. Twenty-five NIKS clones obtained with this method were unable to survive after plating. Fifteen out of 25 clones were grown to 60-70% confluence before being harvested and stored as cell pellets. The pellets obtained were used to carry out western blot analysis (Figure 3.8B). The latter was performed using specific antibodies against p53 and pRb, and revealed that only minimal differences in their expression levels were found between clones (Figure 3.8B). This experiment demonstrated that the NIKS background, in terms of p53 and pRb expression, was essentially comparable in all clones analyzed. The effects of E6 and E7 on p53 and pRb respectively, can be related to a variation in oncogene expression within the NIKS-HPV16 population and was not dependent on internal variations between individual cells that lead to the NIKS cell clones. Furthermore, these assays validated the use of NIKS cells to build a model system for comparative analysis of multiple HPV types.

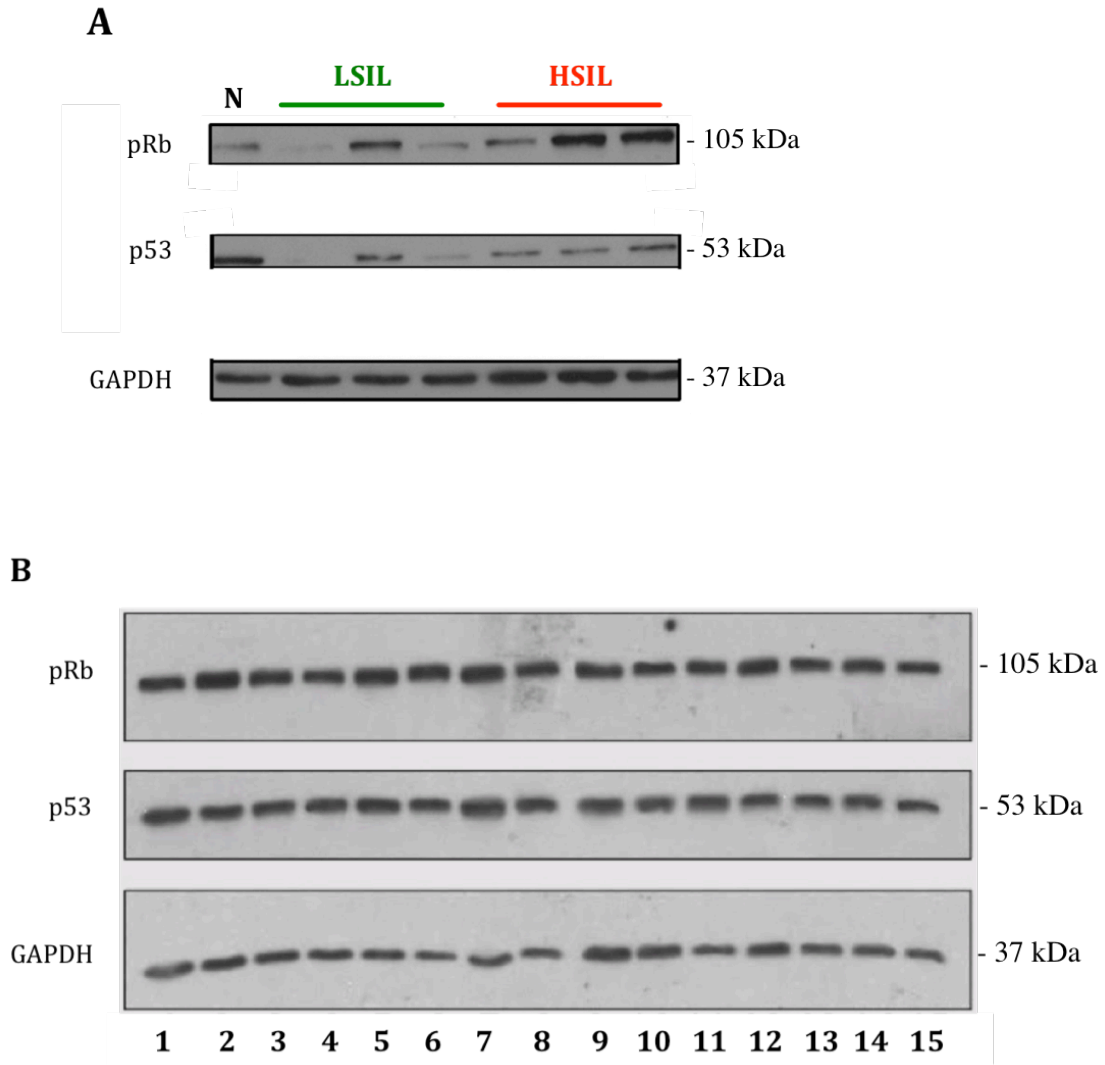

Figure 3.8. The NIKS cloning assay studies variation amongst NIKS cells population prior to HPVs genome transfection. (A) Western blot analysis of pRb and p53 protein expression in HPV16-HSIL, HPV16-LSIL clones and NIKS (N). (B) Western blot analysis of the pRb, p53 obtained from protein extracts of 15 NIKS parental clones. GAPDH expression was used to determine the loading control.

3.7 Discussion

The main focus of this Chapter was to carry out a detailed analysis of the NIKS and NIKS-HPV16 cells cultured in monolayer in order to verify their suitability for the study of wound healing *in vitro*.

In particular, we describe an analysis of the cell line background that we are using in our *in vitro* model system. We confirmed that NIKS-HPV16 HSIL and LSIL cell lines were producing a cell phenotype distinct from that of NIKS cells when propagated in monolayer culture (Figure 3.1). Moreover, we show the ability of cells containing HPV16 genome to proliferate faster than NIKS. Although HSIL and LSIL cell lines produce a different phenotype when propagated in monolayer cultures (Isaacson et al 2012), we now show that these lines are indistinguishable in the early stages of monolayer proliferation. However, the difference between NIKS and NIKS-HPV16 cells doubling time was significant. These results suggest that HPV16 genome containing cells might have a competitive advantage against cells not containing the virus.

Following the study of the growth characteristics of the NIKS-HPV16 HSIL and LSIL cell lines we were intrigued by the possibility that the viral oncogene expression may vary during the early stages of cell proliferation. We, in fact, hypothesized that in NIKS-HPV16 HSIL and LSIL cell lines, changes in oncogene expression levels may explain the different cell phenotype at later stages (Figure 3.3). Thus, to determine whether the viral oncogenes in these cell lines were functional we analysed the levels of the host p53 and pRb proteins, which are the host cellular targets of the HPV16 E6 and E7 proteins. Interestingly, we noticed

from data presented here (and from data presented by Isaacson 2012) that the presence of E6 and E7 proteins were related to the loss of p53 and pRb at all stages of the monolayer proliferation (Figure 3.4). We illustrated that in NIKS-HPV16 clones the levels of the viral oncoprotein targets are dramatically reduced. However, we were not able to determine oncogene variations across the NIKS-HPV16 clones analysed. No obvious differences were apparent however between the HSIL and LSIL clones at least at the level of E7 expression. Recent investigations give evidence of the role of HPV16 E7 in the proliferation of HPV16 containing cells. The studies suggest in fact that inhibiting the HPV16 E7 binding to Rb by using mRNA aptamers (small, single- stranded oligonucleotides selected for high-affinity binding), produce an apoptotic effect on cell lines derived from cervical carcinoma (Nicol et al., 2011; Nicol et al., 2013).

Results led us to investigate the expression of viral oncogenes during the first few days after plating where no difference in cell growth was apparent. During this period the E6 and E7 proteins appear to have a role in increasing the cycling speed of the NIKS-HPV16 containing cells. A recent investigation suggests that inhibiting the HPV16 E7 binding to Rb by using mRNA aptamers (small, single-stranded oligonucleotides selected for high-affinity binding), produce an apoptotic effect on cell lines derived from cervical carcinoma (Nicol et al., 2013). This period of growth, when the HPV-containing cells have space to grow, resembles in some ways, the situation that occurs following infection at wound sites.

In order to model the early stages of infection, however, we also need to be certain that the HPV genomes are predominantly episomal.

The modest increase of E7 expression during the early phase of cell proliferation led the study of the integrity of viral genome state. In fact, we needed to understand whether the viral genome expression was promoted by the viral genome integration into the host DNA during the cell proliferation. Therefore, the analysis of the monolayer model system focused on proving that NIKS-HPV16 cell lines were exclusively episomal. We studied several NIKS-HPV16 cell lines and demonstrated that the genome was contained as episomal. Furthermore, by analysing specific sequences of E4 and E7 in the amplified episomal transcripts we confirmed that the viral expression originates exclusively from viral episomes. At present, data in this thesis suggest that the oncogene levels are exclusively regulated from non-integrated viral genes. Thus, we excluded that viral expression coming from viral integrants are responsible of the modest increased in E7 expression during the cell proliferation in monolayer.

This however does not rule out that a level of heterogeneity in the host cell line could also contribute to these phenotypes in individual clonal cell lines. As mentioned earlier, NIKS arose as a spontaneously immortalized cell line with a near diploid genome, and they were shown to be maintained as an isogenic cell line (Allen-Hoffmann et al., 2000). It was then necessary to verify that the parental NIKS is still a homogeneous cell line, and the cells did not acquire further genomic instability over time that might contribute to these phenotypes. We deemed useful to perform the analysis of the NIKS background in terms of the

expression levels of the cellular counterparts of the HPV16 oncoproteins. We found that NIKS clonal cells were steadily expressing p53 and pRb, so we concluded that the NIKS clonal cells are analogous. Thus, we established that NIKS cells were suitable for further studies and transfection within our model.

Although the expression of E6 and E7 genes was consistent in the early state of cell proliferation, we aimed to understand the differentiation state the transfected keratinocytes during monolayer proliferation. We raised the possibility that keratinocyte differentiation might differ between cell lines resulting in altering in the genome amplification and viral gene expression. We confirmed that the differentiation state of the HPV16 cell lines, evidenced by K10 expression, was comparable between the HSIL and LSIL cell lines (Figure 3.7a; 3.7b). Furthermore, we found that the cell differentiation in the early stages of monolayer proliferation was extremely low. These results indicate that, during the first three days, the proliferation of the cell lines in monolayer resembles closely the amplification of the epithelial basal cells in terms of cell differentiation.

4. The use of NIKS monolayer system to study wound healing *in vitro*

4.1 Introduction

Wound healing is a complex process that occurs in timely defined stages and involves many different cell types. It is referred to the repair process starting when the outer covering of the skin, the epidermis or the mucosal epithelia become injured (Singer and Clark, 1999). This highly coordinated physiological process involves inflammation, wound cell proliferation and migration, neovascularization, and regeneration of the extracellular matrix (Martin, 1997). The epidermal keratinocytes are the main cells of the epidermis and they retain a key role in the tissue repair process (Santoro and Gaudino, 2005).

The physical stimuli that result from the loss of cellular continuity trigger a range of tissue responses in order to repair the damage (Shaw TJ, 2009). These are regulated by the local production of peptide growth factors, which influence cells in the wounded area through autocrine and paracrine mechanisms (Shirakata, 2010; Werner and Grose, 2003). Two structurally related peptide growth factors, the EGF and TGF-alpha, play important roles in wound healing of tissues such as the skin, cornea, and gastrointestinal tract (Schultz et al., 1991). Many types of cells including skin keratinocytes, fibroblasts, vascular endothelial cells, and epithelial cells express EGF/TGF-alpha receptors (Santoro and Gaudino, 2005). In addition, several cells involved in wound healing including platelets, keratinocytes, and activated macrophages synthesize growth factors including EGF or TGF-alpha (Schultz et al., 1991). Keratinocyte-derived growth factors as well as cytokines and chemokines also contribute to the regulation of tissue renewal (Shirakata, 2010). The role of EGF has been extensively investigated in normal and pathological wound healing. It is implicated in keratinocyte

migration, fibroblast function and the formation of granulation tissue (Breuing et al., 1997). Several studies have demonstrated that healing of a variety of wounds in animals and patients was enhanced by treatment with EGF or TGF-alpha (Breuing et al., 1997; Brown et al., 1986). Epidermal regeneration of partial thickness burns on pigs or dermatome wounds on patients was accelerated with topical application of EGF or TGF-alpha, and EGF treatment accelerated healing of gastroduodenal ulcers (Breuing et al., 1997; Buckley et al., 1987). EGF also increased tensile strength of skin incisions in rats and corneal incisions in rabbits, cats, and primates (Grant et al., 1992; Kwon et al., 2006)

The mechanisms of the wound healing have been previously studied using both *in vivo* and *in vitro* model systems (Croft and Tarin, 1970; Escamez et al., 2004; Werner and Grose, 2003). The use of animal model systems allows the study of sequential phases of wound repair, from the moment of injury until the repair is accomplished. However, this method has a number of limitations. One of the major limitations in the study of wound healing and HPV *in vivo* is the absence of an animal model system that supports the viral life cycle of HPVs, as the permissive propagation of papillomaviruses outside their natural host is not possible. Several models however, have been described to permit the growth and propagation of HPV in subcutaneous and cutaneous human skin grafts implanted in the severe combined immunodeficiency (SCID) mouse (Bonnez, 2005). However, animal models have been successfully employed to study other types of PVs, such as rabbit oral papillomavirus (ROPV) or cottontail rabbit papillomavirus (CRPV) (Christensen and Kreider, 1991; Maglennon et al., 2011).

Although such model systems are useful for the study of the formation, regression and reappearance of PVs lesions, their use to investigate the initial phases of lesion formation upon establishment of PV infections in the basal epithelia result laborious.

In the recent years, it has been reported that transgenic mouse lines expressing the E6 and E7 oncogenes of HPV16 in the skin have been used for wound healing studies (Escalante-Alcalde et al., 2000). In these experiments, such mice showed a remarkable ability to regenerate an ear portion after a wound was created. Such effects appear to be primarily due to E6 and E7 expression, which plays an active role in re-epithelization and epidermal growth (Davies et al., 1993). In addition, HPV16 oncogenes have also been shown to increase the migratory ability of keratinocytes during wound healing scratch assay (Au Yeung et al., 2011).

In the absence of an animal model system that allows the use of HPV, an alternative *in vitro* epithelial cell culture approach was attempted (Liang CC, 2007). One of the major advantages of using such an *in vitro* approach is that it allows specific aspects or the behavior of 'healing' cells to be examined without the extraneous influences of the body (Bentley, 1936). As HPV infection would in many cases occur in a wounded epithelia, experiments were performed using a monolayer culture system *in vitro* that resemble some of the features of the epithelia healing cells.

By using such a model system, we aimed to study the effect that the expression of HPVs may have on the wound healing process. In particular we make use of the wound healing scratch assay to examine cell colonization potential and make a close comparison between LR- and HR-HPV types.

4.2 NIKS cells harboring HPV16 present a higher proliferative ability in an *in vitro* scratch assay

Wound healing requires both migration and proliferation of many cell types including neutrophils, fibroblasts, endothelial cells, and keratinocytes. During the proliferative phase of wound healing, the keratinocytes respond to growth stimuli generated by fibroblasts and epithelial cells as a result of loss of cell-to-cell contact (Martin, 1997; Santoro and Gaudino, 2005). These stimuli cause re-organization of the keratin network in cells in the wounded epidermis in preparation for their efficient migration (Wojcik et al., 2000). Keratinocyte cell migration is a complex process that involves a coordinated sequence of distinct functions including the formation of lamellipodia protrusions at the leading edge of the cell, formation of cell-substrate adhesion at the tips of lamellipodia, actomyosin-powered contraction of the cell body, and detachment of the cell rear (Kirfel et al., 2004; Sheetz, 1994). Cell migration during wound healing involves also the expression of a number of growth factors and cytokines. One of these factors, the transforming growth factor-beta (TGF-β), controls many aspects of normal and pathological cell behaviour (Joo and Seomun, 2008), including the migration of keratinocytes in wounded skin and epithelial cells in damaged cornea (Philipp et al., 2004).

With regard to wound healing, the specific questions that we aimed to address were: firstly, whether the enhanced proliferation of NIKS-HPV16 might facilitate a more rapid wound repair in a competitive wound environment, and secondly, whether HPV16 'infection' can have a positive impact on the migration of the NIKS infected cells.

Previous investigations have shown that the expression in trophoblastic cells of the HR-HPV E6 and E7 proteins under the control of the long-control region endogenous promoter, in absence of normal E6/E7 regulation, can cause a growth advantage and an increase in motility and invasivity compared to uninfected cells (Boulenouar et al., 2010). Other studies have specifically evaluated HPV16 the E6 protein in enhancing the migration ability of infected keratinocytes (Au Yeung et al., 2011), and when taken together, suggest that the early proteins of HR-HPVs can modulate migration and proliferation.

It remains to be established to what extent these proteins exert this function on infected keratinocytes harboring viral episomes.

In this thesis, the proliferative and migratory properties of human keratinocytes infected with HR-HPVs were considered using an *in vitro* scratch assay. To do this, the NIKS episomal cell lines were used.

The *in vitro* scratch assay is a well-developed method to measure cell migration *in vitro* (Liang CC, 2007), and involves the generation of a "scratch" in a monolayer culture in order to generate the wound-like situation. As a mechanistic level scratching the cell monolayer relieves contact inhibition, and induces surviving cells near the wound edge to move and proliferate. The movement of the cells can then be monitored through a time-lapse microscope by capturing the images at the start of the scratch and at defined intervals as the scratch-area is colonized. The acquired images can then be compared to quantify the cell migration rates.

To perform the scratch assay we have cultured the NIKS and NIKS-HPV16 cells to confluence in order to obtain an even tissue-like monolayer. Once the cells were confluent, they were physically scratched with the use of a pipette tip. The scratches were performed as accurately and consistently as possible in order to create a regular gap size across the various experiments. Scratched plates were washed twice using pre-warmed culture medium in order to remove cell debris and the plates were immediately positioned in a time-lapse microscope equipped with a 37 °C chamber with 5% CO_2 to support cell growth. Two hours from the time when cells were placed on the microscope define the starting point of our measurements (Figure 4.1A). The scratched section images were acquired every fifteen minutes as the scratched area was colonized. Three selected image area for each set of cells were visualized in each experiment, which was replicated three times. To determine how cells were recovering from the scratch we measured the area of the dish unoccupied by cells at each time point using Image-J® software. We averaged the measurements, which describe the ability of the edge cells to proliferate and move towards the empty space created by the scratch and plotted this in a chart (Figure 4.1 B).

The results obtained demonstrate that the NIKS cell lines containing the HPV16 genome are able to recover the artificial wound in a shorter time than the NIKS control cells. We report a significantly different re-epithelization rate at 8 hours from scratch formation, with NIKS-HPV16 cells covering an area three times larger than the area covered by the NIKS in the same time frame. The measurement reveals that the LSIL-like cell line recovers the free cell area in about 16 hours whereas the NIKS cells take up to 24 hours to completely heal the

wound (Figure 4.1B). Interestingly, these data are in accordance with the proliferation rate studies shown in the previous chapter. In fact, the proliferation advantage presented previously in the HSIL-like and LSIL-like cell growth rates (see Chapter 3) appears aligned with the LSIL-like cells ability to recover a scratched area *in vitro*. The HSIL-like NIKS-HPV16 cells were not employed in this study as their proliferation rate resulted comparable with the proliferation rate of LSIL-like NIKSHPV16 cells in the early stage of monolayer proliferation (Section 3.2).

This experiment shows that keratinocyte cell lines containing HPV16 episomes have a 'healing' advantage over the control cells as they recover a scratch in a shorter time.

We hypothesize that in a competitive environment, such as it would be present during wound healing, HR-HPV infected cells gain a growth advantage that allows them to prevail over surrounding 'uninfected' cells.

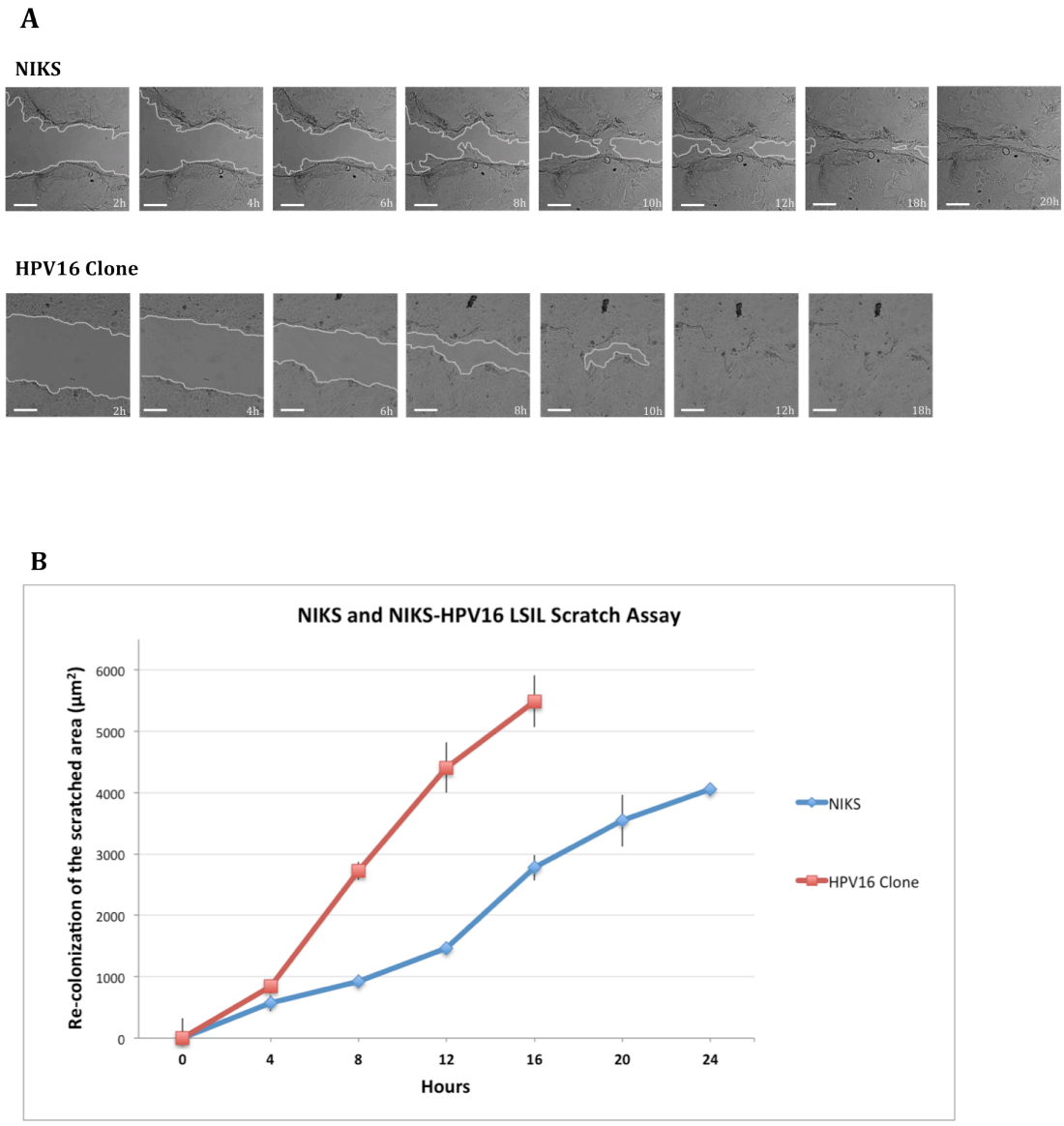

Figure 4.1. Wound healing scratch assay. (A) NIKS and NIKS-HPV16 containing clone (LSIL-like) were grown to confluence in glass bottom dishes and then scratched with a P200 tip. The wound closure was observed using a time-lapse microscope and pictures analyses was carried out using Image J software. The bar sale represent 100 µm. (B) The chart represents the average of twelve measurements of the recovered free cell area of the wounds. The error bars represent the standard deviation of the mean values. The experiment was repeated three times.

4.3 Mitomycin C treatment impede the proliferation of both NIKS and NIKS HPV16 containing cells

The results presented in the previous section support the hypothesis that HPV16 containing cells have a proliferative advantage, which is demonstrated by the increased speed at which the scratch is colonized. Because wounding of the epithelia is necessary for HPV infection at many sites, our results suggest that during the proliferative phase of wound healing, HPV16 infected cells may have the potential to proliferate faster than infected cells in order to colonize the space available around them. During this proliferative phase, keratinocytes are stimulated by growth factors in order to both proliferate and to migrate towards the wounded site. In the experiments described previously (Section 4.2), the migration rate of the keratinocytes could not properly be assessed because both cell proliferation and migration were occurring simultaneously. In order to evaluate the migration ability of the HPV-containing keratinocytes, the proliferation rate must therefore be controlled.

This was achieved by treating NIKS and NIKS-HPV16 cell lines with Mitomycin C. Mitomycin C is a well-established chemotherapeutic agent that is used to block the proliferation of tumour cells. The use of Mitomycin C in a pilot experiment was first required to assess its ability to inhibit NIKS and NIKS-HPV16 cell proliferation. Growth rate experiments were performed in presence of 0.5 ug/mL Mitomycin C and compared with their relative untreated controls (Figure 4.2). The use of this agent in both NIKS and NIKS-HPV16 containing cells showed that the proliferation was impeded. In fact, following Mitomycin C treatment the

average number of cells counted at 24-, 48-, and 72-hours never exceeded the number of cells plated (Figure 4.2 –A, -B).

Moreover, we observed that the use of Mitomycin C did not cause any visible change in the cell morphology suggesting that the drug affected only their mitotic activity.

The ability to selectively stop the proliferation of keratinocytes was subsequently used to assess the migratory activity during the scratch assay.

Figure 4.2. Growth rate analysis +/- Mitomycin C. (A) NIKS cells were cultured in triplicate in monolayer using 6 well plates. Cells were seeded at the same number and stimulated with complete medium and complete medium to which was added 0.5 μg/mL of Mitomycin-C. The blue bars represent the average cell numbers of the untreated cells. The Bars in red represent the average number of cells in the treated samples. The error bars represent the standard deviation of the triplicate values. (B) NIKS-HPV16 cells were used in this experiment as described in (A). The blue bars represent the average cell numbers of the untreated cells. The green bars represent the average number of cells in the Mitomycin C treated samples. The error bars represent the standard deviation of the triplicate values. There was significant difference between the Mitomycin C-treated and untreated samples ($p < 0.05$). The experiment was repeated three times.

A

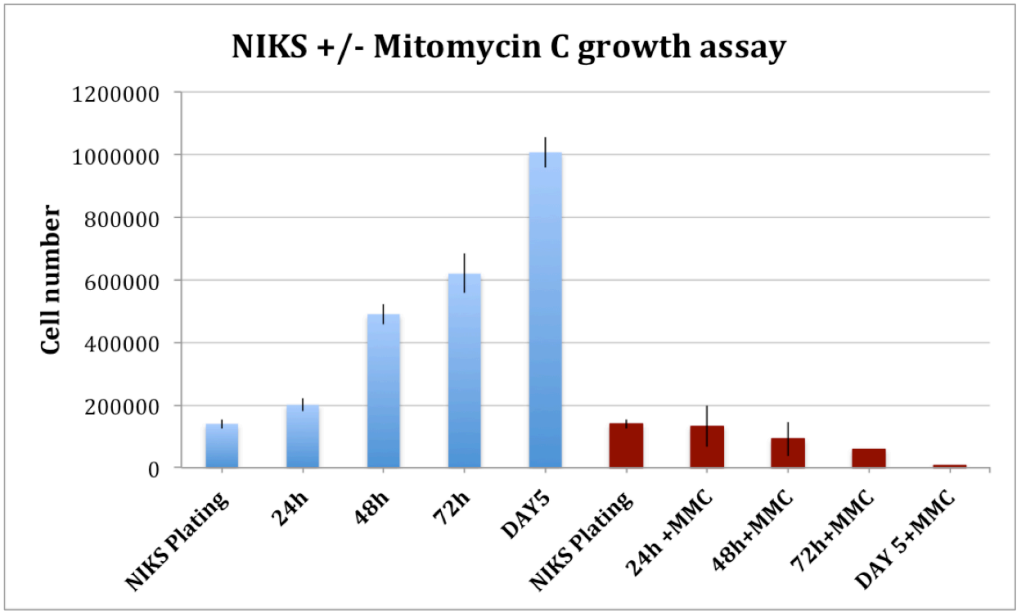
NIKS +/- Mitomycin C growth assay
Cell number
1200000
1000000
800000
600000
400000
200000
0
NIKS Plating
24h
48h
72h
DAY5
NIKS Plating
24h +MMC
48h+MMC
72h+MMC
DAY 5+MMC

B

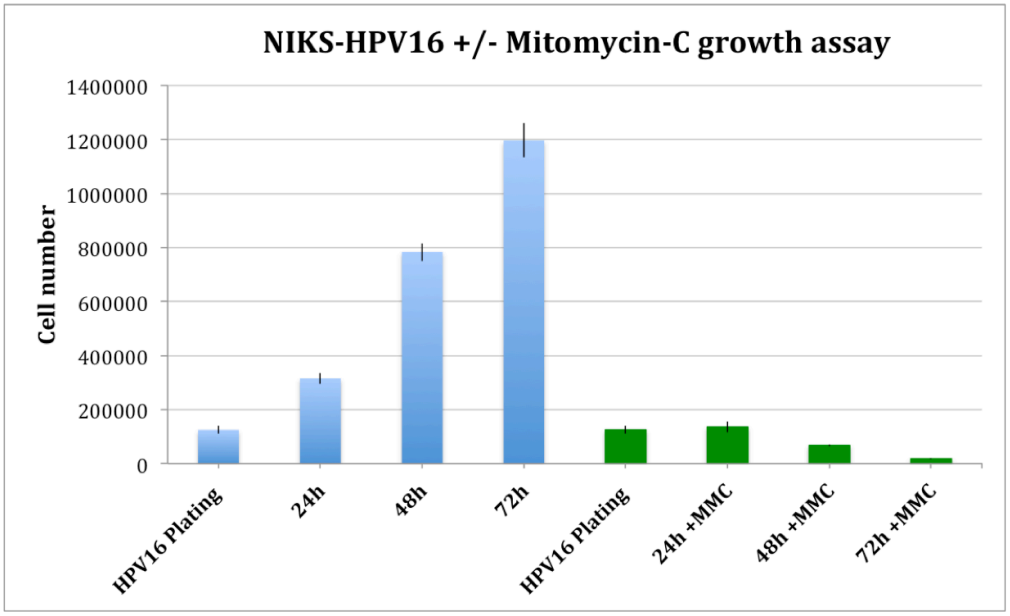
NIKS-HPV16 +/- Mitomycin-C growth assay
Cell number
1400000
1200000
1000000
800000
600000
400000
200000
0
HPV16 Plating
24h
48h
72h
HPV16 Plating
24h +MMC
48h +MMC
72h +MMC

4.3.1 Mitomycin-C treated monolayers show limited Histone H3 phosphorylation

An additional complementary experiment was performed using Mitomycin C to directly evaluate the effect of Mitomycin C treatment on the mitotic activity of NIKS and NIKS-HPV16 populations in monolayer. To do this, the cells for the growth rate experiment were also employed in cover-slip staining experiments using antibodies against a specific mitotic marker, the phosphorylated form of the Histone H3 (H3P) (Hans and Dimitrov, 2001).

During mitosis, H3 phosphorylation is involved in two processes: transcriptional activation requiring chromatin fiber de-condensation, and chromosome compaction during cell division (de la Barre et al., 2000; Nowak and Corces, 2000; Thomson et al., 1999). As the detection of H3P necessarily indicates that cells are going through mitosis, H3P levels were measured in the presence of Mitomycin C in order to establish the extent of cellular mitotic activity. To do this, NIKS and NIKS-HPV16 populations were grown for 72 hours on cover slips, and then lifted every 24 hours to perform H3P immuno-staining (Figure 4.3). NIKS cells were grown under standard conditions as control.

The results show that the Mitomycin C treatment significantly decreases the number of H3P positive cells for both NIKS and NIKS-HPV16 cells (Figure 4.3A, B). The data are collected in Table 4.1.

These data support the growth rate experiment shown in Fig. 4.2, and confirm that Mitomycin C treatment is effective in limiting the mitotic activity of NIKS and NIKS-HPV16 cells.

A

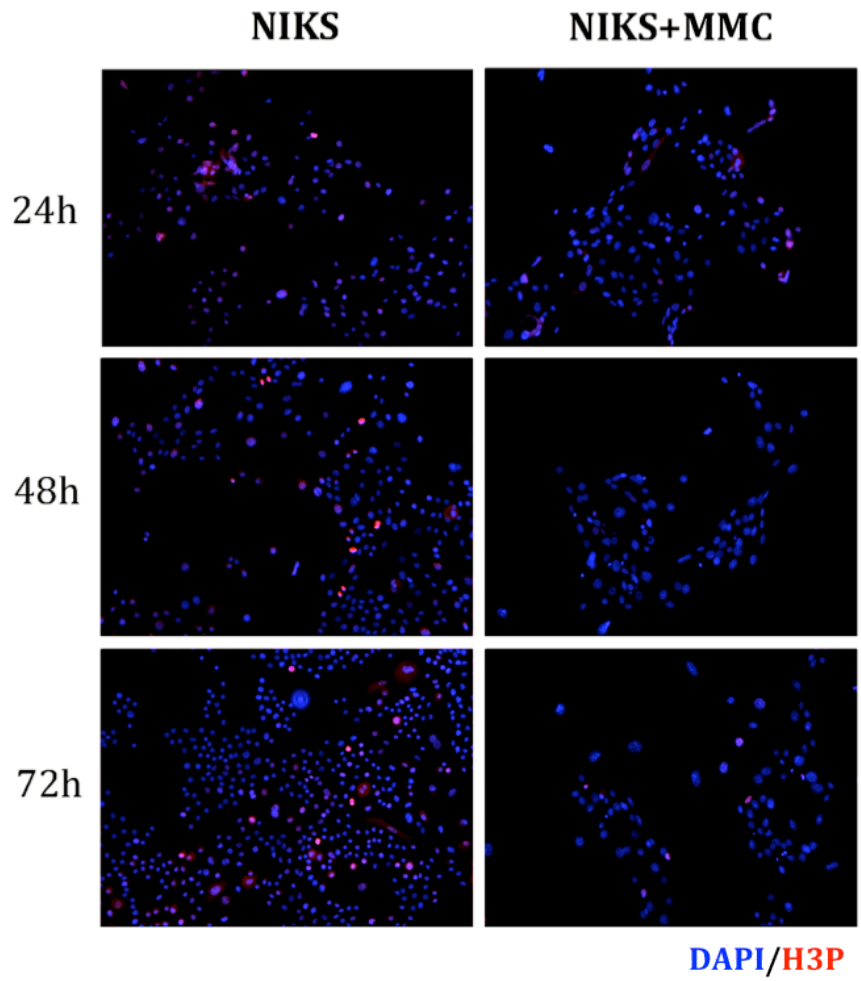

Figure 4.3 H3P expression in NIKS and NIKS-HPV16 populations. (A) NIKS cells grown on cover slips were immuno-stained for H3P (red) and DAPI (blue) at 24-, 48-, and 72-hours post plating. The samples treated with Mitomycin C are shown on the right hand side column. (B) NIKS-HPV16 cells were cultured and stained as above.

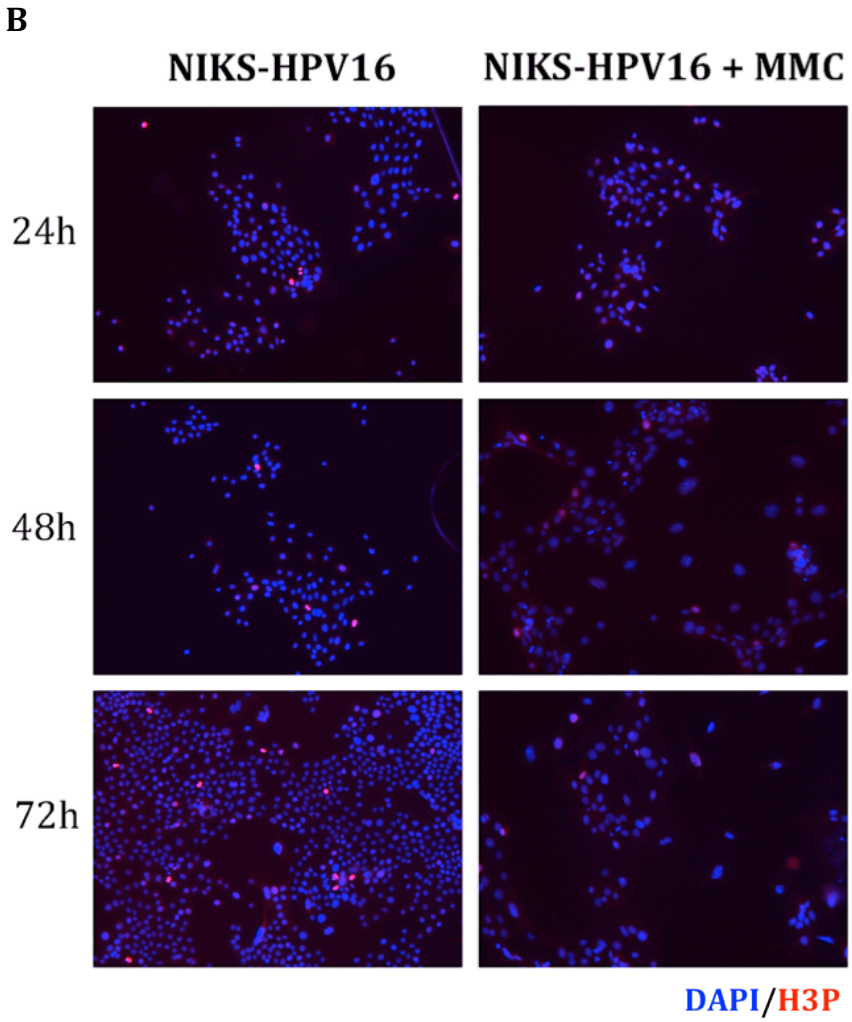

Table 4.1 Percentages of H3P positive cells. The number of H3P positive cells is represented as a percentage of the total number of keratinocytes staining positive for DAPI. Counting was performed from three independent experiments for each time point considered.

	24h	48h	72h
NIKS	19/302 (6.2%)	21/461 (4.5%)	46/978 (4.7%)
NIKS-HPV16	28/469 (5.9%)	31/567 (5.4%)	62/1342 (4.6%)
NIKS+MMC	0/335 (<0.1%)	0/328 (<0.1%)	0/225 (<0.1%)
NIKS-HPV16+MMC	3/437 (0.68%)	1/389 (0.25%)	0/247 (<0.1%)

4.4 NIKS-HPV16 cells migrate faster than NIKS HPV negative cells in a wound healing scratch assay

During wound healing cells are stimulated to proliferate and to move towards the region of injury in order to reconstitute the cellular continuity of the tissue (Singer and Clark, 1999). The ability of keratinocytes to migrate is also important in other processes such as cell invasion during tumour progression and metastasis (Friedl and Wolf, 2003). The capability of infected cells to migrate towards the region of injury during wound healing is a key aspect of the HPV life cycle that needs to be investigated.

One strategy to evaluate cell migration ability in a wound-healing assay is to control cell proliferation. As shown in section 4.2 and 4.3 this can be achieved with the use of Mitomycin C as anti-mitotic agent (Tomasz, 1995). Interestingly, the effect of Mitomycin C on cell migration was previously investigated (Carragher, 2009), and although high concentrations of Mitomycin C were shown to inhibit the migration of cancer cells lines, 0.5 ug/ml Mitomycin C was found to have no significant effect on migration capability (Carragher, 2009).

Following the inhibition of cell proliferation with Mitomycin C, the movement of the cells was examined (Figure 4.4).

As described in section 4.1, the cells were grown to confluence before the monolayer was mechanically scratched in order to monitor over time the cell response to the 'wound' and the migration of cells into the empty space created in the dish.

After the scratch was applied the plates were washed in Mitomycin C containing medium to remove floating cell debris. The scratched plates were then incubated

in a culture medium containing 0.5 μg/mL of Mitomycin C placed in a temperature-controlled chamber of a time-lapse microscope. A time-lapse digital camera was used to follow the development of the scratch 'healing' and to monitor the movement of the keratinocytes into the empty space of the dish. The wound site was photographed digitally at two-hour intervals and images were analysed with Image-J® Software (Figure 4.4A). The repopulation of the free cell area was calculated as the difference between the repopulated free-cell area at any given time compared with the dimension of the free-cell area at 2-hour time point.

The results show that although the infected cells were treated with the anti-proliferative agent Mitomycin C, they were efficiently recovering the scratch area (Figure 4.4B). The analysis of the images demonstrates that the NIKS cells containing HPV16 genome were able to migrate significantly faster than control cells (Figure 4.4B).

We measured essentially the migration of the entire front moving towards the empty space. The movement of single cells leaving the wound edge was in fact very rare. The methodology used to create the scratch cause the detachment of the fibroblasts, however these are used by keratinocytes as a source of collagen and as a physical support, and their loss could feasibly limit the ability of single keratinocytes to detach from the wound edge. However, such a scenario was difficult to properly investigate using the available methodologies.

Nevertheless, the results obtained indicate that the HPV16 containing cells were more efficient in undergoing wound healing-like repopulation of the scratched area than respective control cells, even in the presence of Mitomycin C.

The migratory ability apparent in NIKS-HPV16 containing cells suggest that keratinocytes infected with HR-HPVs acquire several important features that result in an increase of both migration and proliferation rates.

The enhanced migration rate of the infected cells is likely to be important during wound healing and lesion formation, as these cells have the possibility to expand into a relatively large area and to possibly able to out-compete the un-infected cells in terms of their growth rate.

Interestingly, these characteristics were evidenced in both NIKS-HPV16 clones and populations, suggesting that the expression of the viral genome is contributing to the establishment of this phenotype from the initial stages.

The comparison of the migration rates obtained from treated and un-treated cells suggested that the NIKS-HPV16 cells were indeed migrating at a similar rate than those untreated. The contribution of the increased proliferation rate (Section 3.2; 4.2) is however important in the repopulation of the scratched area.

The results obtained using the NIKS-HPV16 model system are in accordance with what has been suggested previously in other systems (Au Yeung et al., 2011; Boulenouar et al., 2010). The presence of HPV16 in both clones and populations is apparent, with cell migration likely to be an important feature that keratinocytes acquire during HPV infection.

Figure 4.4 Wound healing scratch assay performed with Mitomycin C treated samples. (A) Scratched monolayers in Mitomycin C containing medium were observed by time-lapse microscopy and measurements of the free cell area taken using Image-J software. A reproducibility test showed that repeated annotation of the same image produced an average difference of 1.4% of the total image area between replicates and that the difference never exceeded 3.5%. (B) Migration rate of the Mitomycin C treated samples. The chart shows the average of the measurements from three independent experiments. The error bars represent the standard deviation of the triplicate values.. The cell migration rate is measured as cell-movement in the free cell area. The dimension of the free-cell area at 2-hour time point is used as comparative starting-value for each sample. The error bars represent the standard deviation of the triplicate values. The experiment was repeated three times.

A

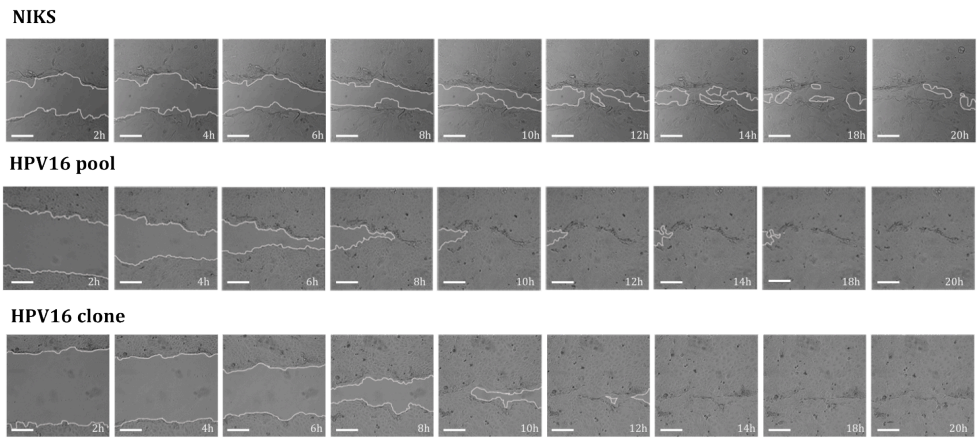
NIKS
2h
4h
6h
8h
10h
12h
14h
18h
20h
HPV16 pool
HPV16 clone

B

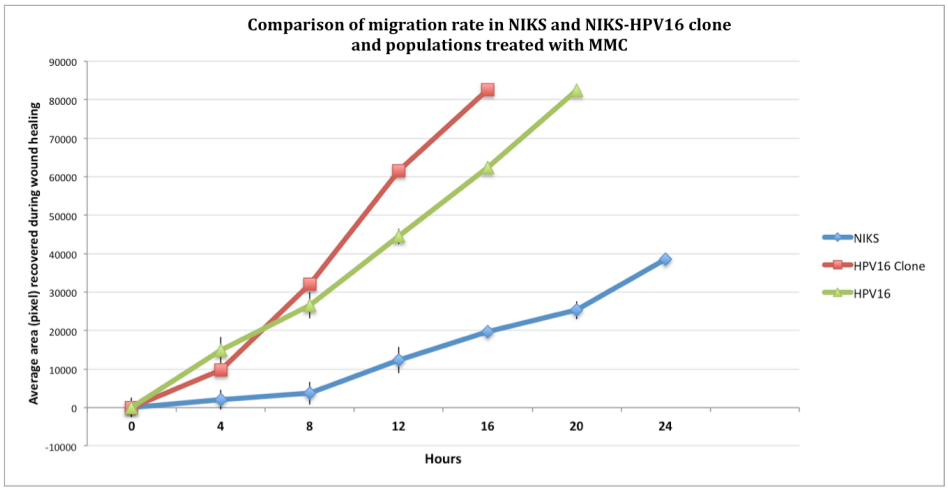
Comparison of migration rate in NIKS and NIKS-HPV16 clone and populations treated with MMC
Average area (pixel) recovered during wound healing
90000
80000
70000
60000
50000
40000
30000
20000
10000
0
-10000
0
4
8
12
16
20
24
Hours
NIKS
HPV16 Clone
HPV16

C

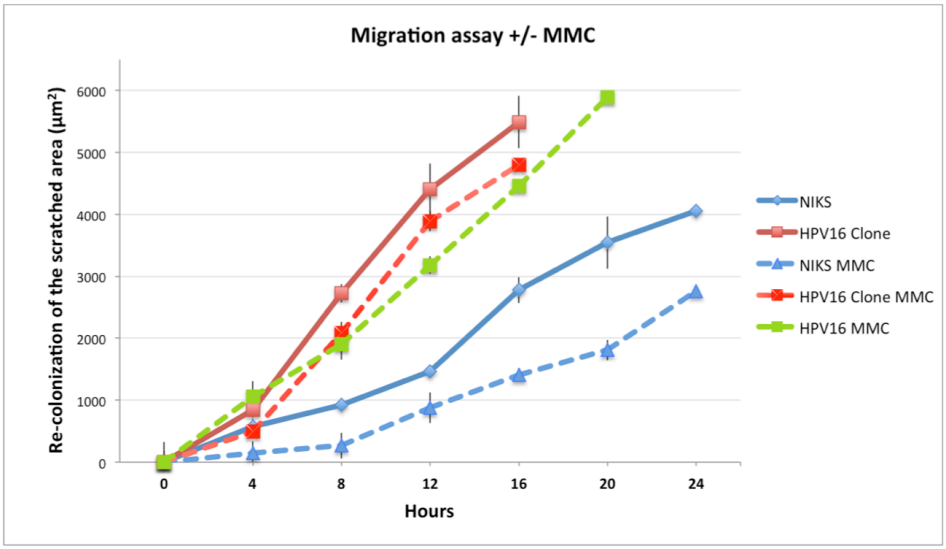
Migration assay +/- MMC
Re-colonization of the scratched area (µm²)
6000
5000
4000
3000
2000
1000
0
0
4
8
12
16
20
24
Hours
NIKS
HPV16 Clone
NIKS MMC
HPV16 Clone MMC
HPV16 MMC

4.5 Comparative analysis of NIKS-HPV 16 and NIKS-HPV 11 genome containing cells during monolayer proliferation *in vitro*

The data obtained so far suggest that the wound healing-environment may favour the proliferation and migration of cells infected with high-risk HPVs, with both HSIL- and LSIL-like cell lines showing an increased proliferation rate when compared to untransfected cells. The reduction in cell doubling time was apparent both before and after cell confluence was achieved, and is likely to be a consequence of viral gene expression from HPV episomes.

In order to understand whether this characteristic is also seen with to LR-HPV types we next went on to perform a comparative study with NIKS populations containing either HR- or LR-HPV types.

A key aim was to address the question of how lesions form and to further our understanding of the differences these broad groups of papillomaviruses.

4.5.1 NIKS cells containing HPV11 genome have lower proliferation rate than NIKS-HPV16 and NIKS-HPV negative cells

HPV11 causes benign papillomas and is a prototype for non-malignant, low-risk papillomaviruses from the Alpha genera.

To determine whether NIKS cells containing the HPV11 genome are able to proliferate as well as NIKS-HPV16 cells, we performed a comparative proliferation assay using the approaches described in section 3.2 (Figure 4.5).

Growth assays were performed in triplicate in order to demonstrate the statistical significance, with cells being plated at the same density at the start of each experiment. Two internal controls were added to the assay; NIKS cells were

used to assess the growth rate in absence of HPV, while the NIKS-HPV16 HSIL-like clone was used as a positive 'hyper-proliferative' control.

NIKS cells transfected with HPV16 and HPV11 genomes showed significantly different growth patterns. NIKS-HPV16 populations grow quicker than NIKS (HPV-negative) cells, proliferating beyond confluence (80-90% confluence is reached with a number of cells of approximately $1x10^6$/well). The NIKS-HPV11 transfected cells shoved a rather slow growth, more like the untransfected NIKS (Figure 4.5).

The failure of the NIKS-HPV11 populations to recreate a phenotype similar to the NIKS-HPV16 is in accordance with recent data showing that HPV11 genomes when transfected in immortal human keratinocyte line (HaCaT) cells are inefficient in promoting cell proliferation when transfected *in vitro* (Kaczkowski et al., 2012). The inability of the HPV11 genome to increase cell proliferation is also suggested from the analysis of clinical biopsies, where the differential proliferation of basal cells in HPV16- and HPV11-induced lesions was highlighted (see Chapter 1). Given this apparent inability to stimulate enhanced proliferation it is not clear how cells infected with LR-HPV types expand to form a lesion. From previous studies it has been suggested that LR-HPVs stimulate lesion formation only after successfully infection of stem or stem cell-like cells in the basal compartment (Doorbar et al., 2012; Stanley et al., 2007). It has also been proposed that the highly proliferative situation created during the wound healing environment provide the primary stimulation for the proliferation of cells containing LR-HPV genomes (Doorbar et al., 2012).

The contribution of wound healing responses, and in particular the role of growth factors will be discussed later in the thesis.

We conclude that in our model system, the HPV11 genome does not drive cell proliferation.

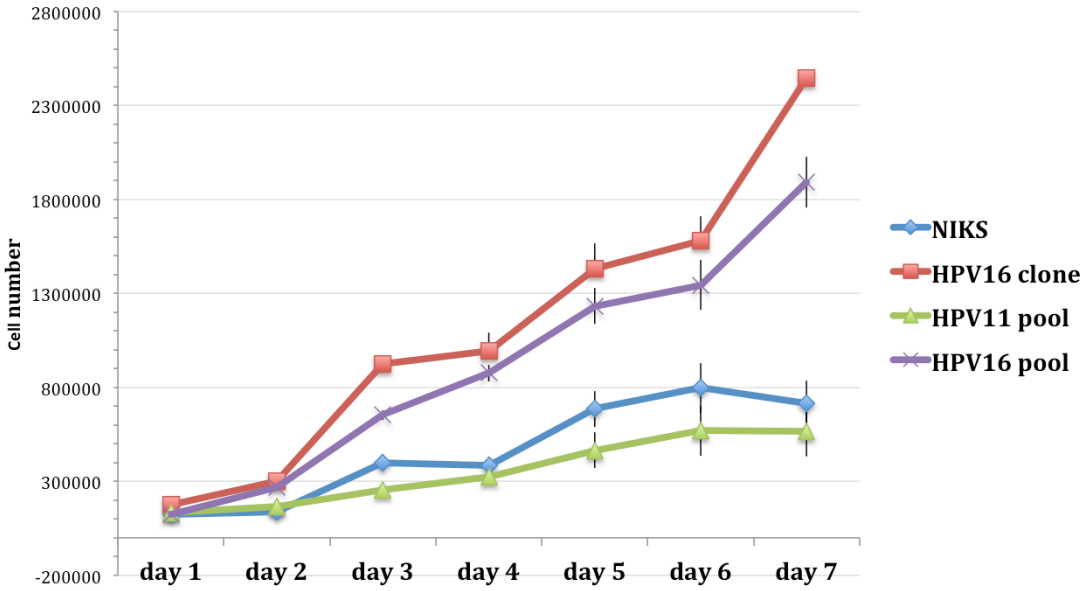

Figure 4.5. NIKS-HPV16/11 and NIKS growth assay. NIKS, NIKS-HPV16 clone and populations (pool) and NIKS-HPV11 populations were grown for 7 days and the cells were counted each day after plating. The chart represents the average number of cells per well obtained from three independent experiments and the error bars show the standard deviation of the triplicate values.

4.5.2 HPV11 genome does no stably persist in NIKS cells after transfection

During the studies on NIKS HPV11 populations we also tested the ability of HPV11 genome to be maintained, and assessed the average copy number per cell immediately following transfection, selection and as the cells were cultured. HPV11 inability to drive cell proliferation, does not allow of to positively select for fast cycling cell populations or clones after transfection. Thus, the presence of the HPV11 genome in the cell populations used had to be regularly tested in all experiments.

The cells were transfected and plated in flasks to acclimatize them to their culture conditions. After recovery from transfection stress, the cultures were typically subdivided into three flasks that were subsequently passaged.

To determine the existence of viral genomes in the transfected cells, the cell cultures were grown to confluence at each passage prior to being harvested in order to perform real time quantitative PCR analysis on the extracted genomic DNA.

The qPCR analysis revealed that the average level of the HPV11 genomes contained in the transfected NIKS populations never exceeded 90 copies per cell at first culture passage (Figure 4.6). Furthermore, we observed a direct correlation between viral copy number and the amount of transfected genome that was used to transfect the NIKS cells (Figure 4.6). Interestingly, the amount of genome used during transfection had no effect on the ability of HPV11 to be maintained in cultured cells after few passages. We observed that the number of HPV11 copies per cell was reduced by about 80% of the initial copy number post-transfection over the period of four culture passages (Figure 4.6).

We believe that the loss of the HPV11 genome was not dependent on the transfection efficiency, which was consistent between experiments when control plasmid was used. With ZsGreen1 Fluorescent Protein transforming vectors a reproducible transfection rate of about 70% of cells was routinely observed using the electroporation system. This was also seen when GFP plasmids were used to spike transfection with HPV11 and HPV16 DNA (Figure 2.1).

To assess further the transfection efficiency of HPV11 genome, the cells were co-transfected with the viral genomes and the pcDNA6 plasmid (which carries a blasticidin-resistance gene), and DNA was extracted from them 48 hours post-transfection. The DNA was then analysed by qPCR to determine the number of HPV copies per cell. In this assay, the cells were first trypsinised and passed onto new plates 24 hours prior to the DNA extraction, to minimize the chances of having any exogenous-DNA complexes attached on the outside of the cells and interfering with the results. The trypsinisation process of these cells involved one quick wash with trypsin-versene, a 2 minute incubation to remove the feeder cells and a 5-10 minute incubation to remove the NIKS cells, followed by neutralization of the trypsin and centrifugation of the detached cells. The copy numbers for the transfection of the HPV16 and HPV18 genomes were normalized to those for the transfection of the HPV11 genome, for three independent experiments (Fig. 4.6). The transfection efficiencies of the three genomes were found to be comparable.

We suspect that the inability of HPV11 to increase cell proliferation and enhance cycling speed means that HPV11 transfected cells do not have any growth

advantage when present as part of a mixed population. This may explain the short life span of the viral genome within the cell populations transfected with HPV11 genomes.

To compensate for this deficiency, in all our experiments employing NIKS-HPV11 populations, we used newly transfected cells in which the presence of HPV11 genome was routinely assessed by qPCR methods. Only when the presence of HPV11 genome within the NIKS population was satisfactorily established, by comparing the number of copies at 48 hours from transfection with the number of HPV11 copies contained in the NIKS after the first culture passage, did we proceed to the use of NIKS-HPV11 cells to perform comparative studies *in vitro*.

A

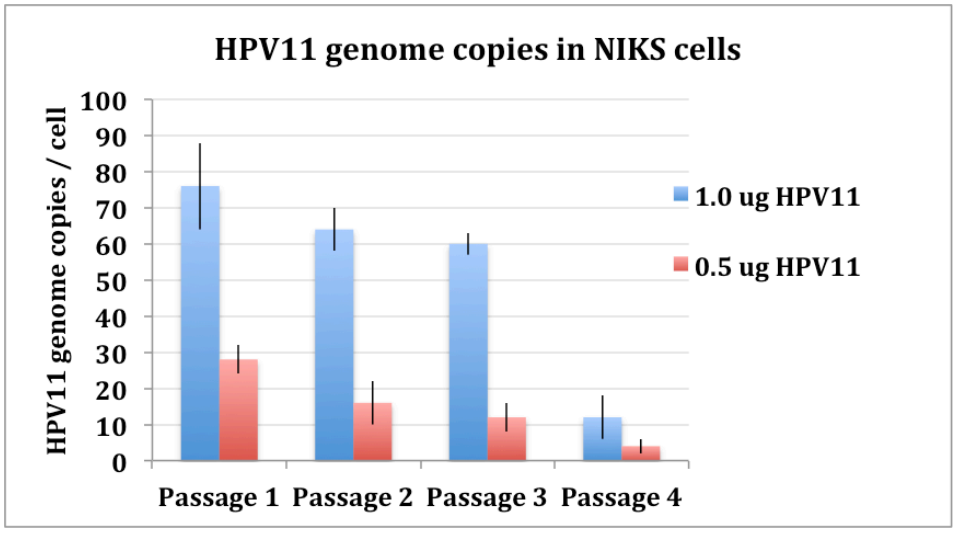

B

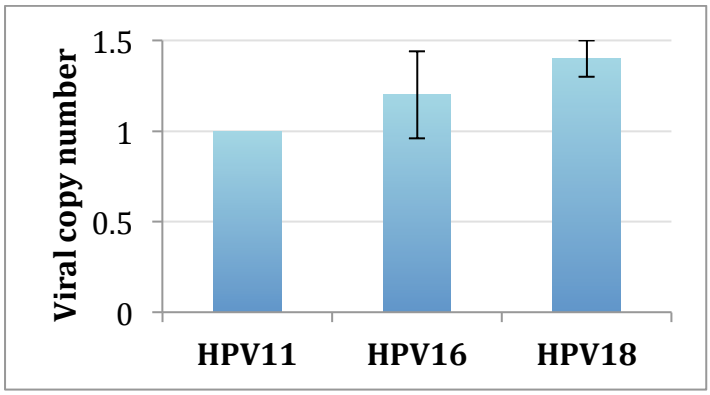

Figure 4.6. Evaluation of HPV11 genome maintenance in NIKS populations. (A) NIKS were transfected with HPV11 genome using 0.5 µg and 1.0 µg of viral genome. The cells were passaged four times and HPV11 copies estimated using qPCR. The chart shows the average copy number obtained from three experiments. The bar graphs show the average of three experiments and the error bars show the range. (B) NIKS cells were co-transfected with HPV11 or HPV16 or HPV18 genomes, and pcDNA6 plasmid and the HPV copies per cell were measured by qPCR at 48 hours post-transfection. The copy numbers for the transfection of the HPV16 and HPV18 genomes were normalised to those for the HPV11 genome. The bar graphs show the average of three independent experiments and the error bars show the range.

4.5.3 Comparative analysis of the colonization ability of NIKS-HPV16 cells and NIKS-HPV11 cell populations

Our model system suggests that NIKS-HPV16 cells might outgrow NIKS-negative cells because of their ability to proliferate faster and to overcome normal cell-to-cell contact inhibition signals. Additionally, the scratch assay experiments performed in the presence of Mitomycin C suggest a possible ability of NIKS-HPV16 genome containing cells to repopulate a wound quicker than control cells. Thus, a higher rate of proliferation and a faster migration characterize NIKS-HPV16 containing cells.

Contrarily to HR-HPV-containing cells cells, NIKS cells transfected with the HPV11 genome have a slow cycling phenotype as shown in the growth rate analysis (Section 4.5.1) suggesting that the LR-HPV genomes have no capacity to increase proliferation.

The differences between NIKS-HPV16 and NIKS-HPV11 cells revealed by the monolayer culture system suggest that these two types of cells may behave differently in an environment crowded by NIKS-HPV negative cells.

In fact, we hypothesize that following HPV infection the cells containing the HR-HPV genome may outcompete neighbouring cells that are not 'infected'.

To determine whether NIKS-HPV16 cells can indeed outgrow NIKS cells we have developed an *in vitro* 'colonization assay'. The colonization assay involves the plating of NIKS-HPV16 positive cells transfected with a GFP-expressing plasmid in dishes containing NIKS cells. The expression of the GFP-positive cells, which is monitored by fluorescent microscopy, is used to track the proliferating HPV16 genome-containing colonies as they increase in size.

In this assay, we used NIKS-HPV16 LSIL-like clones and NIKS-HPV16 cell populations, which were transfected with GFP expressing plasmids in order to help visualize the cells containing the viral genome. Cells expressing GFP were then plated into the midst of un-transfected NIKS cells, which were used as a normal growth reference in comparison with NIKS-HPV16 GFP expressing cells (Figure 4.7). The analysis of the colonies formed by the different types of cells shows that cells containing the HPV16 genome and a GFP plasmid form large clusters of cells over a period of 96 hours. In particular, they were able to outgrow the neighbouring NIKS-HPV negative keratinocytes as expected as a result of their increased growth rate (Section 3.1 and 4.5.1). The control experiment, which involved the analysis of NIKS cells transfected with GFP expressing plasmids plated onto untransfected NIKS cells, showed the typical NIKS HPV-negative cell proliferation rate, with colonies formed by NIKS-GFP expressing cells being small in size. A comparative analysis of the colonies size was carried out by measuring the area covered by GFP expressing cells in three different plating experiments. For each experiment three images for each time point were analysed and the size of the GFP colonies present in the field of view were measured using Image-J® software. The results show that cells lines containing the HPV16 genome produce large colonies 96 hours post plating, whereas the keratinocytes containing only GFP expressing plasmids produce only small colonies and do not outgrow their neighbour cells (Figure 4.7).

The ability of both NIKS HPV16 LSIL-like clones and NIKS –HPV16 populations to overgrow NIKS cells confirms the hypothesis that HPV16 containing cells outcompete the un-infected neighbours.

Furthermore, the analysis of the colony size is in accordance with the doubling time analysis and the growth rate analysis showed previously (see Chapter 3). This experiment shows the ability of keratinocytes containing HPV16 genomes to form colonies that may resemble the early phases of cell proliferation following HPV16 infection in the basal layer of the epithelium.

Figure 4.7 GFP expressing cells colonization assay. (A) NIKS-HPV16 cells were transfected with GFP-expressing plasmid, and plated onto NIKS. NIKS-HPV16 green fluorescent cell proliferation was estimated during 96 hours time course. A control experiment using NIKS-GFP cells plated onto NIKS was carried out to compare the colonization rate of HPV16-negative cells. The scale bars measure 100 μm. (B) The chart shows the number of fluorescent cells of each type (NIKS, NIKS-HPV16 clone LSIL-like and NIKS-HPV16 populations) at 24-, 48-, and 72-hours post plating. The bar graphs show the average of three independent experiments and the error bars show the range. There was significant difference between the colony size formed by NIKS-HPV16 (Pool and L-SIL) and NIKS at 96h time point ($p < 0.05$). The experiment was repeated three times.

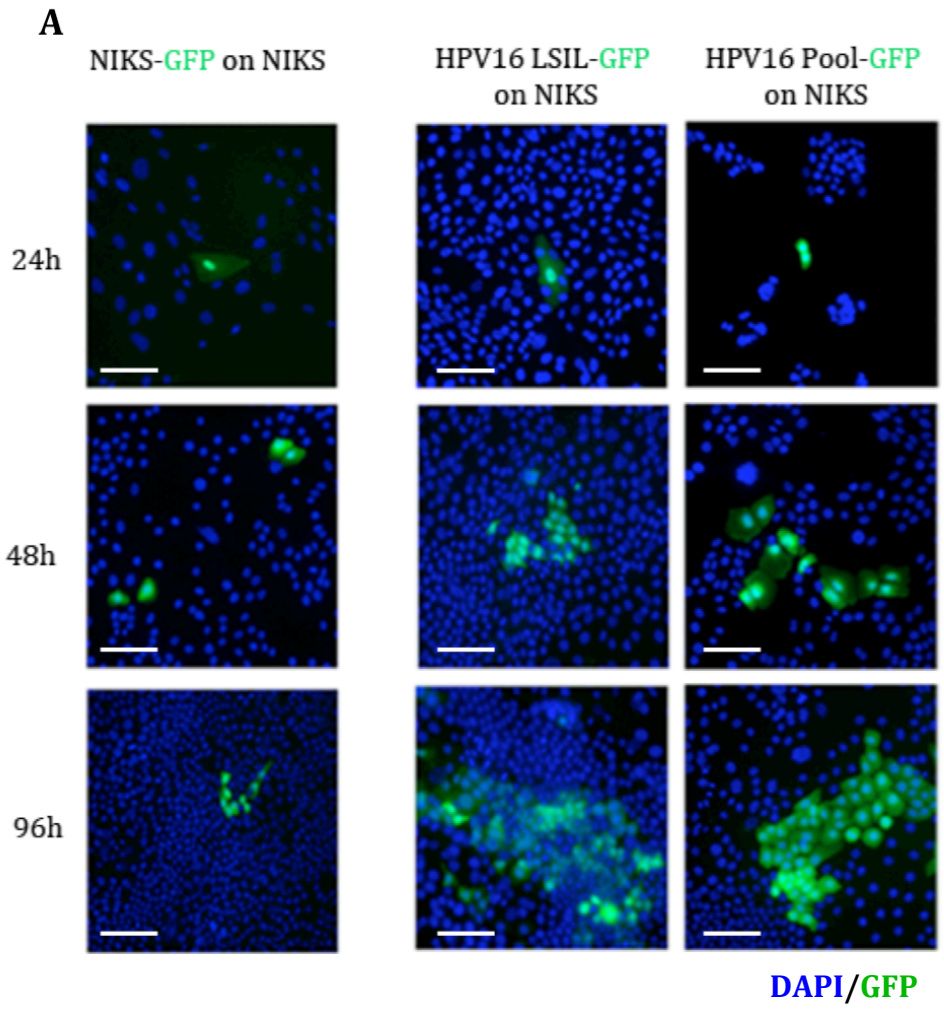
A
NIKS-GFP on NIKS
HPV16 LSIL-GFP on NIKS
HPV16 Pool-GFP on NIKS
24h
48h
96h
DAPI/GFP

B

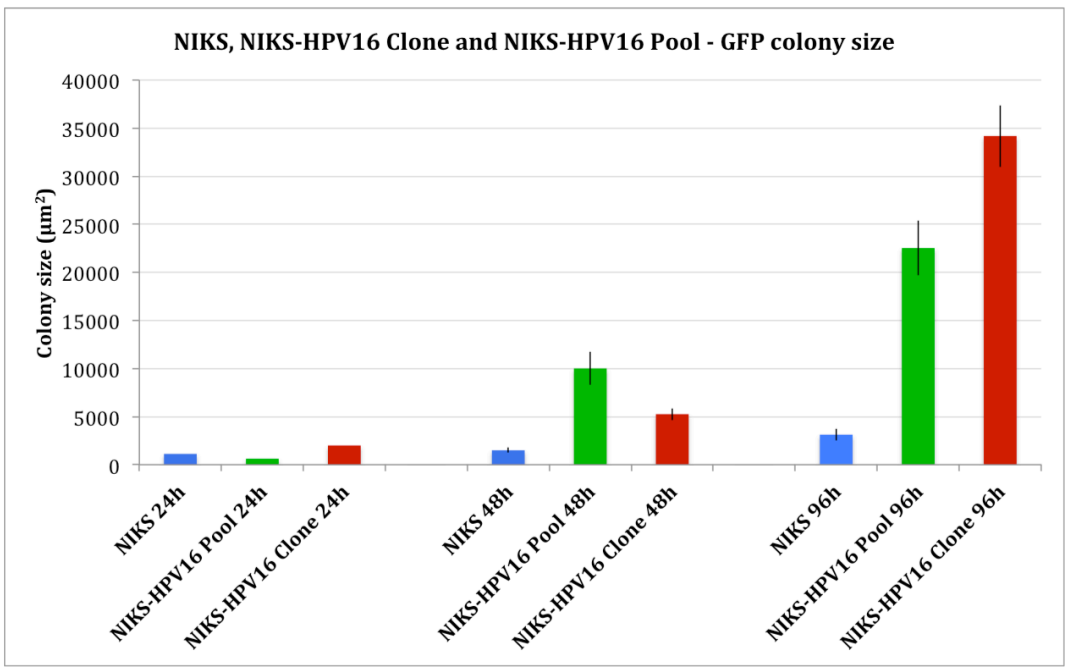
NIKS, NIKS-HPV16 Clone and NIKS-HPV16 Pool - GFP colony size
Colony size (µm²)
40000
35000
30000
25000
20000
15000
10000
5000
0
NIKS 24h
NIKS-HPV16 Pool 24h
NIKS-HPV16 Clone 24h
NIKS 48h
NIKS-HPV16 Pool 48h
NIKS-HPV16 Clone 48h
NIKS 96h
NIKS-HPV16 Pool 96h
NIKS-HPV16 Clone 96h

4.5.4 NIKS-HPV11 cells expressing GFP are not able to outgrow NIKS-HPV negative cells

The colonization assay performed with NIKS and NIKS-HPV16 cells showed that HPV16 genome-containing keratinocytes were able to outgrow NIKS HPV-negative cells in a competitive growth environment. This experiment provides insight as to what might occur in the basal compartment of the epithelia soon after the HR-HPV infection. It is not clear however, whether this mechanism is also a feature of low-risk HPV types which show limited levels of basal layer proliferation in clinical samples.

The study of the NIKS-HPV11 containing cells has already demonstrated that HPV11-containing keratinocytes do not proliferate as fast as HPV16 genome containing cells. To determine the ability of HPV11 and HPV16 genome-containing NIKS to form colonies in a competitive growth environment we made use of the comparative colonization assay outlined in Section 4.5.3.

NIKS-HPV11 and NIKS-HPV16 cell populations were transiently transfected with GFP plasmid and plated onto NIKS (HPV-negative) cells as described earlier. NIKS cells were also transfected with GFP expressing plasmid and used in control experiments. The NIKS-HPV11 and NIKS-HPV16 GFP-transfected cells were subdivided in three vials. One vial of NIKS-HPV16 and one of NIKS-HPV11 populations was used to check for viral genome maintenance before starting the experiment. A second vial was used in the experiment and a third stored at -80° C. In dishes containing cover slips, the GFP-NIKS-HPV11/16 cells were plated so as to obtain an approximately 20:1 ratio between NIKS and NIKS-HPV cells. Cells were subsequently grown for seven days and cover slips were lifted at each day

over a period of seven days. Cover slips were then fixed and stained with DAPI to visualize the cell nuclei (Figure 4.8). Green fluorescent colonies were observed using a Zeiss inverted microscope equipped with a fluorescence lamp and picture acquired digitally using Axion™ Digital Imager Software. The sizes of the GFP positive colonies were assessed using Image-J® software.

Data gathered for each day from two independent experiments were averaged and values obtained at day 2 and day 7 compared. The result showed that the sizes of the colonies of the NIKS-HPV16 GFP-positive cells were significantly larger than those that arose from the NIKS-GFP cells and NIKS-HPV11 GFP-positive cells (Figure 4.8 B).

Furthermore, the number of GFP positive colonies was different between the HPV11 and HPV16 genome containing populations (Table 4.2). A colony was defined as a cluster of minimum three contiguous cells.

We conclude that the formation of colonies from HPV11 genome containing cells was not as efficient as for NIKS-HPV16 cells.

We hypothesize that as NIKS-HPV11 cells do not show enhanced cell proliferation or any ability to outgrow their 'uninfected' neighbours, thus they are unlikely to compete successfully in a wound healing like environment. It is plausible to hypothesize that a long-lived recipient with slow cycling characteristics may favour the proliferation of LR-HPV genotypes. In order to successfully infect the basal epithelia therefore, LR-HPVs may need to enter keratinocytes with stem cell-like characteristics. The comparative analysis of LR- and HR-HPV types provides evidence of differences of HPV types belonging to different groups. The analysis of colony size performed in the monolayer model system may in the

future be exploited in a raft model or in an i*n vivo* system if GFP-HPV genome hybrids can be prepared.

Figure 4.8: Colonization assays of NIKS, NIKS-HPV16 and NIKS-HPV11 populations. (A) Colony formation at day 1 to 7 of NIKS, NIKS-HPV16 and NIKS-HPV11 GFP cells onto NIKS cells. The cells expressing GFP were visualized using a fluorescence microscope and pictures were acquired digitally. DAPI staining (blue) was used to help visualize all keratinocytes present in the field of view and to reveal the cells that were GFP negative. Scale bars measure 100 µm. (B) Two time points were chosen for comparison of the sizes of colonies between NIKS-HPV11 and NIKS-HPV16 GFP cells. (C) The colony measurements from six images of two independent experiments were averaged and plotted in a chart. The bar graphs show the average of three independent experiments and the error bars show the range

A

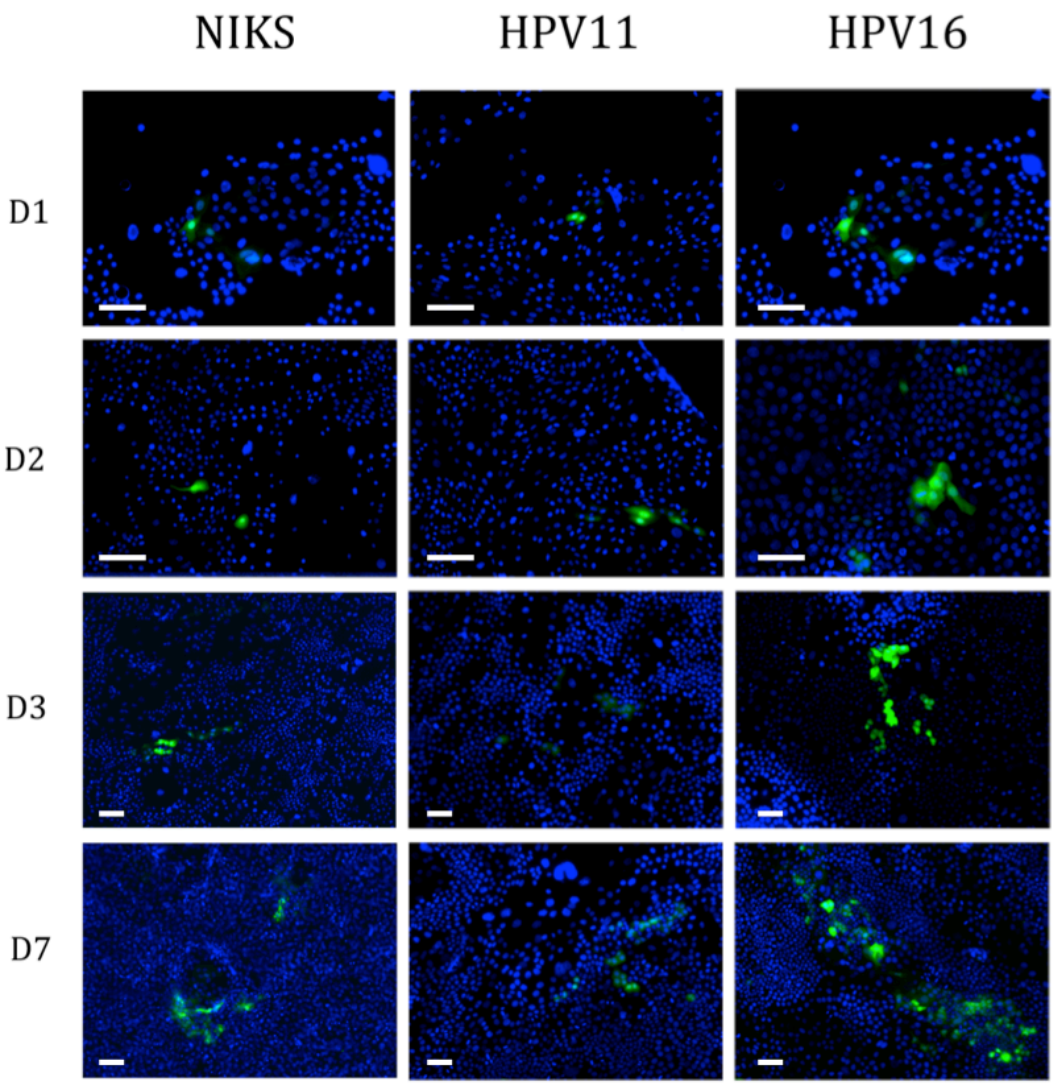

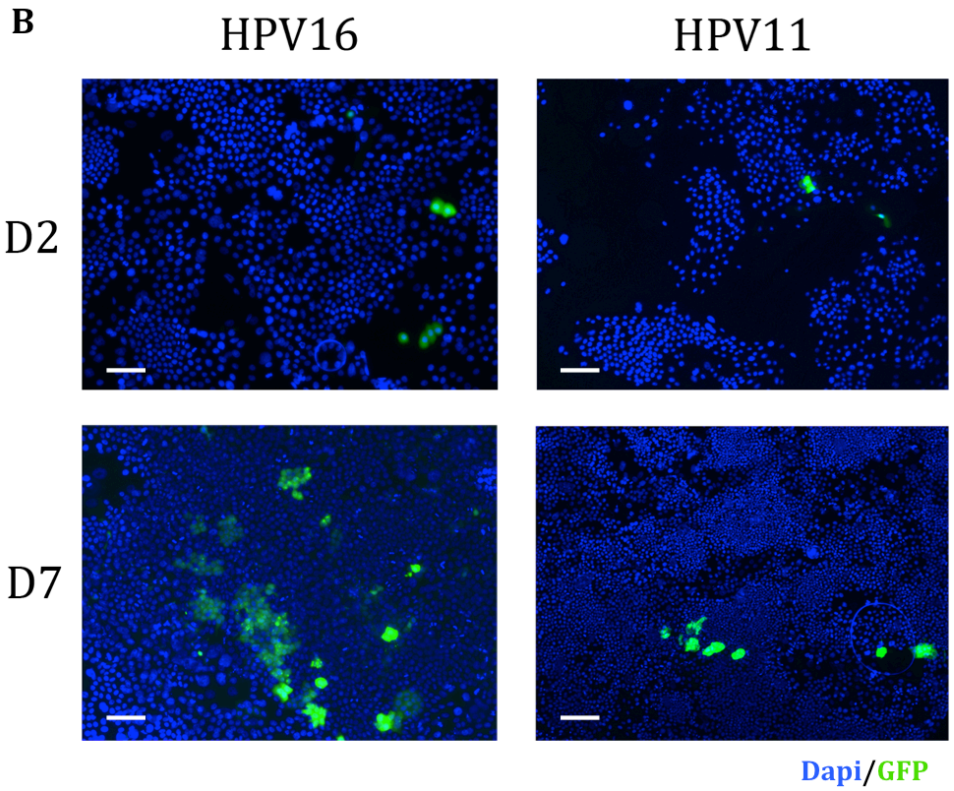
B
HPV16
HPV11
D2
D7
Dapi/GFP

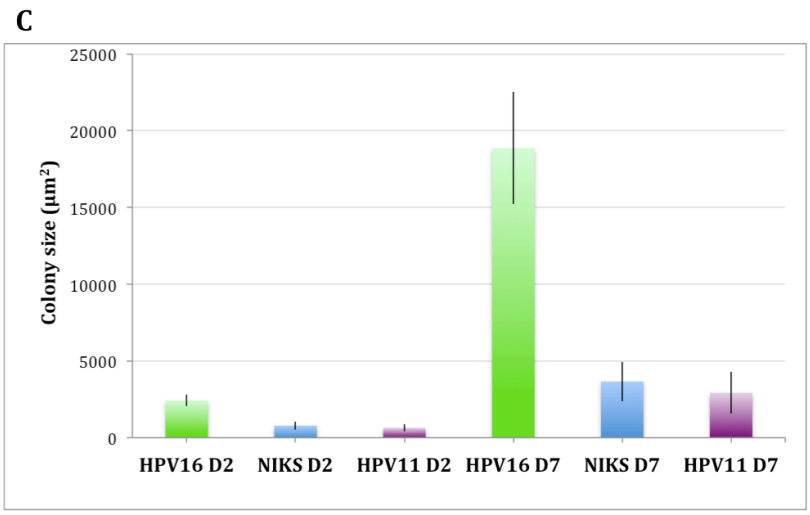
C
Colony size (µm²)
25000
20000
15000
10000
5000
0
HPV16 D2
NIKS D2
HPV11 D2
HPV16 D7
NIKS D7
HPV11 D7

Table 4.2 Number of colonies counted in the images analysed. The table shows the number of the colonies produced in all dishes at day 2 and day 7 by NIKS-GFP, NIKS-HPV11-GFP and NIKS-HPV16-GFP respectively.

	NIKS	NIKS-HPV11	NIKS-HPV16
Day 2	21 colonies	23 colonies	27 colonies
Day 7	18 colonies	12 colonies	26 colonies

4.5 Discussion

In this chapter we have shown that HPV16 genome containing NIKS cells have the ability to recover a scratched monolayer in a shorter time than NIKS cells. More specifically we have shown that the cells containing the viral genome migrate and proliferate faster than NIKS in an *in vitro* scratch assay. This suggests that the HPV16 genome is likely to confer an advantage to an infected cell with regard to competitive proliferation in a wounded epithelium. This characteristic was common to both NIKS-HPV16 clonal cell lines and NIKS-HPV16 newly transfected population. Furthermore, according to previous experiments (see Chapter 3), we suggest that 'infected' HPV16 cells may acquire such a proliferative advantage during the very early phase of virus genome-establishment in the host cells.

The contribution of the migration rate as opposed to the proliferation rate was evaluated in a separate monolayer scratch assay. The results of this investigation, suggested an additional ability of the infected cells to migrate into the empty space created by the newly formed 'wound'. Other studies support the idea that

cells containing HPV16 E6 and E7 may increase their migration rate when propagated in monolayer (Boulenouar et al., 2010).

Although we observed a substantial increase in the migration rate we are conscious of the limitations of the migration assay. Surprisingly, the movements of free cells into the scratched region from the wound edges of the scratched monolayer were not observed. In this case, the removal of the fibroblasts layer during the formation of the scratch might have compromised the ability of single cells to migrate into the unoccupied space. Nevertheless, NIKS-HPV16 cells were consistently quicker than NIKS in performing the scratch repair. We hypothesize that the scratch is occupied as a result of an increase in size of the cells at the periphery of the scratch and also by the continued growth of cells that were previously contact inhibited within the dish. These features are common to NIKS cells independently of whether they contain HPV.

According with data obtained here, we can speculate that the presence of the HR-HPV viral genome is likely to confer to the infected basal cells an ability to contribute to rapid wound repair. Both cell proliferation and cell migration were greater in the NIKS-HPV16 cells, suggesting the possibility that infected cells prevail under the selective pressure of a proliferative wound healing environment. Recent studies using cervical cancer cell lines have also shown that HPV16 containing cells confer a substantial advantage to the repairing cells (Au Yeung et al., 2011). It was reported also that in transgenic mice (Tg(bK6-E6/E7)), the expression of the HPV16 E6 and E7 oncogenes, under the control of the bovine keratin 6 promoter, markedly improves the mouse's capacity to repair portions of the ear after being wounded (Valencia et al., 2008).

Our results suggest that NIKS-HPV16 containing cells may outgrow the cells lacking the viral genome. Interestingly, we found that both NIKS-HPV16 clones and NIKS-HPV16 populations could efficiently outgrow their neighbouring cells when propagated together. During wound healing therefore, an infected cell would be able to establish a colony by exploiting its increased cycling speed and proliferation efficiency. Interestingly, a comparison between the LR-HPVs and HR-HPVs genome containing cells showed that the LR-HPVs were inefficient in forming large colonies and were not outgrowing the parental NIKS cells. Although we suppose that NIKS cells may not be an ideal host environment to study LR-HPVs due to their inefficient genome establishment, it was interesting to note that the LR-HPV cells were not able to support efficient proliferation, and were not able to outgrow the NIKS cells. We can therefore raise the possibility that LR-HPVs infections occur in basal cells with particular characteristics. We also believe that the cycling speed of the NIKS cells used, as our LR-HPV host may be not ideal for efficiently establishing the viral genome. Although recent studies suggest the ability to culture HPV11 cell lines for an extended length of time (Fang et al., 2006), our current thinking suggest that we should perhaps select slow-cycling NIKS cells (the more stem cell-like) to perform further analysis on HPV11 genome maintenance in NIKS.

The comparison between NIKS-HPV11 and NIKS-HPV16 containing cells, as shown in this study, suggest that HR-HPV containing cells acquire a selective advantage over against the uninfected cells. LR-HPVs appear not to have this characteristic, as NIKS-HPV11 containing cells did not proliferate as fast as

parental NIKS cells. We speculate that LR-HPVs infections occur in basal cells with characteristics similar to stem cells, in which the viral genome is preserved for long period through slow cellular replication.

5. Study of wound healing responses in an *in vitro* model system

5.1 Introduction

The events during papillomavirus lesion-formation are not well understood, but are likely to differ between high and low risk HPV types, which have different effects on the infected basal layer. These differences most likely reflect differences in protein function and gene expression patterns that have evolved to support the different biology of the two virus groups. While high-risk HPV types such as HPV 16 or 18 can drive cell proliferation in the basal and suprabasal layers, low-risk types such as HPV 6 and 11 appear not to possess this function (Doorbar et al., 2012).

In order to compare the two virus groups, we have introduced the HPV genomes into genetically identical keratinocyte background and examined their effect on functions required for lesion formation following epithelial trauma.

In this model, high-risk HPV types increase cell growth and migration rate when cells have space to grow, such as would occur during wound healing. Such viruses can also overcome normal cell-to-cell contact inhibition as the cells pack-up, and this is manifest in organotypic rafts as an increase in basal and parabasal cell division similar to that seen in neoplasia (Isaacson Wechsler et al., 2012; Doorbar et al., 2012). This growth advantage would allow a single infected cell to outgrow its uninfected neighbours following infection or during lesion expansion after wounding. Interestingly, the low-risk HPV types appear to have a negative effect on the cell growth rate, allowing the uninfected cells to predominate as a result of their more rapid cell division. These observations suggest a fundamental difference in the biology of the two HPV group, and support the idea that low-risk types may reside in a long-lived, slow-cycling cell such as a stem cell. For the high-

risk HPV types this model may not hold true, with lesion-formation being directed actively through functional changes in the infected basal layer.

In this chapter we aim to consider the effects that wound healing responses may have on lesion-formation following epithelial trauma. We hypothesize that due to the presence of growth factors during wound healing, infected cells may receive a proliferative 'boost' allowing them to expand into the injured region.

The contribution of wound healing responses to the development of a HPV–related lesion is not well understood. It is supposed that the abundance of growth factors during wound–healing may favour the expansion of infected basal cells. In fact, the presence of proliferative growth factors increases immediately after epithelial trauma (Sheardown and Cheng, 1996; Wilson et al., 1999). Thus, the area of injury is infiltrated by growth factors and cytokines, which act to stimulate keratinocytes in an autocrine and paracrine manner. The growth of keratinocytes is stimulated by the members of the epidermal growth factor family (EGF), fibroblast growth factor (FGF), nerve growth factor (NGF), and insulin-like growth factor (IGF) families, as well as hepatocyte growth factor (HGF), granulocyte-macrophage colony-stimulating factor (GM-CSF), and endothelin-1; their growth is suppressed by the transforming growth factor-β, vitamin D3, and interferon-γ (Shirakata, 2010). Keratinocyte-derived growth factors, cytokines, and chemokines contribute to the skin's cytokine network. These components play important roles during inflammation, immune responses and wound healing (Nickoloff et al., 2007; Werner and Grose, 2003). During the re-epithelization phase of wound healing, the concentration of growth factors increases in order to stimulate the cells to proliferate and migrate (Sheardown and Cheng, 1996; Zhang

et al., 1999). EGF level content in tears showed a significant increase after corneal injury (Brightwell et al., 1985). The variation of the EGF protein and EGF mRNA during corneal wounding is estimated to increase several about 70 fold immediately after trauma and to return to a basal level within 24-72 hours (Wilson et al., 1999).

EGF is known to be an important proliferative agent and is used in tissue culture to stimulate the proliferation of NIKS cells. Thus, in order to understand whether the variation of the growth factor concentration produces a stimulating effect on infected cells we first aimed to recreate wound healing-like conditions by varying its concentration in the culture medium. Our studies aimed to establish whether a wound-healing environment might affect the establishment of a HPV-induced lesion. As part of this, we hypothesized that changing the EGF levels may simulate to some extent, the changes that occur upon wound healing *in vivo* when cells are infected with either low or high risk HPVs.

5.2 Increasing EGF concentration results in increased HPV16 viral copy number in monolayer cultures.

A series of experimental and clinical studies have demonstrated a positive effect of EGF, TGF-α and heparin binding-EGF (HB-EGF) on wound repair, suggesting that the endogenous growth factors are also involved in the healing process (Martin, 1997; Schultz et al., 1987). In particular, such growth factors are released in abundance (mainly by eosinophils and macrophages) and are key regulators of keratinocyte proliferation at the wound site. Furthermore, epidermal keratinocytes at the wound edge were identified as a source of EGF and TGF- α

(Yu et al., 1994). HB-EGF was also localized in the advancing epithelial margin and also at the marginal surface of keratinocytes in murine burn wounds (Cribbs et al., 2002).

EGF, TGF-α and HB-EGF bind the Epidermal Growth Factor Receptor (EGFR), which is a trans-membrane receptor tyrosine kinase that is expressed on many different cell types (Yarden, 2001). The binding of ligands to the EGF receptor results in a proliferative signalling response at wound sites during re-epithelisation (Santoro and Gaudino, 2005).

Thus, the environment is enriched with growth factors that may contribute to the expansion of HPV infected cells during the wound healing response. Moreover, it has been suggested that the concentration of EGF in monolayer cancer cell line cultures is able to alter the expression of early viral genes (Collins et al., 2005; Rosenberger et al., 2010).

We hypothesise that papillomaviruses may have evolved to profit from the environmental condition found during wound healing and that the presence of an increased amount of EGF may favour a pattern of viral gene expression that allows the proliferation and the establishment of HPV-infected cells in the epithelial basal layer.

To determine whether an increased EGF concentration can alter the viral copy number in monolayer culture we have augmented up to 50 fold the concentration of EGF normally contained in the culture medium, during the proliferative phase of sub-confluent NIKS-HPV16 cultures, to mimic the post-wounding increase in EGF concentration found *in vivo* (Brightwell et al., 1985; Wilson et al., 1999). In order to avoid the variations in the viral copy number that might occur as a

consequence of keratinocyte differentiation, we performed the experiment in strictly sub-confluent conditions (NIKS cells differentiation was discussed Section 3.5).

NIKS-HPV16 cells were cultured in standard medium to confluence and re-plated in at three different EGF concentrations. We have chosen to use the standard 10ng/ml EGF concentration alongside two altered concentrations of 100ng/ml and 500ng/ml, which are comparable with the post-wounding EGF increases described *in vivo*. We observed that increasing the EGF concentration had no significant effects on the morphology of the keratinocytes in culture (Figure 5.1). The NIKS-HPVs were grown for 72 hours and cell pellets were harvested for protein, DNA and RNA analysis.

An analysis of the viral copy number in pellets was carried out using a qPCR approach. The results showed that the number of the HPV16 viral genome copies increased at when using 500ng/ml EGF in the culture medium (Figure 5.2). The highest concentration of EGF induces increase of viral copy number 72 hours after EGF addition.

These data suggest that the presence of growth factors at the site of infection is able to enhance viral genome replication. The imitation of such effects *in vivo* would be advantageous for the virus as keratinocytes containing high copy number are more likely to persist and proliferate in latter phases of lesion formation.

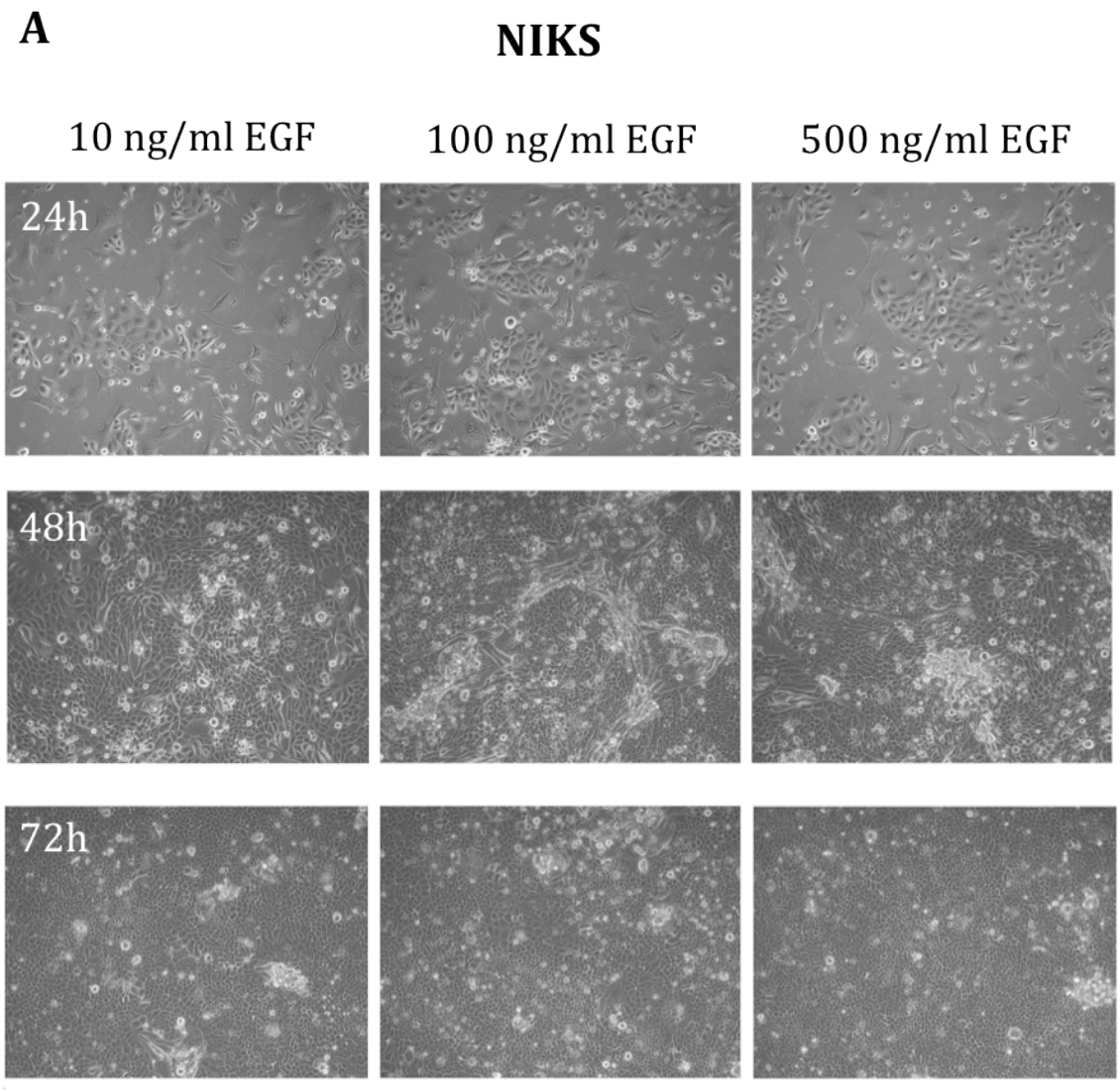
A
NIKS
10 ng/ml EGF
100 ng/ml EGF
500 ng/ml EGF
24h
48h
72h

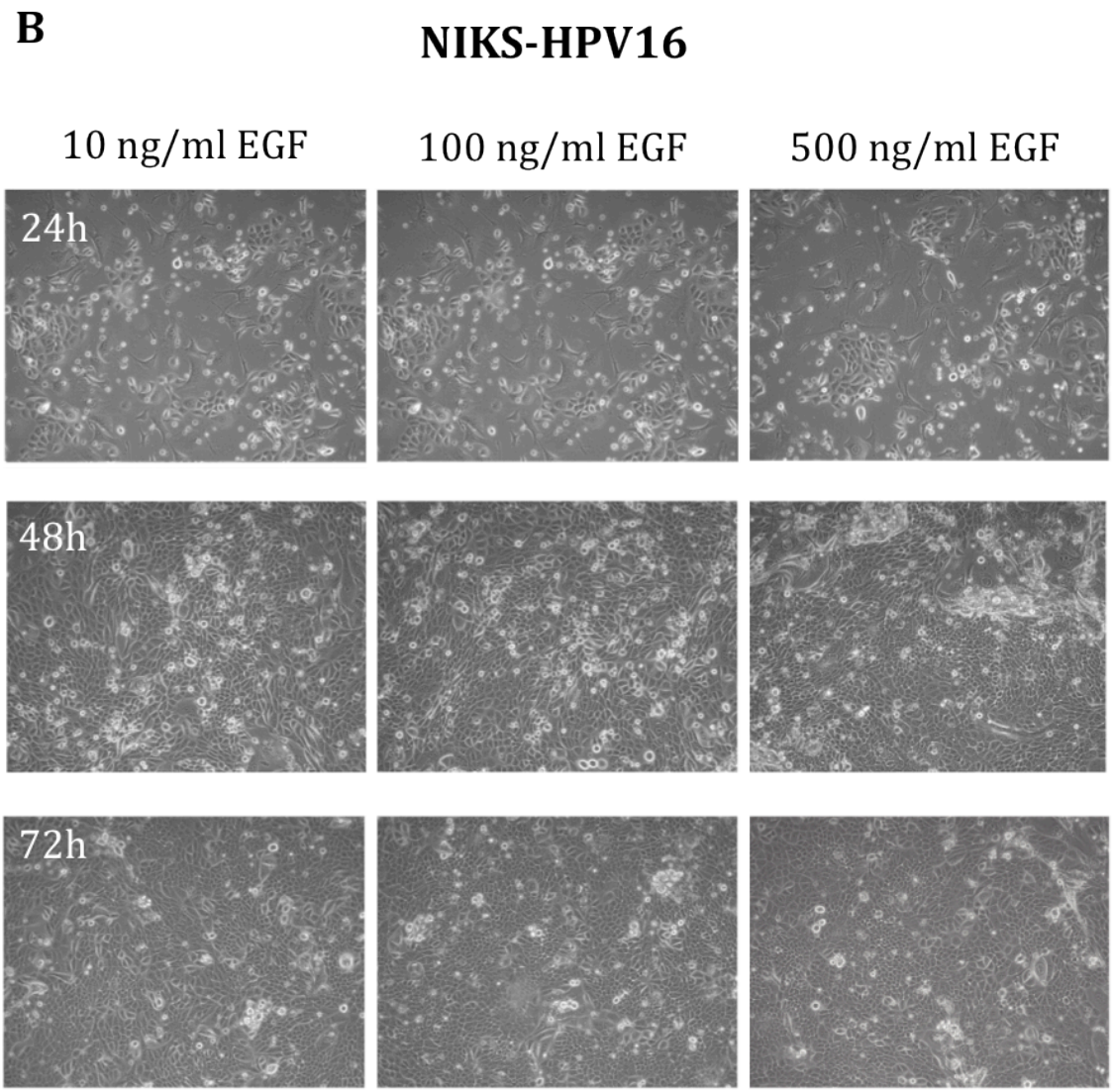

Figure 5.1 Bright-filed Images of monolayer cultures at 24, 48 and 72 hours post-plating. (A) NIKS cells were seeded in equal number and cultured 72 hours using three concentrations of EGF. Pictures show the morphology of the NIKS cells cultured with 10ng/ml EGF, which corresponds to the standard concentration used in monolayer cultures. (B) Images of NIKS-HPV16 cells cultured 72h using standard and wound healing-like EGF concentrations were also acquired. Images were acquired digitally using a 10x magnification objective.

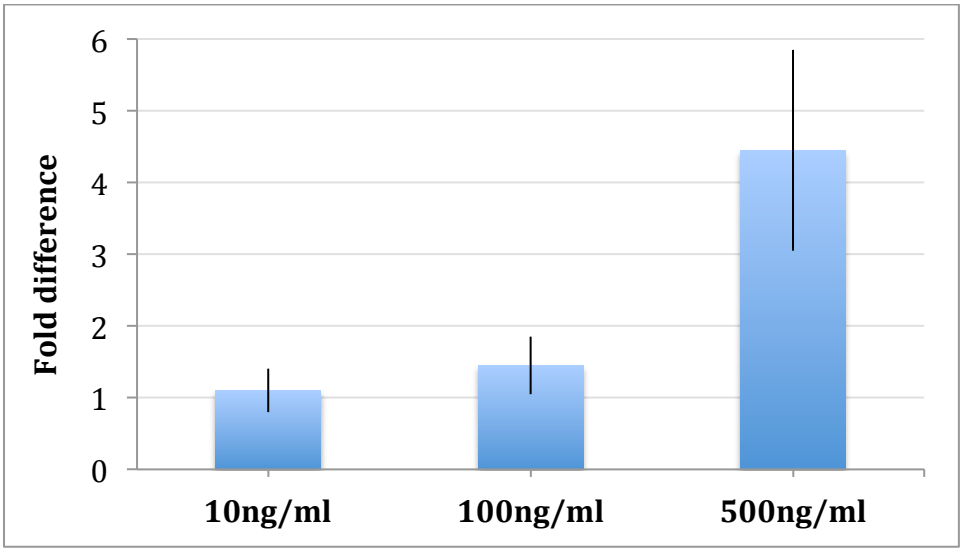

Figure 5.2. NIKS-HPV16 genome copy number at 72 hours compared to HPV16 genome copy number at plating (0h). NIKS-HPV16 populations were harvested at 72 hours post-plating and DNA extracted from cell pellets. During the 72 hours time period the NIKS-HPV16 cells were treated with 10ng/ml, 100ng/ml and 500ng/ml EGF. Quantitative PCR analysis was used to determine the absolute copies of HPV16 genome and GAPDH house keeping genes at plating time and 72 hours post-plating. The GAPDH copies were used to estimate the number of NIKS-HPV16 cells. The bar graphs show the average of three experiments and the error bars show the range.

5.2.1 EGF-rich medium treatment has a long-term effect on the increase the HPV16 genome copy number

During wound healing it has been suggested that the concentration of growth factors rises locally in the area of the injury in order to stimulate the proliferation of keratinocytes. Corneal wound studies have measured the concentration of EGF in the tears and demonstrated that the EGF concentration varies during the days following corneal trauma (Wilson et al., 1999). EGF levels rise up to 10 fold the standard concentration immediately following wound creation with its concentration in tears returning to the basal level within 24 hours of the onset of the trauma. A second significant peak in the EGF concentration was noted at 3 days post-wounding, suggesting that EGF rich environment persists for few days from wound creation (Wilson et al., 1999).

A highly concentrated EGF medium was used in our monolayer culture experiment to determine the effect of the wound healing response on the amplification of the viral genome and on pattern of viral gene expression. As showed earlier, using an EGF supplemented medium resulted in an increase in HPV16 viral copy number by 72h.

In order to determine the possible long-term effect of EGF treatment on HPV16 copy number we evaluated the number of viral genome copies 96 hours after EGF treatment. The experiment aimed to establish whether changes in the number of genome copies were sustained when the lower concentration of 10ng/ml EGF was re-established in the culture, as would happen in the days following epithelial wound.

To do this, NIKS-HPV16 cell populations were seeded at equal density in 7 six-well plates in order to obtain triplicate wells for each time point. The NIKS-HPV16 cells were cultured using three concentration of EGF, corresponding to 10-, 100-, and 500-ng/ml. The monolayer cultures (6 plates) were left in EGF enriched medium for 72 hours. A separate monolayer culture of NIKS-HPV16 cells grown in a 10ng/ml EGF Medium was used as control. After 72 hours, the first set of cells contained in three plates was harvested and DNA extracted for quantitative PCR analysis. In order to simulate the restoration of normal/steady-state of EGF after epithelial trauma, the remaining three plates of NIKS-HPV16 populations were kept in culture for further 96 hours in standard complete medium (10 ng/ml EGF), prior to harvesting and DNA extraction for quantitative PCR analysis.

The comparison of viral copy number obtained with the first and the second set of cells showed no significant variation. In fact, the cells cultured in the highest EGF concentrations maintained the viral copy number at unvaried levels when EGF had returned to basal levels (Figure 5.3).

This suggests that even short exposures to high concentration of EGF might trigger a mechanism that elevates the viral copy number in the infected cell. We hypothesize that such a mechanism would be advantageous during the early phases of viral infection when the number of viral copies in the newly infected basal cells is believed to be very low. The virus might have evolved a mechanism that exploits the particular environment that the infected cell finds itself in a wound situation

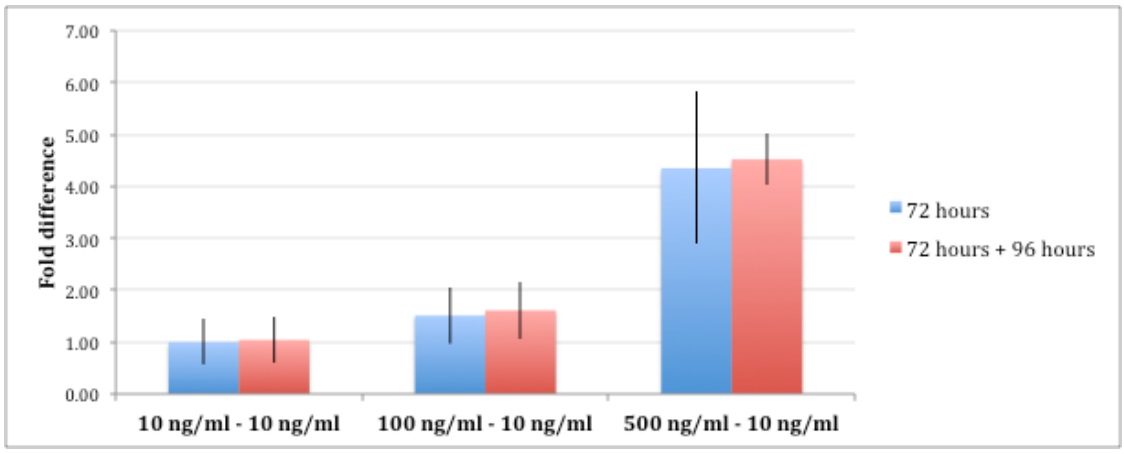

Figure 5.3 Evaluation of the copy number change in NIKS-HPV16 populations. NIKS-HPV16 cells were plated in equal number and cultured in complete medium supplemented with 10 ng/ml, 100 ng/ml or 500 ng/ml EGF in each plate. After 72 hours the monolayers were cultured for a further 96 hours in 10 ng/ml EGF only. The copy number estimated at 72 hours post plating and the copy number evaluated at 96 hours post-treatment were normalized with the copy number measured at plating point. The bar graphs show the average of three experiments and the error bars show the range. The experiment was repeated three times.

5.3 EGF treatment increases the HPV11 genome copy number but the effect is not maintained over time

As wounding of epithelia is necessary for HPV infection at some sites, virus establishment in the basal layers is thought to occur concurrently with tissue repair (Joyce et al., 1999; Kines et al., 2009). Thus, wound-healing responses might influence the establishment of viral infection. Moreover, it is plausible that the expansion of infected cells is essentially driven by proliferative stimuli from repairing cells during the early phases of wound healing. This would be particularly useful when low-risk HPV types infect the epithelium as we reported

that they are unable to drive proliferation of basal cells (Section 4.5.1). As shown previously in section 5.2, environmental changes such as changes in growth factor concentration are able to influence the levels of the viral genome contained in NIKS cells. To determine whether the concentration of EGF may interfere with the replication of HPV11 viral episomes, we performed a similar experiment using NISK-HPV11 populations.

NIKS-HPV11 populations were obtained by transfection of NIKS with full-length HPV11 genomes. The NIKS were harvested and plated on 60 mm 6-well plates at a density of $5x10^5$ cells per well on a layer of $1x10^5$ feeders and left to grow overnight in FC medium. Transfections were carried out using the Nucleofector® Transfection Equipment (Lonza) following the manufacturer's instructions. Cells were transfected with up to a total of 1 µg of circular DNA together with a blasticidin resistance plasmid, which were purified from bacterial cultures. Six hours after transfection cells were given fresh FC selective medium. Cells were cultured to confluence and HPV11 content was assessed using a quantitative PCR approach. The NIKS-HPV11 populations were harvested at confluence and re-seeded in (12) 60mm 6-well plates. The cultures were treated with increasing EGF concentrations as described in Section 5.2. Cells grown in a 10ng/ml EGF containing medium were used as control. Half of the cultured plates were harvested at day 1, 3, 5 and 7. These cultures, which were cultured in 10ng/ml EGF medium showed a constant level of viral genome copies (≅80 copies/cell) throughout the duration of the experiment (Figure 5.4A). The number of HPV11 copies contained at the plating time was used as reference. Results showed that HPV11 viral copy number remained unchanged.

The second set of NIKS-HPV11 populations was cultured in EGF enriched medium (500 ng/ml) (Figure 5.4B). The EGF treatment was maintained for 7 days and cells harvested at day 1 and every other day. DNA was extracted from cell pellets and HPV11 copies estimated with the use of the q-PCR. The data obtained showed that high concentration of EGF produce a stimulative effect in the replication of the HPV11 genome, similar to what showed in Section 5.2.1 for HPV16. Contrary to what was seen with NIKS-HPV16, the viral genome copies in NIKS-HPV11 cells were not maintained over time. The HPV11 copy number increased during the first three days of treatment but had returned to pre-treatment level by day 7.

We believe that the mechanisms underlying the decrease in the viral copy number in cells transfected with HPV11 genome are worth investigating.

A

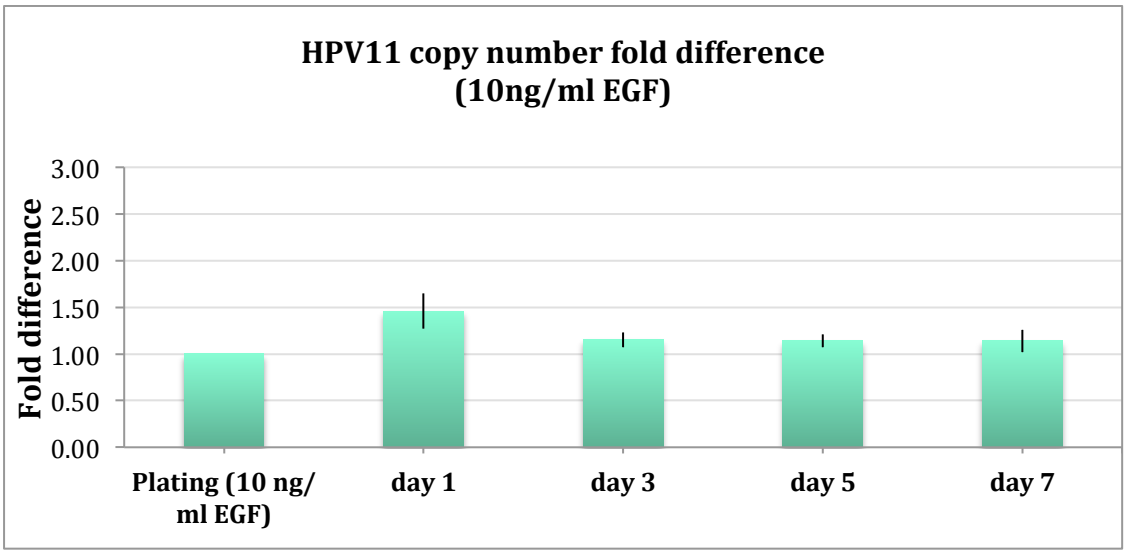

B

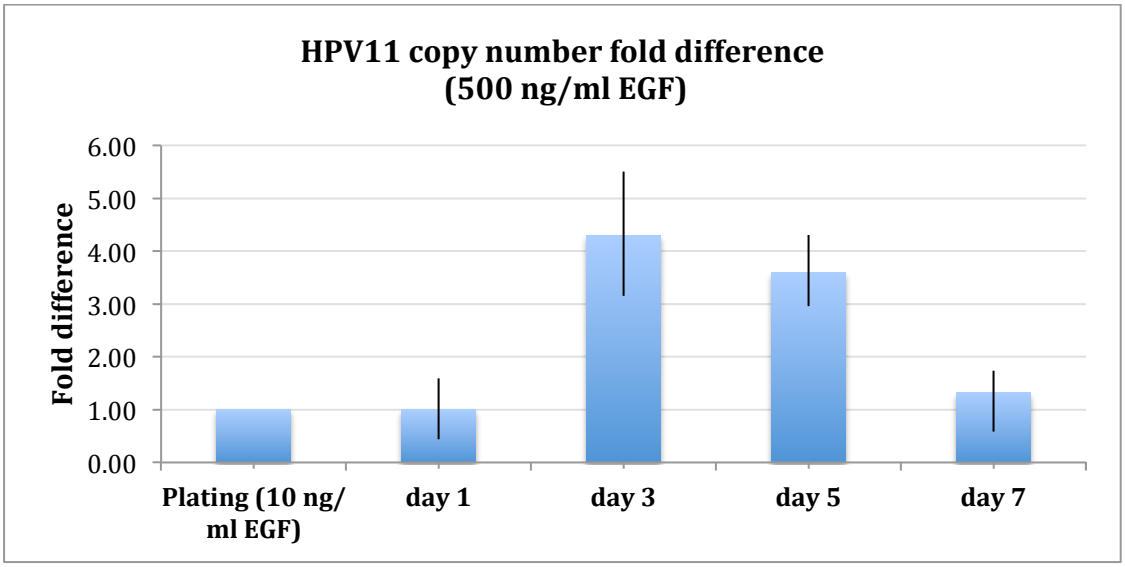

Figure 5.4 NIKS-HPV11 copy number variations in monolayer cultures. (A) Viral genome copy number variation amongst cells cultured in standard medium. (B) Viral genome copy number variation amongst cells cultured in EGF-rich medium (500 ng/ml). GAPDH was used as reference control gene. The copy numbers of the HPV11 genome at each time point were normalised to those measured at plating point. The bar graphs show the average of three experiments and the error bars show the range.

5.4 EGF concentration correlates with NIKS-HPV11 and NIKS-HPV16 copy number increase

During the proliferative phase of wound healing, keratinocytes are stimulated by a variety of growth factors, cytokines and chemokines. It is plausible that the duration of such stimuli varies depending on the tissue and the severity of the injury. To look at this, we have reproduced *in vitro* such conditions by altering the concentration of EGF in the culture medium. This was increased up to 500 ng/ml and cells were analysed for HPV genome content. As shown previously for HPV16 the EGF treatment also stimulated the replication of HPV11 viral genomes.

In order to compare the effects of EGF concentration on the low-risk and high-risk HPV types, we went on to reproduce the experiment using NIKS transfected with HPV11 and HPV16 genomes. NIKS cells were transfected in parallel and once the presence of viral genome had been established the cells were cultured to 50-60% confluence and then re-plated in triplicate culture plates. The medium added to the culture plates was equal except for the content of diluted EGF. Three concentrations were used to culture the cell populations: 10 ng/ml, 50 ng/ml and 500ng/ml.

The cells were cultured 72 hours and viral copy number was analysed with q-PCR.

Both cell populations displayed a similar increase in the viral copy number (Figure 5.5). Interestingly, the number of genome copies was not similar between the two cell populations, with the HPV16 genome-containing NIKS having a greater number of copies.

In conclusion, an EGF-rich medium stimulates HPV-containing cells, resulting in an increase in the quantity of genome copies. This effect is common to both low-risk and high-risk HPV types analysed during the proliferative time frame (0-72 hours) (Figure 5.5).

However, as shown earlier, the NIKS-HPV11 cells are not likely to maintain a high virus copy number and return to basal level when cells are confluent. Furthermore, the number of established HPV11 copies in the transfected NIKS is always lower than that observed for NIKS-HPV16, suggesting that low-risk HPVs may ideally establish in slow-cycling cells or cells with a specific phenotype.

The significant effect on the viral copy number obtained with a temporary EGF treatment show that HPVs have evolved to exploit the transitory conditions created during wound healing.

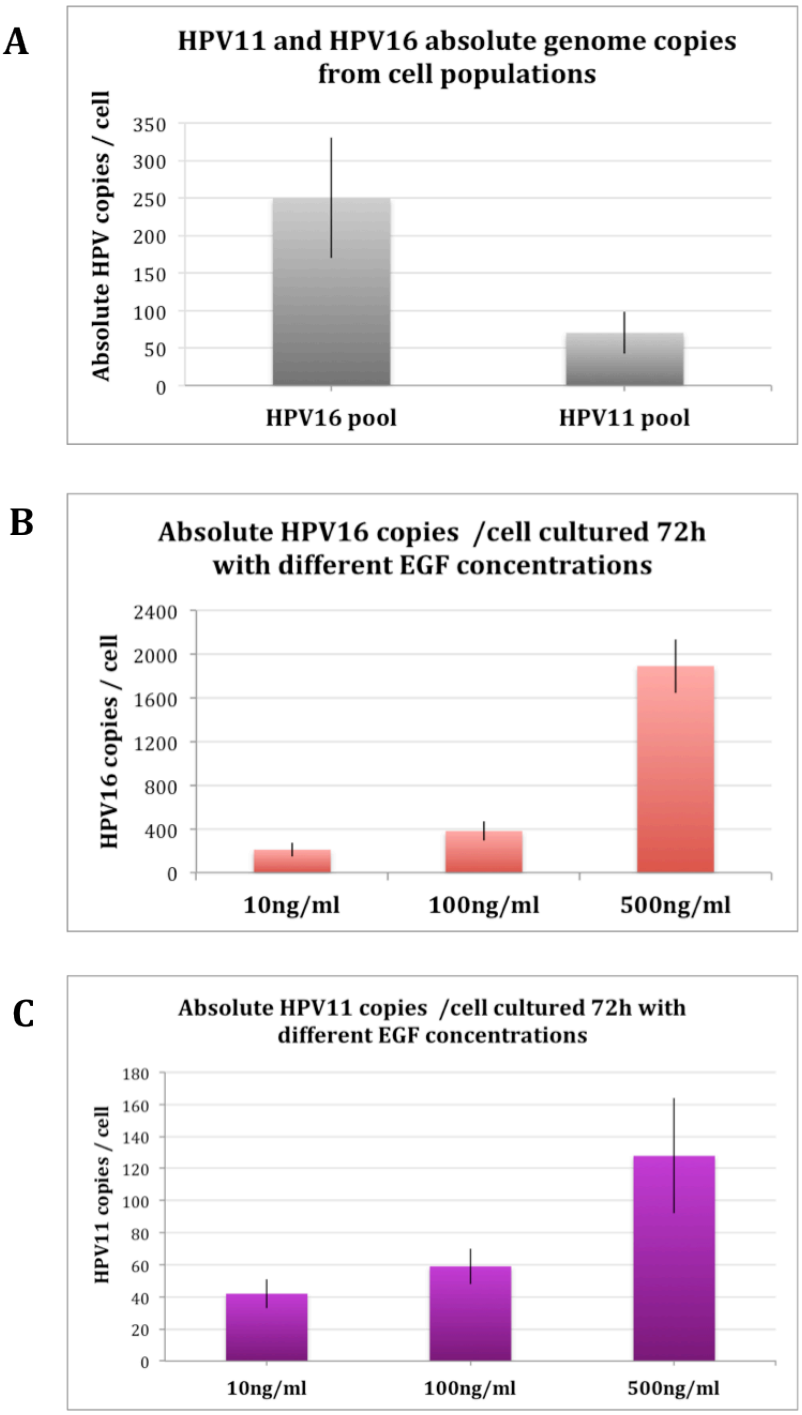

Figure 5.5. Absolute viral genome copies measured in NIKS-HPV16 and NIKS-HPV11 populations. (A) Average from three independent experiments of the absolute viral genome copies measured in NIKS cells after genome transfection. (B-C) HPV16/11 copies in NIKS cultured with different concentrations of EGF. The bar graphs show the average of three experiments and the error bars show the range.

5.5 Increasing EGF concentration does not produce a proliferative effect in monolayer cultures

Treating NIKS-HPV11 and NIKS-HPV16 populations with increased concentration of EGF lead to an increase in the of genome copy number in the transfected NIKS. The effect is particularly noticeable in NIKS-HPV16 cells, which maintain the elevated copy number for an extended period of time, once the EGF stimulus was removed. NIKS-HPV11 cells were also stimulated by the high-EGF medium to increase copy number, but the copy number rise was only transient. EGF has well-established growth-stimulative properties, and thus we aimed to determine whether the high EGF concentration could also lead to an increase in cell number during monolayer growth.

In order to understand whether the EGF concentration used in the latter experiment could also lead to enhanced cell proliferation in monolayer, we went onto develop a specific growth assay. This proliferation assay was carried out using both NIKS-HPV11 and NIKS-HPV16 cell populations.

Cells were seeded for measurement of proliferation rate, which was conducted without blasticidin selection. Cultures were harvested for proliferation measurement every at day 1 and every 48 hours for a total of 7 days. Triplicate wells were set-up for each cell type and time-point.

The results show NIKS-HPV16 cells cultured at high EGF concentration (50 ng/ml and 500 ng/ml) produce a greater number of cells by day 5 and day 7 than NIKS-HPV16 cultured in standard medium (10 ng/ml) (Figure 5.6). Interestingly the number of NIKS-HPV16 cells counted at day 3 was lower than NIKS-HPV16 cells cultured in standard EGF medium. Although the cell number increase was modest

we believe that the medium rich of growth factors allowed the NIKS-HPV16 cells to proliferate more efficiently post-confluence. Contrary to this, culturing NIKS-HPV11 cells in EGF rich medium did not produce any appreciable effect on the number of the cells counted at any time-point.

Thus, we conclude that NIKS-HPV16 and NIKS-HPV11 populations contain elevated copies of the viral genome when exposed to high concentrations of EGF (Figure 5.5), but do not necessarily show a concomitant elevation in cell proliferation. We hypothesise however, that cells containing a greater number of viral genome copies may have limited proliferative ability due to a more robust activation of cellular mechanisms of DNA replication control (DDR), or other inhibitions signals in response to the replication of foreign viral DNA within the cell. It is plausible that NIKS cells containing HPV16 may have a more effective ability to overcome the DDR check points, whereas NIKS-HPV11 cells are more susceptible of being inhibited, given that HPV11 genomes appear not to be maintained long-term in rapidly dividing cells *in vivo*.

We believe that the role of the DNA damage response pathways in NIKS-HPVs cells is worth investigating to examine these hypotheses.

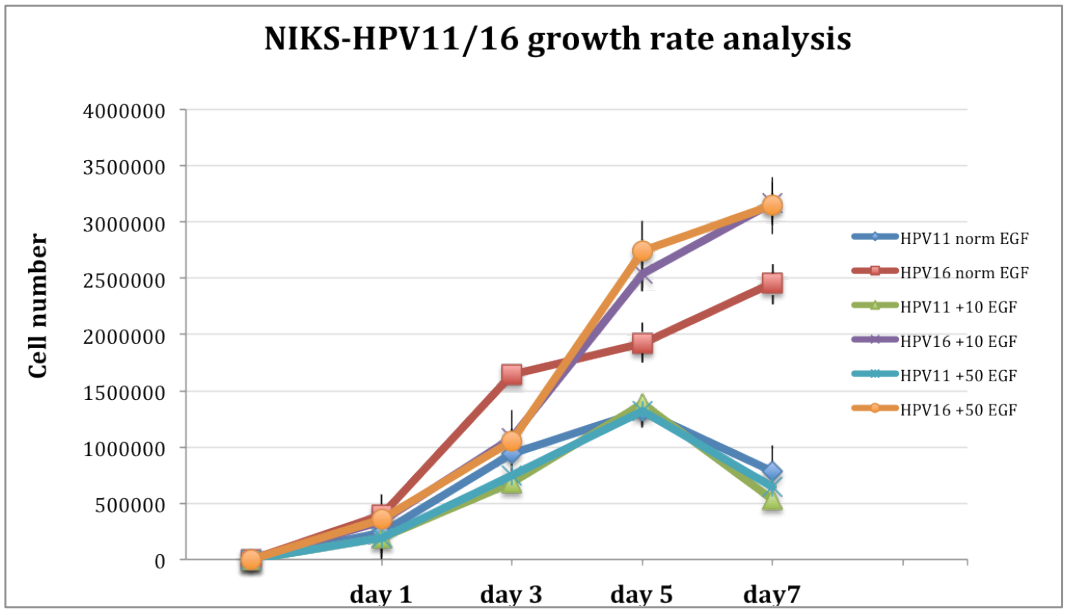

Figure 5.6. NIKS-HPV11 and NIKS-HPV16 growth assay. Cells were cultured seven days in Medium containing different concentration of EGF (norm=10ng/ml; +10=100ng/ml; +50= 500ng/ml). The cell number of six different wells/time points was obtained using a coulter counter. Cell numbers were averaged for each time point and plotted in a chart. The error bars represent the standard error of the measured values.

5.6 NIKS-HPV16 cells exposed to high concentration of EGF show variations in the splicing pattern of E6/E6* mRNA

As mentioned in the introduction, two main promoters, the early p97 and the late p670 promoter regulate HPV16 gene transcription. The activation and suppression of these promoters is differentiation dependent, and results in the production of a number of polycistronic mRNAs (Figure 1.10). Differential splicing can further regulate the polycistronic mRNAs (Jia et al., 2009; Schwartz, 2008). Alternative splicing of the early pre-mRNAs leads to the translation of a number of functional proteins such as E6, E6* and E7, which have specific biological functions (Grassmann et al., 1996; zur Hausen, 2002).

Alternative splicing can also be regulated by extracellular stimuli as a number of pathways and splicing factors have been discovered that regulate this process (Blaustein et al., 2007). Amongst these exogenous stimuli, growth factors activated signal pathways are known to influence the splicing patterns of a number of genes, including CD44v5 and fibronectin. The mechanism by which the growth factors exert these functions includes activation and suppression of different splicing factors leading enhanced exon exclusion (Blaustein et al., 2007).

With regard to HPVs, splicing of the polycistronic E6/E7 mRNA produces a new ORF termed E6*, where the first 5' exon is excluded. The E6* mRNAs have been described only in high-risk HPVs (Zheng and Baker, 2006). In particular, the E6 gene of HPV16 has the potential to encode full-length as well as truncated E6 proteins (E6*I and E6*II) by alternative splicings. HPV16 E6*I alternative splicing is produced via exclusion of a 183-bp fragment of the E6 ORF, which leads to a premature termination codon. Interestingly, only full-length E6 demonstrate

transforming capacity. E6* ORF species are the most abundant transcripts in HPV16 caused lesions, cervical carcinoma biopsies and in explanted carcinoma cell lines (Bohm et al., 1993). E6* protein functions include the modulation of E6 in HPV18 by rescuing the p53 levels *in vivo* and, in HPV16, the 8-kDa E6* protein can induce apoptosis by stabilizing procaspase-8 which is otherwise targeted by E6 (Filippova et al., 2007; Pim and Banks, 2010).

Although some biochemical differences regarding the different E6 isoforms have been examined, less information exists about the regulation of alternate splicing *in vivo* and its biological function within the epithelia (Schwartz, 2008). Additionally, the *in vivo* regulation of E6/E6* splicing is not yet fully understood.

Interestingly, a recent study has suggested that HPV16 E6 alternate splicing is dependent on the presence of EGF, and that the MEK1/2-Erk1/2 MAP kinases act as key regulatory components in promoting or inhibiting the exon exclusion (Rosenberger et al., 2010). This study suggests a model for HPV16 viral oncogene regulation during cell differentiation, as the concentration of EGF is known to vary in the differentiating epithelia (Collins et al., 2005).

Because EGF concentration also varies during wound healing we aimed to monitor HPV16 oncogene alternative splicing in our monolayer model system.

To determine the E6/E6* ratios produced from the viral episomes, we used specific primers covering the complete first alternative exon (Figure 5.7A). When NIKS containing the HPV16 genome were exposed to a high concentration of EGF (100 ng/ml or 500 ng/ml) we detected an increased level of E6 full-length mRNA compared with the untreated samples (Figure 5.7B).

These data suggest that EGF concentration is capable of interfering with the regulation of HPV16 viral oncogene regulation. We hypothesize that during wound healing, the virus may require high levels of E6 to prevent apoptosis and to elevate copy number by creating a more sustained replication competent environment. Such a mechanism might be brought about by the high concentration of growth factors at the site of infection. When the wound is repaired the concentration of EGF would be expected to return to basal level and the virus may require an alternate splicing pattern in order to properly regulate basal cell proliferation and to maintain or increase E7 production, which is beneficial to the virus as it can enhance the proliferation rate of the basal and parabasal cells.

We have shown that EGF levels are involved in the mechanism of E6/E6* alternate splicing regulation in cells harbouring viral episomes *in vitro*. Further investigation will be necessary to assess the mechanism by which the E6/E6* splicing regulation is achieved and to understand whether splicing patterns of other ORFs are also altered by the concentration of growth factors.

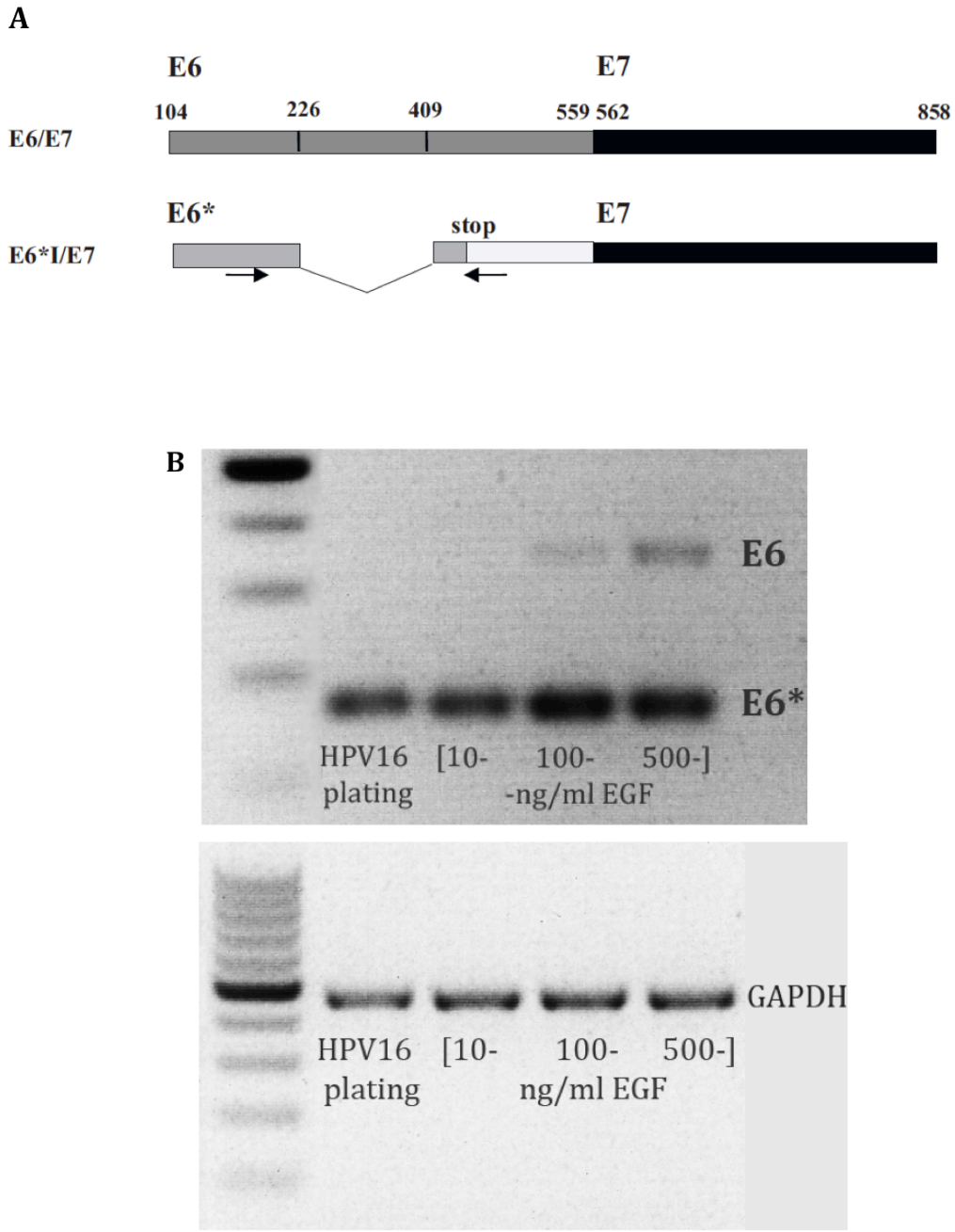

Figure 5.7 Analysis of splicing patterns in NIKS-HPV16 cells. (A) Organization of HPV16 E6/E7 and E6*/E7 early mRNA; base pair numbers are given relative to HPV genome localization. Exclusion of the exon 226-409 results in formation of E6* ORF, which contains a premature stop-codon. Arrows indicate primer localisation for semi-quantitative RT-PCR. (B) Analysis of E6 splicing pattern in NIKS-HPV16 populations treated 72h with Medium containing different concentration of EGF (10 ng/ml; 100 ng/ml; 500 ng/ml). GAPDH primers were used as control.

5.7 Exogenous EGF treatment affects EGFR expression and its related molecular targets in NIKS-HPV cells

It is known from a number of studies that EGF is a mitogen for oestrogen receptor (ER). It has been shown that EGF mimics the oestrogen functions and cross-talk with ER-α to exert its activity (Clark et al., 2001). The EGFR is highly expressed in breast and ovarian cancers (Arteaga, 2002; Yokota et al., 1986). As mentioned earlier, the EGFR half-life is influenced by the expression of the HPV protein E5, which prevents the recycling of the receptor (Venuti et al., 2010). Recent studies performed on HPV-positive cervical cancer cell lines have demonstrated that the treatment with exogenous EGF stimulated the expression of EGFR (Narayanan et al., 2012). According to what has been reported in previous studies, the mechanism by which EGF stimulates the cell proliferation of cervical cancer cells upon exogenous treatment might be dependent on the activation of the EGFR and Cyclin D1 (Narayanan et al., 2012). EGF also stimulates NIKS cellular proliferation via the EGF signaling pathway (Roy and King, 2013).

We hypothesize that in our wound healing model system the expression of the EGF receptor might be influenced by the extensive and/or prolonged EGF administration.

To determine whether the amount of EGF contained in the culture medium has an effect on EGFR expression we decided to estimate the EGFR level using a western blotting approach.

NIKS HPV-negative and NIKS-HPV16 cell lines were initially cultured in standard medium for a period of seven days and cell pellets harvested for protein analysis.

This preliminary analysis was carried out in order to understand whether the confluence state of the monolayer culture had an effect on EGFR expression.

The western blot analysis showed that in the samples containing the HPV16 genome, the expression of EGFR increased compared to the samples not containing the virus when confluence was reached (Figure 5.8A).

Thus, in order to counter the possibility that the expression of EGFR was altered by the confluence state of the cells we decided to successively culture the NIKS-HPV16 genome containing cells up to 72 hours. The culture media used in these experiment was supplemented with EGF in order to reach the concentration used in the previous experiments. The EGF concentrations employed were 10 ng/ml, 100 ng/ml and 500 ng/ml. The cells cultured for 72 hours were harvested and protein levels assessed using specific EGFR antibodies.

The western blot showed an increase in EGFR expression in the NIKS-HPV16 cells cultured with 100 and 500 ng/ml of EGF (Figure 5.8B).

These data suggest that exogenous EGF is able to alter the number of the EGF receptor present on the cell surface.

We hypothesise that the number of the receptors may be increased in response to the EGF treatment and that their half-life may be elongated by the expression of viral proteins such as E5.

The increased EGFR expression levels and the change in viral copy number led us to investigate the effects of exogenous EGF treatment on the various molecular targets of EGFR. To do this, we examined the transcription levels of EGFR, Akt-1,

Cyclin D1 p21, p53, Caspase-3 and GAPDH. The RNA was extracted from EGF-stimulated cells and a quantitative RT-PCR was performed.

Although we have not examined EGFR expression increase in NIKS-HPV11 samples, we also performed the RT-PCR analysis on NIKS-HPV11 populations cultured 72 hours in culture medium containing 10ng/ml, 100ng/ml and 500ng/ml EGF.

Using qPCR, we found on average a >2.0-3.0-fold increase in p21, Caspase-3, and p53 transcripts levels in the samples treated with 100ng/ml and 500ng/ml EGF when compared to cells grown at 'normal' EGF levels (Figure 5.9). Exogenous EGF did not significantly alter the transcript levels of Cyclin D1 and EGFR, suggesting that cell proliferation at the G0➔G1➔S boundary was not stimulated. A decrease of >2.0-3.0-fold of the steady state level of Akt mRNA in the samples stimulated with 100ng/ml and 500ng/ml was also measured (Figure 5.9).

Collectively, these data suggest that culturing NIKS-HPV11 cells with high concentration of EGF does not produce a stimulatory effect in terms of cell proliferation as the mRNA level of EGFR and MAP kinase (Akt-1) and Cyclin D1 were not significantly altered.

Contrarily, the level of EGFR, Akt, Cyclin D1, and p53 transcripts were significantly increased by EGF stimulation in NIKS-HPV16 treated cells (Figure 5.10). A greater stimulatory effect was obtained by culturing NIKS-HPV16 cells with medium containing 100ng/ml and 500ng/ml EGF. Although we did not observe a significant difference in the level of mRNA expression for p53 following EGF stimulation, the steady state level of mRNA of p21 and Capsase-3 were

decreased by EGF treatment, suggesting a negative regulation of the tumour suppressor genes.

We also have observed an increased p97 promoter activity as consequence of EGF stimulation (Figure 5.11). However, such effect might not be common to low-risk HPVs, as two independent promoters regulate the transcription messages that contain the E7 ORF (DiLorenzo and Steinberg, 1995).

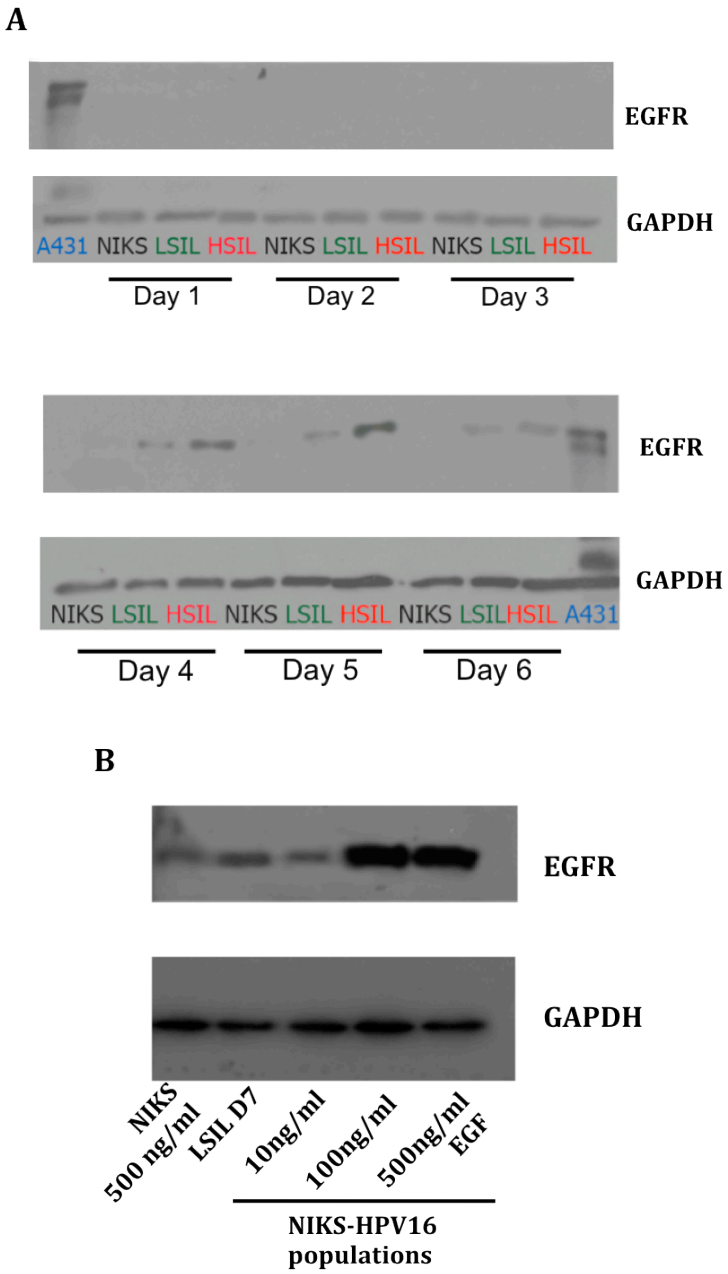

Figure 5.8 Expression level of EGFR in NIKS and NIKS-HPV16 clones and populations. (A) Expression level of EGFR was determined by western blot analysis on protein extracts from NIKS and NIKS-HPV16-HSIL and -LSIL clones cultured over a period of 6 days in monolayer. The A-431 cell extract was used as comparative positive EGFR control. (B) Western blot analysis of EGFR indicating a specific stimulatory effect by exogenous EGF administration (10ng/ml, 100ng/ml and 500ng/ml) to the culture medium. NIKS-HPV16 populations were cultured in monolayer for 72 hours. NIKS (EGF 500ng/ml) and NIKS-HPV16 LSIL (EGF 10ng/ml) samples were used for comparative analysis.

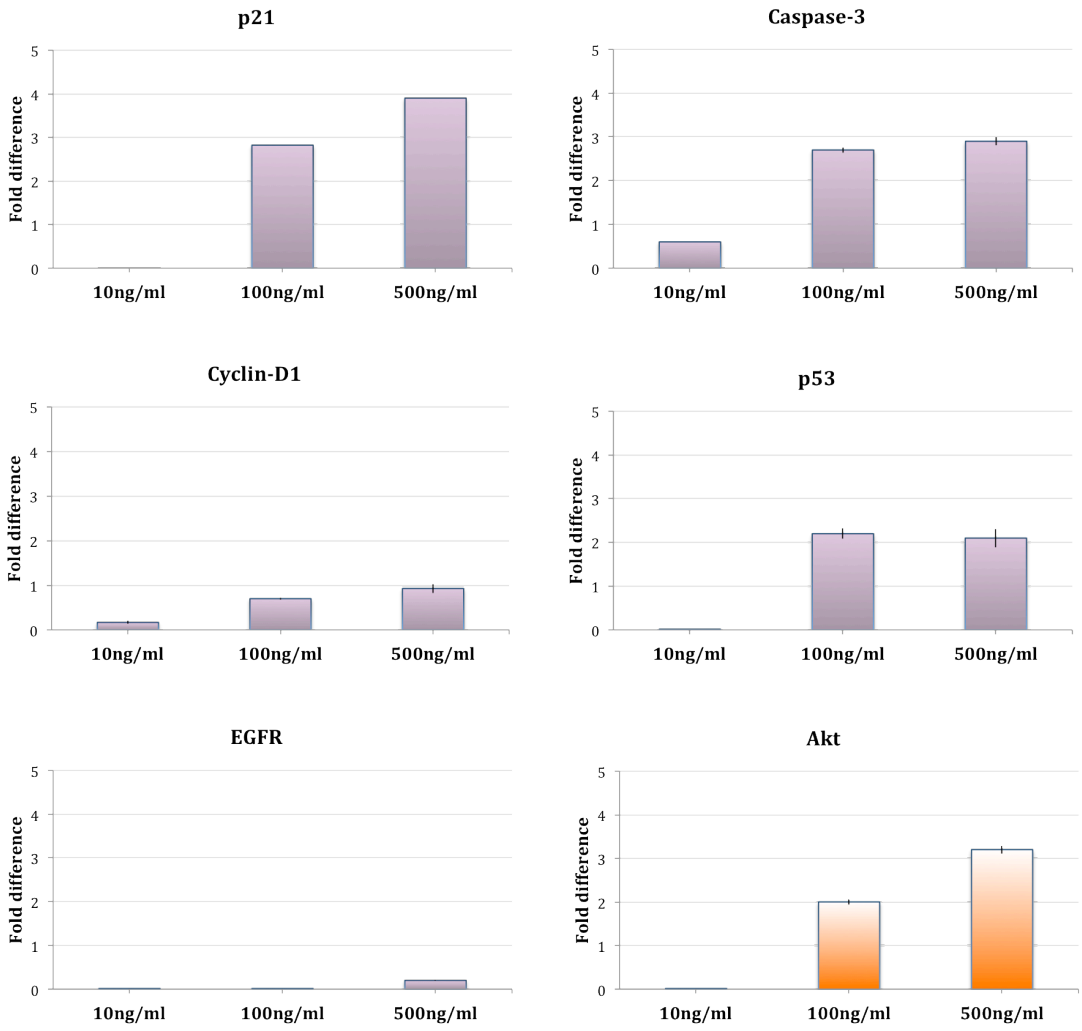

Figure 5.9 Quantitative real-time RT-PCR analysis of EGF-modulated molecular targets in NIKS-HPV11 populations. The mRNA expression level of EGFR, Akt, Cyclin D1, p53, p21 and Caspase-3 was determined by performing quantitative RT-PCR analysis with the total RNA extracted from EGF-stimulated NIKS-HPV11 cells cultured in monolayer for 72 hours using 10ng/ml, 100ng/ml and 500ng/ml of EGF. The fold increase in the expression level was normalized to the expression level measured at seeding point. GAPDH expression was used as reference gene. Expression levels of Akt indicate >2.0-3.0-fold decrease in the 100ng/ml and 500ng/ml samples respectively. The data presented generated from the mean values of three independent experiments and the standard deviation (±) is presented as error bars.

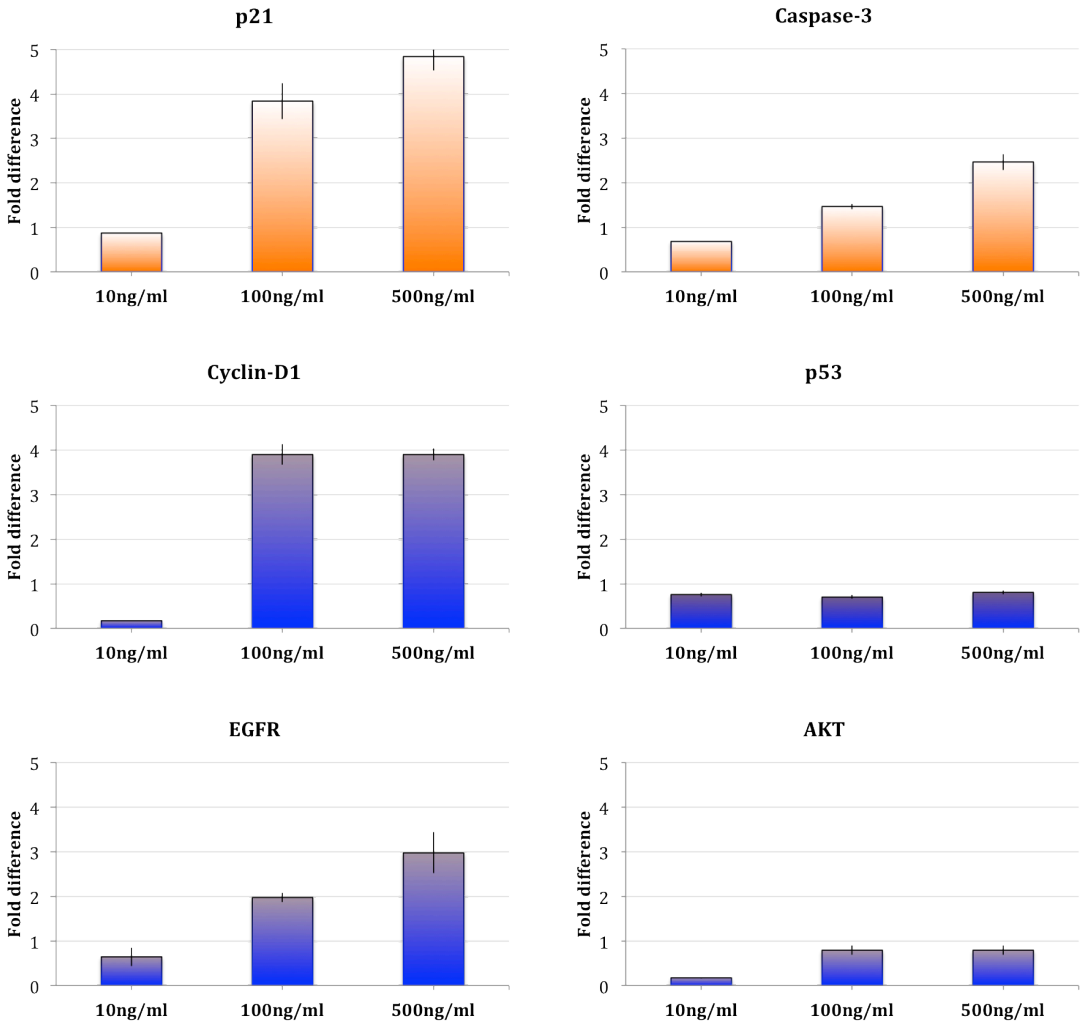

Figure 5.10 Quantitative real-time RT-PCR analysis of EGF-modulated molecular targets in NIKS-HPV16 populations. The mRNA expression level of EGFR, Akt, Cyclin D1, p53, p21 and Caspase-3 was determined by performing quantitative RT-PCR analysis with total RNA extracted from EGF-stimulated NIKS-HPV16 cells cultured in monolayer for 72 hours, using 10ng/ml, 100ng/ml and 500ng/ml of EGF. The fold increase in the expression level was normalized to the expression level measured at seeding point. GAPDH expression was used as reference gene. Expression levels of p21 and Caspase-3 indicate >2.0-4.5-fold decrease in the 100ng/ml and 500ng/ml samples respectively. The data presented generated from the mean values of three independent experiments and the standard deviation (±) is presented as error bars.

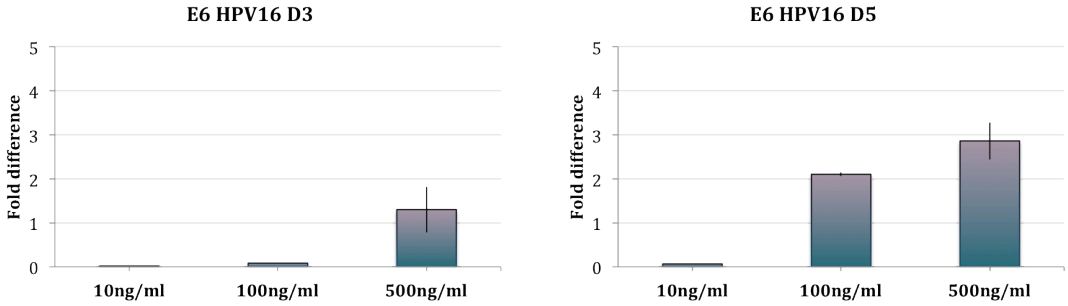

Figure 5.11 Quantitative real-time RT-PCR analysis of E6 transcripts in NIKS-HPV16 populations. The mRNA expression level of E6 mRNAs was determined by performing quantitative RT-PCR analysis with total RNA extracted from EGF-stimulated NIKS-HPV16 cells cultured in monolayer for 3 and 5 days, using 10ng/ml, 100ng/ml and 500ng/ml of EGF. The fold increase in the expression level was normalized to the expression level measured at seeding point. GAPDH expression was used as reference gene. Expression levels of E6 indicate >2.0-3.0-fold increase at day 5 in the 100ng/ml and 500ng/ml samples respectively. The data presented generated from the mean values of three independent experiments and the standard deviation (±) is presented as error bars.

5.8 Discussion

In Chapter 5 we have shown that exogenous growth factors interfere with the production of HPV viral genome in the NIKS transfected cells. More specifically the experiments have shown that by increasing the amount of available EGF in the culture medium, an increased number of the viral copies could be detected. We have also observed that such increase in the EGF administration was well tolerated by the keratinocytes in culture. Thus, we speculate that in an EGF rich environment, the presence of the growth factors may have a significant effect on

viral copy number. Overall the amount of viral copies in HR-HPV transfected cells increased significantly, suggesting that such HPV types are particularly susceptible to changes in the external environment. Interestingly, we reported that although the LR-HPV types showed a similar copy number increase, the copy number per cell was lower than HR-HPV transfected cells. We therefore raise the possibility that NIKS cells may tolerate HPV16 viral episomes better than HPV11 genomes, where the viral copy number was found to decline.

In NIKS-HPV16 cells after EGF treatment the elevated copy number was maintained long-term at the higher levels. In contrast, in NIKS-HPV11 cells, the copy number increase caused by the administration of increased exogenous growth factors was not maintained upon continued growth. We therefore hypothesise that during the initial phases of PVs infection, infected cells containing LR-HPV types would benefit from the presence of high concentrations of growth factors as this could stimulate an initial rise in genome copy number. The inability of NIKS-HPV11 to maintain a high number of genome copies might be related to the inefficiency of HPV11 in counteracting the host cell mechanisms that control the replication of exogenous DNA.

The spontaneous rise in HPV episomal levels after EGF administration was a recent finding with the NIKS monolayer system. Previous studies have shown that the levels in growth factors increase during wound healing (Cribbs et al., 2002; Schultz et al., 1991). Therefore we speculate that during viral infection, the basal cell environment enriched ingrowth factors may play a fundamental role in the establishment of a successful HPV infection.

We have also made an interesting correlation between the levels of exogenous EGF and HPV16 viral genome expression. In this case, we found that when high concentrations of EGF were added to NIKS-HPV16 cell cultures, the levels of E6 and E6* transcripts were altered. In particular we found that high levels of EGF increase the expression of HPV16 E6 full-length mRNAs. Therefore, it is reasonable to assume that during initial phases of viral infection HR-HPVs might require high levels of full-length E6 to prevent apoptosis. Interestingly, recent studies using cervical cancer cell lines have also shown that changes in EGF levels in the culture medium can modulate E6/E6* splicing patterns (Collins et al., 2005; Rosenberger et al., 2010).

When we studied the effects of exogenous EGF we also found that this produced an increased expression level of the EGF receptor. The downstream effects of EGFR activation may contribute to cell proliferation and the enhancement of viral genome amplification. Thus, we decided to look at the EGFR molecular targets that may be altered by the presence of exogenous EGF. Preliminary data suggest in fact, that in the NIKS-HPV16 cell populations, the activation of EGFR contributes to the proliferative response when monolayer cells reach the confluence state. I found also that at this stage the HPV16 E6 transcripts increased, which might be as a result of the activation of the p97 promoter. By contrast, the EGFR targets analysed in NIKS-HPV11 cells showed that exogenous EGF did not produce a proliferative stimulus as seen in NIKS-HPV16 cells. These observations suggest that different mechanisms might control cell proliferation in NIKS-HPV11 and NIKS-HPV16 cell populations. Further investigations are necessary to elucidate the molecular pathways involved.

Although these data suggested that NIKS-HPV16 cells might have a proliferative advantage when EGF is administrated at high concentration, we observed a modest increase in the number of cells produced during a seven-day growth period. As EGF treatment had no significant effect on the cell proliferation of NIKS-HPV11, we hypothesize that host cellular mechanisms that control the replication of exogenous DNA may be activated in response to the increased copies of viral genome contained in the cells. These responses limit our ability to study HPV11 in cell culture models at the moment. In vivo, this limitation may control the expansion of the LR-HPV infections; perhaps to restrict immune system intervention that would otherwise eliminate infected cells. This strategy might differ between low- and high-risk types. We also hypothesise that in NIKS-HPV16 cell populations the activation of the DNA Damage Responses (Edwards et al., 2013) might be better tolerated as a modest increase in the cell proliferation was measured in the growth assay. Future work will be aimed at understanding the role of these pathways in HPV lesion formation.

6. Final discussion

6.1 General Discussion

Despite the recent introduction of prophylactic vaccines for cervical cancer and other HPV-associated diseases, it is estimated that this will not dramatically affect the burden of cervical cancer for 30-50 years (Stanley, 2012). Although most work so far has focused out on the study of high-risk HPV types such as HPV16 and HPV18, it is necessary to increase the understanding of the different risks associated with different HPV types, pursuing also the understanding of the molecular pathways that these viruses destabilise. Advancements in these areas are likely to yield better strategies for disease treatments, which are necessary to complement current methods of disease management and disease prevention. Furthermore, it will also be necessary to extend the knowledge of the high-risk associated disease occurring not only at cervical sites, but at other important sites as well, such as the oropharynx and oesophageal squamocolumnar junction. A final important area of study focuses on the mechanisms by which low-risk HPV types produce benign lesions, such as laryngeal-papillomatosis, which in some rare cases can progress to cancer.

In this thesis we have examined the mechanisms of lesion formation caused by HPV. To accomplish this, we have developed a model system in which we can mimic in the most reasonable way, the environment in which a HPV lesion are thought to develop.

Initially, I characterised the model system that has been used in this study. Experiments were performed to understand the dynamics of the infected cell, in the way that they proliferate and migrate, as would happen during the initial

phases of HPV infection following a micro wound. The work presented in this thesis also focuses on the comparison of different HPV types using this model system. Comparison of HPV11 and HPV16 episome-containing NIKS revealed that cells containing low-risk HPV genomes (unlike those containing the high-risk HPV) lacked the ability to enhance cell proliferation rate. The inability of low-risk HPV containing cells to form large colonies in a competitive growth environment suggest such HPV types lack an important characteristic that high-risk HPV types can impart on NIKS cells. These observations support the hypothesis that HPV11-containing cells, and maybe also other low-risk HPV types cannot impart a highly proliferative phenotype onto the cells that they infect. This hypothesis is compatible with observations made on clinical lesions caused by HPV11 and HPV16, as discussed in Section 1.6. This comparative study is also in accordance with recent reports in which the authors suggest a disadvantageous growth of HPV11 containing cells in culture (Kaczkowski et al., 2012; Klingelhutz and Roman, 2012). In this study, I have made use of exclusively of episomal cell lines, which are grown in an undifferentiated basal-like environment, which we believe provides us with key insight into the differential biologies of the LR- and HR-HPVs.

The role of the basal-cell environment in the formation of an HPV lesion was evaluated, considering in particular the hypothesis that many infections occur following creation of epithelial trauma that exposes the basement membrane and allows the attachment of the virus (Kines et al., 2009). Following this hypothesis, we aimed to recreate *in vitro* the conditions that would be comparable to those

created during wound healing. We focused initially on understanding the dynamics of repopulation of the HR-HPV containing NIKS in a scratched area of a keratinocyte monolayer culture *in vitro*. The data obtained showed that the 'infected' cells (in this case cells transfected with recircularised HPV episome) have the ability to proliferate and migrate at a greater speed than 'uninfected' cells. It is plausible to hypothesize that such a phenotype would confer a competitive advantage to the infected cells during wound healing. Thus, in accordance with previous investigations that employed cancer cell lines expressing HR-HPV oncogenes (Au Yeung et al., 2011; Valencia et al., 2008), we report for the first time that in an *in vitro* system the presence of HR-HPV viral episomes can similarly induce a highly proliferative phenotype to the 'infected' cells in a wound like environment.

This study was extended to look at the additional effects that a growth factor-rich environment might produce on the behaviour of the infected cells. In fact, during normal wound healing the cells not only have increased space to proliferate, but they are also actively stimulated by the presence of higher concentration of growth factors than they would be in unwounded epithelium (Sheardown and Cheng, 1996). Under normal circumstances, the presence of such growth factors is necessary to increase the proliferation of cells at the wound site. We have tested the effect that an increased concentration of EGF has on episomal genome replication and viral gene expression from viral episomes. Interestingly, the rise in EGF concentration corresponds to an increase in viral genome copy number in both HPV16 and HPV11 genome-containing cells. The effect on HR-HPV genome replication was however greater, and was more prolonged. Although I report here

that NIKS cells containing either HPV16 or HPV11 are responsive to EGF stimulation, our observations are in contrast to previously inhibitory reported effects of EGF on HPV16 E6/E7 gene expression (Yasumoto et al., 1991). The sustained effect of EGF on genome replication seen in the NIKS HPV16 cells suggest an important role for external signalling in the establishment of HR HPV types. If we are correct that HPV11 persists long-term in slow cycling stem-like cells without an elevation in cell proliferation rate, then it may be that EGF also contributes to an elevation in copy number soon after infection here as well. Having made observations on EGF-mediated copy number regulation, we next evaluated the effect of increasing concentrations of EGF on viral gene expression. Recent work has suggested that an epithelial EGF gradient can control the splicing of E6/E7 transcripts (Rosenberger et al., 2010). Although such studies were carried out using cancer cell lines that contain integrated HPV sequences, and which express high level of viral oncogenes, we wondered whether wound healing-like changes in EGF levels may exert similar effects on NIKS-HPV16 episomal lines. Indeed, when high concentrations of EGF were added to the culture medium, HPV16 E6 mRNA were found to become more abundant. We hypothesize that the activation of EGFR is necessary to modify the balance between E6* and E6 after infection and to elevate the level of the E6 protein. In normal epithelium, the expression of the EGFR can be detected throughout the epidermis, with elevated levels in the basal and parabasal layers (Nanney et al., 1984). Thus, EGFR activation and alternative splicing of the HPV early gene may be linked, especially during the early phases of infection and lesion formation. Such mechanisms might counteract apoptotic stimuli in newly infected basal

keratinocytes or enhance their growth potential. We also reported that an increased expression of EGFR was mediated by high levels of EGF in the culture medium in NIKS-HPV16 genome-containing cell populations. Such increases in EGFR expression seem however to correlate with increased cell proliferation only in NIKS-HPV16 cells. In fact, when we assessed whether the stimulative effect of EGF might correspond with an increase in cell proliferation, we found to our surprise that the proliferation of NIKS-HPV11 was not significantly altered by the increasing concentration of EGF. NIKS-HPV16 by contrast, showed an increase in cell number after the cells reached confluence, with the continuous stimulus appearing to push the cells to even a more extreme highly proliferative phenotype. In the context of HPV-mediated immortalization and transformation, it is plausible to hypothesize that the increased concentration of EGF could favour the production of full-length E6 protein expression, which is necessary for efficient p53 degradation. When the EGF concentration returns to resting levels, as when for example microwounds are repaired, the preferential E6 exon exclusion would result in a higher expression of E7, that would be expected to give to the infected cells a selective growth advantage during proliferation.. This might also explain the prevalence of E6* mRNA in most cervical carcinomas cells lines and high-grade cervical lesions *in vivo* (Bohm et al., 1993; Hafner et al., 2008). We also report an apparent increase in p97 promoter activity as a consequence of increasing EGF level in tissue culture (as evidenced by the increase in transcripts spanning E6/E7 region (Fig. 5.11)). However, such mechanism is not likely to be preserved in low-risk HPVs such as HPV11, as two independent promoters regulate the transcription of mRNAs that encode the E6

and E7 gene products (DiLorenzo and Steinberg, 1995). We have not measured the level of the HPV11 E7 proteins or compared them with the expression levels of the high-risk E7 proteins in HPV16 NIKS cells. However, my data indicates clearly that HPV11 has no obvious proliferative effect on the phenotype of the NIKS cells following transfection. Furthermore, the administration of high concentrations of EGF to the culture medium produced only a temporary fluctuation in the HPV11 copy number, with no significant growth advantage apparent when elevated concentration of EGF were added to the culture medium. Upon extended passage of cells in culture, I also observed that the levels of HPV11 genomes decreased. The study of episomal maintenance in the HPV11 transfected cells is complicated by the lack of immortalizing ability of the low-risk HPV types. We believe that the inability of HPV11 genomes to be stably maintained in NIKS might be linked to the fact that HPV11 is not normally maintained in rapidly dividing cells *in vivo*. We therefore hypothesize that HPV11 genome may be better maintained in cells that more closely resemble the slow-cycling epithelial stem cell. Although the use of a different type of recipient cell was considered, previous investigations reported variation in episomal maintenance levels when HPV11 genomes were transfected into primary keratinocytes derived from diverse donors (Oh et al., 2004). We suspect that a slow-cycling clonal cell line derived from NIKS might be helpful in understanding the maintenance of low-risk HPV genomes however, and such slow cycling variant cell lines have now been isolated in the lab. Alternatively, host cell lines with compromised p53 expression may be used to examine the efficiency of long-term episomal maintenance and replication of low-risk HPV genome following transfection. Recent studies using in HPV18

transfected human primary keratinocytes, suggest that p53 and additional host proteins are involved in regulating viral DNA amplification (Kho et al., 2013). Such cells might also be useful in better understanding the biology of the low-risk E6 proteins, which do not inactivate p53 as efficiently as the high-risk E6 proteins, and show a weaker p53 binding and degradation ability (Klingelhutz and Roman, 2012).

Another difference between NIKS-HPV11 and NIKS-HPV16 cell populations noticed during our investigations lies in their ability to stimulate Cyclin D1 and EGFR transcription. Recent studies have suggested that exogenous EGF stimulation may enhance HPV-mediated proliferation as consequence of EGFR and Cyclin D1 activation (Narayanan et al., 2012). I report here that there is an increase in EGFR protein levels in NIKS-HPV16 cells when high concentrations of EGF are added to the monolayer culture. This change appears to coincide with an increase in EGFR and Cyclin D1 mRNA levels in these cells. In contrast, NIKS cells, and NIKS cells transfected with HPV11 do not produce high levels of EGFR and Cyclin D1 transcripts on EGF stimulation, suggesting a differential activation of promoter activity across the cell populations analysed. The presence of high levels of EGFR and Cyclin D1 transcripts, and the loss of p53 protein in NIKS-HPV16 cells may contribute to their characteristic more proliferative phenotype. Further analysis of the protein levels between low- and high-risk HPV cell populations will be needed to fully understand how the various functions of both E6 and E7 work together to drive neoplasia. In NIKS-HPV11 cells the levels of EGFR and Cyclin D1 transcripts did not increase suggesting a negative regulation of the cell cycle, as the transcript levels of Akt-1 decreased upon EGF treatment.

Although the analysis of EGFR molecular targets carried out here was limited only to the analysis of transcript levels, important differences were clearly apparent between the HPV11 and HPV16 genome-containing cells. My findings are consistent with the reports from other studies, which suggest that Cyclin D1 expression is dependent on autocrine stimulation through EGFR (Robles et al., 1998).

One mechanism that may be important in regulating the proliferation rate of NIKS-HPV11 cells could be their sensitivity to growth arrest resulting from the detection of extra chromosomal DNA by the cell. The presence of HPV episomes (i.e. extra chromosomal DNA) is in fact likely to be sensed as a DNA damage stimulus. The ability of HPV to interfere with the control mechanisms has been suggested to be crucial to allow the persistence of the viral episomes (Moody and Laimins, 2009). It is plausible that an increasing number of HPV copies may lead to activation of such cellular checkpoint responses, with the host cell being inclined to progress towards apoptosis unless the virus expresses proteins that are able to efficiently counteract these defence mechanisms. The inability of low-risk HPVs to immortalise primary keratinocytes (Woodworth et al., 1989) may explain why the cells transfected with HPV11 genomes are not efficient in maintaining the viral episomes in culture (Oh et al., 2004). Further studies on the DNA damage pathway in low- and high-risk HPV-infected cells may better elucidate the fundamental differences between these two HPV groups.

6.2 The further evaluation of the biology of low-risk and high-risk HPV types using a monolayer culture system as laboratory model for comparison

The studies presented in this thesis aimed to reproduce *in vitro,* the phenotype of cells infected with HPV11 and HPV16 genomes. Although the of the model systems have a number of limitations, our data identifies several key principles that allow us to better understand the biology of the high- and low-risk HPVs. The laboratory model described here will allow us to study the episomal maintenance and persistence of both low- and high-risk HPV types. Future work will be aimed at evaluating whether the phenotypic variation seen in NIKS-HPV11 and 16 episomal cell populations extends also in primary cell. The investigation of cells derived from clinical biopsies may also elucidate the various hypotheses that we have made using the culture system. The selection and transfection of basal keratinocyte sub-populations from clinical samples may in the future help clarify the molecular basis of how these viruses can be maintained long-term in culture.

7. References

Agarwal, M.L., Agarwal, A., Taylor, W.R., Stark, G.R., 1995. p53 controls both the G2/M and the G1 cell cycle checkpoints and mediates reversible growth arrest in human fibroblasts. Proceedings of the National Academy of Sciences of the United States of America 92, 8493-8497.

Allen-Hoffmann, B.L., Schlosser, S.J., Ivarie, C.A., Sattler, C.A., Meisner, L.F., O'Connor, S.L., 2000. Normal growth and differentiation in a spontaneously immortalized near-diploid human keratinocyte cell line, NIKS. The Journal of investigative dermatology 114, 444-455.

Androphy, E.J., Lowy, D.R., Schiller, J.T., 1987. Bovine papillomavirus E2 trans-activating gene product binds to specific sites in papillomavirus DNA. Nature 325, 70-73.

Arends, M.J., Buckley, C.H., Wells, M., 1998. Aetiology, pathogenesis, and pathology of cervical neoplasia. Journal of clinical pathology 51, 96-103.

Arteaga, C.L., 2002. Epidermal growth factor receptor dependence in human tumors: more than just expression? The oncologist 7 Suppl 4, 31-39.

Au Yeung, C.L., Tsang, T.Y., Yau, P.L., Kwok, T.T., 2011. Human papillomavirus type 16 E6 induces cervical cancer cell migration through the p53/microRNA-23b/urokinase-type plasminogen activator pathway. Oncogene 30, 2401-2410.

Baldwin, P., Laskey, R., Coleman, N., 2003. Translational approaches to improving cervical screening. Nature reviews. Cancer 3, 217-226.

Barbosa, M.S., Edmonds, C., Fisher, C., Schiller, J.T., Lowy, D.R., Vousden, K.H., 1990. The region of the HPV E7 oncoprotein homologous to adenovirus E1a and Sv40 large T antigen contains separate domains for Rb binding and casein kinase II phosphorylation. The EMBO journal 9, 153-160.

Barnard, P., McMillan, N.A., 1999. The human papillomavirus E7 oncoprotein abrogates signaling mediated by interferon-alpha. Virology 259, 305-313.

Barrow-Laing, L., Chen, W., Roman, A., 2010. Low- and high-risk human papillomavirus E7 proteins regulate p130 differently. Virology 400, 233-239.

Bechtold, V., Beard, P., Raj, K., 2003. Human papillomavirus type 16 E2 protein has no effect on transcription from episomal viral DNA. Journal of virology 77, 2021-2028.

Belnap, D.M., Olson, N.H., Cladel, N.M., Newcomb, W.W., Brown, J.C., Kreider, J.W., Christensen, N.D., Baker, T.S., 1996. Conserved features in papillomavirus and polyomavirus capsids. Journal of molecular biology 259, 249-263.

Bentley, F.H., 1936. Wound Healing in vitro. J Anat. July; 70 (Pt 4);, 498-506.493.

Berg, M., Stenlund, A., 1997. Functional interactions between papillomavirus E1 and E2 proteins. Journal of virology 71, 3853-3863.

Bernard, H.U., Chan, S.Y., Delius, H., 1994. Evolution of papillomaviruses. Curr Top Microbiol Immunol 186, 33-54.

Blaustein, M., Pelisch, F., Srebrow, A., 2007. Signals, pathways and splicing regulation. The international journal of biochemistry & cell biology 39, 2031-2048.

Bohm, S., Wilczynski, S.P., Pfister, H., Iftner, T., 1993. The predominant mRNA class in HPV16-infected genital neoplasias does not encode the E6 or the E7 protein. International journal of cancer. Journal international du cancer 55, 791-798.

Bonnez, W., 2005. The HPV xenograft severe combined immunodeficiency mouse model. Methods in molecular medicine 119, 203-216.

Bosch, F.X., Munoz, N., 2002. The viral etiology of cervical cancer. Virus research 89, 183-190.

Boukamp, P., Petrussevska, R.T., Breitkreutz, D., Hornung, J., Markham, A., Fusenig, N.E., 1988. Normal keratinization in a spontaneously immortalized aneuploid human keratinocyte cell line. The Journal of cell biology 106, 761-771.

Boulenouar, S., Weyn, C., Van Noppen, M., Moussa Ali, M., Favre, M., Delvenne, P.O., Bex, F., Noel, A., Englert, Y., Fontaine, V., 2010. Effects of HPV-16 E5, E6 and E7 proteins on survival, adhesion, migration and invasion of trophoblastic cells. Carcinogenesis 31, 473-480.

Boyer, S.N., Wazer, D.E., Band, V., 1996. E7 protein of human papilloma virus-16 induces degradation of retinoblastoma protein through the ubiquitin-proteasome pathway. Cancer research 56, 4620-4624.

Brake, T., Lambert, P.F., 2005. Estrogen contributes to the onset, persistence, and malignant progression of cervical cancer in a human papillomavirus-transgenic mouse model. Proceedings of the National Academy of Sciences of the United States of America 102, 2490-2495.

Branca, M., Ciotti, M., Santini, D., Bonito, L.D., Benedetto, A., Giorgi, C., Paba, P., Favalli, C., Costa, S., Agarossi, A., Alderisio, M., Syrjanen, K., 2004. Activation of the ERK/MAP kinase pathway in cervical intraepithelial neoplasia is related to grade of the lesion but not to high-risk human papillomavirus, virus clearance, or prognosis in cervical cancer. Am J Clin Pathol 122, 902-911.

Breuing, K., Andree, C., Helo, G., Slama, J., Liu, P.Y., Eriksson, E., 1997. Growth factors in the repair of partial thickness porcine skin wounds. Plastic and reconstructive surgery 100, 657-664.

Brightwell, J.R., Riddle, S.L., Eiferman, R.A., Valenzuela, P., Barr, P.J., Merryweather, J.P., Schultz, G.S., 1985. Biosynthetic human EGF accelerates healing of Neodecadron-treated primate corneas. Investigative ophthalmology & visual science 26, 105-110.

Brown, G.L., Curtsinger, L., 3rd, Brightwell, J.R., Ackerman, D.M., Tobin, G.R., Polk, H.C., Jr., George-Nascimento, C., Valenzuela, P., Schultz, G.S., 1986. Enhancement of epidermal regeneration by biosynthetic epidermal growth factor. The Journal of experimental medicine 163, 1319-1324.

Buck, C.B., Thompson, C.D., Pang, Y.Y., Lowy, D.R., Schiller, J.T., 2005. Maturation of papillomavirus capsids. Journal of virology 79, 2839-2846.

Buckley, A., Davidson, J.M., Kamerath, C.D., Woodward, S.C., 1987. Epidermal growth factor increases granulation tissue formation dose dependently. The Journal of surgical research 43, 322-328.

Buckley, C.H., 1994. The pathology of intra-uterine contraceptive devices. Current topics in pathology. Ergebnisse der Pathologie 86, 307-330.

Camus, S., Menendez, S., Cheok, C.F., Stevenson, L.F., Lain, S., Lane, D.P., 2007. Ubiquitin-independent degradation of p53 mediated by high-risk human papillomavirus protein E6. Oncogene 26, 4059-4070.

Carpenter, G., 2000. EGF receptor transactivation mediated by the proteolytic production of EGF-like agonists. Science's STKE : signal transduction knowledge environment 2000, pe1.

Carragher, N., 2009. Evaluation of the Effects of Mitomycin C on Wound Healing Rates for HT1080 and MDA-MB231 Cells. Cell-IQ Application Note 10;.

Chan, S.Y., Bernard, H.U., Ratterree, M., Birkebak, T.A., Faras, A.J., Ostrow, R.S., 1997. Genomic diversity and evolution of papillomaviruses in rhesus monkeys. J Virol 71, 4938-4943.

Chang, J.L., Tsao, Y.P., Liu, D.W., Huang, S.J., Lee, W.H., Chen, S.L., 2001. The expression of HPV-16 E5 protein in squamous neoplastic changes in the uterine cervix. Journal of biomedical science 8, 206-213.

Chen, X.S., Garcea, R.L., Goldberg, I., Casini, G., Harrison, S.C., 2000. Structure of small virus-like particles assembled from the L1 protein of human papillomavirus 16. Molecular cell 5, 557-567.

Cheng, S., Schmidt-Grimminger, D.C., Murant, T., Broker, T.R., Chow, L.T., 1995. Differentiation-dependent up-regulation of the human papillomavirus E7 gene reactivates cellular DNA replication in suprabasal differentiated keratinocytes. Genes & development 9, 2335-2349.

Choo, K.B., Pan, C.C., Han, S.H., 1987. Integration of human papillomavirus type 16 into cellular DNA of cervical carcinoma: preferential deletion of the E2 gene and invariable retention of the long control region and the E6/E7 open reading frames. Virology 161, 259-261.

Chow, L.T., Duffy, A.A., Wang, H.K., Broker, T.R., 2009. A highly efficient system to produce infectious human papillomavirus: Elucidation of natural virus-host interactions. Cell cycle (Georgetown, Tex.) 8, 1319-1323.

Christensen, N.D., Kreider, J.W., 1991. Neutralization of CRPV infectivity by monoclonal antibodies that identify conformational epitopes on intact virions. Virus research 21, 169-179.

Clark, D.E., Poteet-Smith, C.E., Smith, J.A., Lannigan, D.A., 2001. Rsk2 allosterically activates estrogen receptor alpha by docking to the hormone-binding domain. The EMBO journal 20, 3484-3494.

Clark, R.A., Ashcroft, G.S., Spencer, M.J., Larjava, H., Ferguson, M.W., 1996. Re-epithelialization of normal human excisional wounds is associated with a switch from alpha v beta 5 to alpha v beta 6 integrins. The British journal of dermatology 135, 46-51.

Cole, S.T., Danos, O., 1987. Nucleotide sequence and comparative analysis of the human papillomavirus type 18 genome. Phylogeny of papillomaviruses and repeated structure of the E6 and E7 gene products. Journal of molecular biology 193, 599-608.

Collins, A.S., Nakahara, T., Do, A., Lambert, P.F., 2005. Interactions with pocket proteins contribute to the role of human papillomavirus type 16 E7 in the papillomavirus life cycle. Journal of virology 79, 14769-14780.

Cornelissen, M.T., Smits, H.L., Briet, M.A., van den Tweel, J.G., Struyk, A.P., van der Noordaa, J., ter Schegget, J., 1990. Uniformity of the splicing pattern of the E6/E7 transcripts in human papillomavirus type 16-transformed human fibroblasts, human cervical premalignant lesions and carcinomas. The Journal of general virology 71 (Pt 5), 1243-1246.

Cribbs, R.K., Harding, P.A., Luquette, M.H., Besner, G.E., 2002. Endogenous production of heparin-binding EGF-like growth factor during murine partial-thickness burn wound healing. The Journal of burn care & rehabilitation 23, 116-125.

Cripe, T.P., Haugen, T.H., Turk, J.P., Tabatabai, F., Schmid, P.G., 3rd, Durst, M., Gissmann, L., Roman, A., Turek, L.P., 1987. Transcriptional regulation of the human papillomavirus-16 E6-E7 promoter by a keratinocyte-dependent enhancer, and by viral E2 trans-activator and repressor gene products: implications for cervical carcinogenesis. The EMBO journal 6, 3745-3753.

Croft, C.B., Tarin, D., 1970. Ultrastructural studies of wound healing in mouse skin. I. Epithelial behaviour. Journal of anatomy 106, 63-77.

Crusius, K., Rodriguez, I., Alonso, A., 2000. The human papillomavirus type 16 E5 protein modulates ERK1/2 and p38 MAP kinase activation by an EGFR-independent process in stressed human keratinocytes. Virus genes 20, 65-69.

Dall, K.L., Scarpini, C.G., Roberts, I., Winder, D.M., Stanley, M.A., Muralidhar, B., Herdman, M.T., Pett, M.R., Coleman, N., 2008. Characterization of naturally occurring HPV16 integration sites isolated from cervical keratinocytes under noncompetitive conditions. Cancer research 68, 8249-8259.

Davies, R., Hicks, R., Crook, T., Morris, J., Vousden, K., 1993. Human papillomavirus type 16 E7 associates with a histone H1 kinase and with p107 through sequences necessary for transformation. Journal of virology 67, 2521-2528.

Davy, C.E., Jackson, D.J., Wang, Q., Raj, K., Masterson, P.J., Fenner, N.F., Southern, S., Cuthill, S., Millar, J.B., Doorbar, J., 2002. Identification of a G(2) arrest domain in the E1 wedge E4 protein of human papillomavirus type 16. Journal of virology 76, 9806-9818.

Day, P.M., Lowy, D.R., Schiller, J.T., 2003. Papillomaviruses infect cells via a clathrin-dependent pathway. Virology 307, 1-11.

De Geest, K., Turyk, M.E., Hosken, M.I., Hudson, J.B., Laimins, L.A., Wilbanks, G.D., 1993. Growth and differentiation of human papillomavirus type 31b positive human cervical cell lines. Gynecologic oncology 49, 303-310.

de la Barre, A.E., Gerson, V., Gout, S., Creaven, M., Allis, C.D., Dimitrov, S., 2000. Core histone N-termini play an essential role in mitotic chromosome condensation. The EMBO journal 19, 379-391.

de Villiers, E.M., Fauquet, C., Broker, T.R., Bernard, H.U., zur Hausen, H., 2004a. Classification of papillomaviruses. Virology 324, 17-27.

de Villiers, E.M., Gunst, K., Stein, H., Scherubl, H., 2004b. Esophageal squamous cell cancer in patients with head and neck cancer: Prevalence of human papillomavirus DNA sequences. International journal of cancer. Journal international du cancer 109, 253-258.

Demers, G.W., Halbert, C.L., Galloway, D.A., 1994. Elevated wild-type p53 protein levels in human epithelial cell lines immortalized by the human papillomavirus type 16 E7 gene. Virology 198, 169-174.

Derkay, C.S., 1995. Task force on recurrent respiratory papillomas. A preliminary report. Archives of otolaryngology--head & neck surgery 121, 1386-1391.

DiLorenzo, T.P., Steinberg, B.M., 1995. Differential regulation of human papillomavirus type 6 and 11 early promoters in cultured cells derived from laryngeal papillomas. Journal of virology 69, 6865-6872.

DiMaio, D., Mattoon, D., 2001. Mechanisms of cell transformation by papillomavirus E5 proteins. Oncogene 20, 7866-7873.

Disbrow, G.L., Hanover, J.A., Schlegel, R., 2005. Endoplasmic reticulum-localized human papillomavirus type 16 E5 protein alters endosomal pH but not trans-Golgi pH. Journal of virology 79, 5839-5846.

Donne, A.J., Clarke, R., 2010. Recurrent respiratory papillomatosis: an uncommon but potentially devastating effect of human papillomavirus in children. International journal of STD & AIDS 21, 381-385.

Doorbar, J., 2005. The papillomavirus life cycle. Journal of clinical virology : the official publication of the Pan American Society for Clinical Virology 32 Suppl 1, S7-15.

Doorbar, J., 2006. Molecular biology of human papillomavirus infection and cervical cancer. Clinical science (London, England : 1979) 110, 525-541.

Doorbar, J., Foo, C., Coleman, N., Medcalf, L., Hartley, O., Prospero, T., Napthine, S., Sterling, J., Winter, G., Griffin, H., 1997. Characterization of events during the late stages of HPV16 infection in vivo using high-affinity synthetic Fabs to E4. Virology 238, 40-52.

Doorbar, J., Parton, A., Hartley, K., Banks, L., Crook, T., Stanley, M., Crawford, L., 1990. Detection of novel splicing patterns in a HPV16-containing keratinocyte cell line. Virology 178, 254-262.

Doorbar, J., Quint, W., Banks, L., Bravo, I.G., Stoler, M., Broker, T.R., Stanley, M.A., 2012. The biology and life-cycle of human papillomaviruses. Vaccine 30 Suppl 5, F55-70.

Duensing, S., Lee, L.Y., Duensing, A., Basile, J., Piboonniyom, S., Gonzalez, S., Crum, C.P., Munger, K., 2000. The human papillomavirus type 16 E6 and E7 oncoproteins cooperate to induce mitotic defects and genomic instability by uncoupling centrosome duplication from the cell division cycle. Proceedings of the National Academy of Sciences of the United States of America 97, 10002-10007.

Duensing, S., Munger, K., 2004. Mechanisms of genomic instability in human cancer: insights from studies with human papillomavirus oncoproteins. International journal of cancer. Journal international du cancer 109, 157-162.

Durst, M., Glitz, D., Schneider, A., zur Hausen, H., 1992. Human papillomavirus type 16 (HPV 16) gene expression and DNA replication in cervical neoplasia: analysis by in situ hybridization. Virology 189, 132-140.

Dyson, N., Guida, P., Munger, K., Harlow, E., 1992. Homologous sequences in adenovirus E1A and human papillomavirus E7 proteins mediate interaction with the same set of cellular proteins. Journal of virology 66, 6893-6902.

Dyson, N., Howley, P.M., Munger, K., Harlow, E., 1989. The human papilloma virus-16 E7 oncoprotein is able to bind to the retinoblastoma gene product. Science (New York, N.Y.) 243, 934-937.

Eckert, R.L., Crish, J.F., Robinson, N.A., 1997. The epidermal keratinocyte as a model for the study of gene regulation and cell differentiation. Physiological reviews 77, 397-424.

Edwards, T.G., Vidmar, T.J., Koeller, K., Bashkin, J.K., Fisher, C., 2013. DNA Damage Repair Genes Controlling Human Papillomavirus (HPV) Episome Levels under Conditions of Stability and Extreme Instability. PloS one 8, e75406.

Eming, S.A., Brachvogel, B., Odorisio, T., Koch, M., 2007. Regulation of angiogenesis: wound healing as a model. Progress in histochemistry and cytochemistry 42, 115-170.

Escalante-Alcalde, D., Recillas-Targa, F., Valencia, C., Santa-Olalla, J., Chavez, P., Marroquin, A., Gutierrez, X., Gariglio, P., Covarrubias, L., 2000. Expression of E6 and E7 papillomavirus oncogenes in the outer root sheath of hair follicles extends the growth phase and bypasses resting at telogen. Cell growth & differentiation : the molecular biology journal of the American Association for Cancer Research 11, 527-539.

Escamez, M.J., Garcia, M., Larcher, F., Meana, A., Munoz, E., Jorcano, J.L., Del Rio, M., 2004. An in vivo model of wound healing in genetically modified skin-humanized mice. The Journal of investigative dermatology 123, 1182-1191.

Fang, L., Meyers, C., Budgeon, L.R., Howett, M.K., 2006. Induction of productive human papillomavirus type 11 life cycle in epithelial cells grown in organotypic raft cultures. Virology 347, 28-35.

Ferlay, J., Forman, D., Mathers, C.D., Bray, F., 2012. Breast and cervical cancer in 187 countries between 1980 and 2010. Lancet 379, 1390-1391.

Ferlay, J., Shin, H.R., Bray, F., Forman, D., Mathers, C., Parkin, D.M., 2010. Estimates of worldwide burden of cancer in 2008: GLOBOCAN 2008. International journal of cancer. Journal international du cancer 127, 2893-2917.

Filippova, M., Johnson, M.M., Bautista, M., Filippov, V., Fodor, N., Tungteakkhun, S.S., Williams, K., Duerksen-Hughes, P.J., 2007. The large and small isoforms of

human papillomavirus type 16 E6 bind to and differentially affect procaspase 8 stability and activity. Journal of virology 81, 4116-4129.

Firth, A.E., Brierley, I., 2012. Non-canonical translation in RNA viruses. The Journal of general virology 93, 1385-1409.

Friedl, P., Wolf, K., 2003. Tumour-cell invasion and migration: diversity and escape mechanisms. Nature reviews. Cancer 3, 362-374.

Fuchs, E., 1990. Epidermal differentiation: the bare essentials. The Journal of cell biology 111, 2807-2814.

Gage, J.R., Meyers, C., Wettstein, F.O., 1990. The E7 proteins of the nononcogenic human papillomavirus type 6b (HPV-6b) and of the oncogenic HPV-16 differ in retinoblastoma protein binding and other properties. Journal of virology 64, 723-730.

Galloway, D.A., 2003. Papillomavirus vaccines in clinical trials. The Lancet infectious diseases 3, 469-475.

Galloway, D.A., McDougall, J.K., 1996. The disruption of cell cycle checkpoints by papillomavirus oncoproteins contributes to anogenital neoplasia. Seminars in cancer biology 7, 309-315.

Genther Williams, S.M., Disbrow, G.L., Schlegel, R., Lee, D., Threadgill, D.W., Lambert, P.F., 2005. Requirement of epidermal growth factor receptor for hyperplasia induced by E5, a high-risk human papillomavirus oncogene. Cancer research 65, 6534-6542.

Gerard, C.M., Baudson, N., Kraemer, K., Ledent, C., Pardoll, D., Bruck, C., 2001. Recombinant human papillomavirus type 16 E7 protein as a model antigen to study the vaccine potential in control and E7 transgenic mice. Clinical cancer research : an official journal of the American Association for Cancer Research 7, 838s-847s.

Gerein, V., Rastorguev, E., Gerein, J., Draf, W., Schirren, J., 2005. Incidence, age at onset, and potential reasons of malignant transformation in recurrent respiratory papillomatosis patients: 20 years experience. Otolaryngology--head and neck surgery : official journal of American Academy of Otolaryngology-Head and Neck Surgery 132, 392-394.

Ghim, S., Newsome, J., Bell, J., Sundberg, J.P., Schlegel, R., Jenson, A.B., 2000. Spontaneously regressing oral papillomas induce systemic antibodies that neutralize canine oral papillomavirus. Experimental and molecular pathology 68, 147-151.

GIbson, A.L.F., 2007. Cutaneous Wound Therapy: A Role for Therapeutic Skin Substitutes. PhD Thesis University of Wisconsin - Madison.

Gonzalez, S.L., Stremlau, M., He, X., Basile, J.R., Munger, K., 2001. Degradation of the retinoblastoma tumor suppressor by the human papillomavirus type 16 E7 oncoprotein is important for functional inactivation and is separable from proteasomal degradation of E7. Journal of virology 75, 7583-7591.

Goodsell, D.S., 2003. The molecular perspective: epidermal growth factor. Stem cells (Dayton, Ohio) 21, 702-703.

Grant, M.B., Khaw, P.T., Schultz, G.S., Adams, J.L., Shimizu, R.W., 1992. Effects of epidermal growth factor, fibroblast growth factor, and transforming growth factor-beta on corneal cell chemotaxis. Investigative ophthalmology & visual science 33, 3292-3301.

Grassmann, K., Rapp, B., Maschek, H., Petry, K.U., Iftner, T., 1996. Identification of a differentiation-inducible promoter in the E7 open reading frame of human papillomavirus type 16 (HPV-16) in raft cultures of a new cell line containing high copy numbers of episomal HPV-16 DNA. Journal of virology 70, 2339-2349.

Gray, E., Pett, M.R., Ward, D., Winder, D.M., Stanley, M.A., Roberts, I., Scarpini, C.G., Coleman, N., 2010. In vitro progression of human papillomavirus 16 episome-associated cervical neoplasia displays fundamental similarities to integrant-associated carcinogenesis. Cancer research 70, 4081-4091.

Griep, A.E., Herber, R., Jeon, S., Lohse, J.K., Dubielzig, R.R., Lambert, P.F., 1993. Tumorigenicity by human papillomavirus type 16 E6 and E7 in transgenic mice correlates with alterations in epithelial cell growth and differentiation. Journal of virology 67, 1373-1384.

Hafner, N., Driesch, C., Gajda, M., Jansen, L., Kirchmayr, R., Runnebaum, I.B., Durst, M., 2008. Integration of the HPV16 genome does not invariably result in high levels of viral oncogene transcripts. Oncogene 27, 1610-1617.

Hamid, N.A., Brown, C., Gaston, K., 2009. The regulation of cell proliferation by the papillomavirus early proteins. Cellular and molecular life sciences : CMLS 66, 1700-1717.

Hanna, E., Bachmann, G., 2006. HPV vaccination with Gardasil: a breakthrough in women's health. Expert opinion on biological therapy 6, 1223-1227.

Hans, F., Dimitrov, S., 2001. Histone H3 phosphorylation and cell division. Oncogene 20, 3021-3027.

He, W., Staples, D., Smith, C., Fisher, C., 2003. Direct activation of cyclin-dependent kinase 2 by human papillomavirus E7. Journal of virology 77, 10566-10574.

Hebner, C.M., Laimins, L.A., 2006. Human papillomaviruses: basic mechanisms of pathogenesis and oncogenicity. Reviews in medical virology 16, 83-97.

Heck, D.V., Yee, C.L., Howley, P.M., Munger, K., 1992. Efficiency of binding the retinoblastoma protein correlates with the transforming capacity of the E7 oncoproteins of the human papillomaviruses. Proceedings of the National Academy of Sciences of the United States of America 89, 4442-4446.

Herfs, M., Yamamoto, Y., Laury, A., Wang, X., Nucci, M.R., McLaughlin-Drubin, M.E., Munger, K., Feldman, S., McKeon, F.D., Xian, W., Crum, C.P., 2012. A discrete population of squamocolumnar junction cells implicated in the pathogenesis of cervical cancer. Proceedings of the National Academy of Sciences of the United States of America 109, 10516-10521.

Ho, L., Chan, S.Y., Burk, R.D., Das, B.C., Fujinaga, K., Icenogle, J.P., Kahn, T., Kiviat, N., Lancaster, W., Mavromara-Nazos, P., et al., 1993. The genetic drift of human papillomavirus type 16 is a means of reconstructing prehistoric viral spread and the movement of ancient human populations. J Virol 67, 6413-6423.

Howley, P.M., 1982. The human papillomaviruses. Archives of pathology & laboratory medicine 106, 429-432.

Hsueh, P.R., 2009. Human papillomavirus, genital warts, and vaccines. Journal of microbiology, immunology, and infection = Wei mian yu gan ran za zhi 42, 101-106.

Hu, L., Ceresa, B.P., 2009. Characterization of the plasma membrane localization and orientation of HPV16 E5 for cell-cell fusion. Virology 393, 135-143.

Hughes, F.J., Romanos, M.A., 1993. E1 protein of human papillomavirus is a DNA helicase/ATPase. Nucleic acids research 21, 5817-5823.

Isaacson Wechsler, E., Wang, Q., Roberts, I., Pagliarulo, E., Jackson, D., Untersperger, C., Coleman, N., Griffin, H., Doorbar, J., 2012. Reconstruction of human papillomavirus type 16-mediated early-stage neoplasia implicates E6/E7 deregulation and the loss of contact inhibition in neoplastic progression. Journal of virology 86, 6358-6364.

Jia, R., Liu, X., Tao, M., Kruhlak, M., Guo, M., Meyers, C., Baker, C.C., Zheng, Z.M., 2009. Control of the papillomavirus early-to-late switch by differentially expressed SRp20. Journal of virology 83, 167-180.

Johansson, C., Somberg, M., Li, X., Backstrom Winquist, E., Fay, J., Ryan, F., Pim, D., Banks, L., Schwartz, S., 2012. HPV-16 E2 contributes to induction of HPV-16 late gene expression by inhibiting early polyadenylation. The EMBO journal 31, 3212-3227.

Johnson, K.M., Kines, R.C., Roberts, J.N., Lowy, D.R., Schiller, J.T., Day, P.M., 2009. Role of heparan sulfate in attachment to and infection of the murine female genital tract by human papillomavirus. Journal of virology 83, 2067-2074.

Joo, C.K., Seomun, Y., 2008. Matrix metalloproteinase (MMP) and TGF beta 1-stimulated cell migration in skin and cornea wound healing. Cell adhesion & migration 2, 252-253.

Joseph, A.W., D'Souza, G., 2012. Epidemiology of human papillomavirus-related head and neck cancer. Otolaryngologic clinics of North America 45, 739-764.

Joyce, J.G., Tung, J.S., Przysiecki, C.T., Cook, J.C., Lehman, E.D., Sands, J.A., Jansen, K.U., Keller, P.M., 1999. The L1 major capsid protein of human papillomavirus type 11 recombinant virus-like particles interacts with heparin and cell-surface glycosaminoglycans on human keratinocytes. The Journal of biological chemistry 274, 5810-5822.

Kaczkowski, B., Rossing, M., Andersen, D.K., Dreher, A., Morevati, M., Visser, M.A., Winther, O., Nielsen, F.C., Norrild, B., 2012. Integrative analyses reveal novel strategies in HPV11,-16 and -45 early infection. Scientific reports 2, 515.

Kamper, N., Day, P.M., Nowak, T., Selinka, H.C., Florin, L., Bolscher, J., Hilbig, L., Schiller, J.T., Sapp, M., 2006. A membrane-destabilizing peptide in capsid protein L2 is required for egress of papillomavirus genomes from endosomes. Journal of virology 80, 759-768.

Katzenellenbogen, R.A., Vliet-Gregg, P., Xu, M., Galloway, D.A., 2009. NFX1-123 increases hTERT expression and telomerase activity posttranscriptionally in human papillomavirus type 16 E6 keratinocytes. Journal of virology 83, 6446-6456.

Khan, J., Davy, C.E., McIntosh, P.B., Jackson, D.J., Hinz, S., Wang, Q., Doorbar, J., 2011. Role of calpain in the formation of human papillomavirus type 16 E1^E4 amyloid fibers and reorganization of the keratin network. Journal of virology 85, 9984-9997.

Kho, E.Y., Wang, H.K., Banerjee, N.S., Broker, T.R., Chow, L.T., 2013. HPV-18 E6 mutants reveal p53 modulation of viral DNA amplification in organotypic cultures. Proceedings of the National Academy of Sciences of the United States of America 110, 7542-7549.

Kim, M.K., Kim, H.S., Kim, S.H., Oh, J.M., Han, J.Y., Lim, J.M., Juhnn, Y.S., Song, Y.S., 2010. Human papillomavirus type 16 E5 oncoprotein as a new target for cervical cancer treatment. Biochemical pharmacology 80, 1930-1935.

Kines, R.C., Thompson, C.D., Lowy, D.R., Schiller, J.T., Day, P.M., 2009. The initial steps leading to papillomavirus infection occur on the basement membrane prior to cell surface binding. Proceedings of the National Academy of Sciences of the United States of America 106, 20458-20463.

Kirfel, G., Rigort, A., Borm, B., Herzog, V., 2004. Cell migration: mechanisms of rear detachment and the formation of migration tracks. European journal of cell biology 83, 717-724.

Klaes, R., Woerner, S.M., Ridder, R., Wentzensen, N., Duerst, M., Schneider, A., Lotz, B., Melsheimer, P., von Knebel Doeberitz, M., 1999. Detection of high-risk cervical intraepithelial neoplasia and cervical cancer by amplification of transcripts derived from integrated papillomavirus oncogenes. Cancer research 59, 6132-6136.

Klingelhutz, A.J., Roman, A., 2012. Cellular transformation by human papillomaviruses: lessons learned by comparing high- and low-risk viruses. Virology 424, 77-98.

Kumar, A., Zhao, Y., Meng, G., Zeng, M., Srinivasan, S., Delmolino, L.M., Gao, Q., Dimri, G., Weber, G.F., Wazer, D.E., Band, H., Band, V., 2002. Human papillomavirus oncoprotein E6 inactivates the transcriptional coactivator human ADA3. Molecular and cellular biology 22, 5801-5812.

Kwon, Y.B., Kim, H.W., Roh, D.H., Yoon, S.Y., Baek, R.M., Kim, J.Y., Kweon, H., Lee, K.G., Park, Y.H., Lee, J.H., 2006. Topical application of epidermal growth factor accelerates wound healing by myofibroblast proliferation and collagen synthesis in rat. Journal of veterinary science 7, 105-109.

Lace, M.J., Anson, J.R., Thomas, G.S., Turek, L.P., Haugen, T.H., 2008. The E8--E2 gene product of human papillomavirus type 16 represses early transcription and replication but is dispensable for viral plasmid persistence in keratinocytes. Journal of virology 82, 10841-10853.

Lace, M.J., Yamakawa, Y., Ushikai, M., Anson, J.R., Haugen, T.H., Turek, L.P., 2009. Cellular factor YY1 downregulates the human papillomavirus 16 E6/E7 promoter, P97, in vivo and in vitro from a negative element overlapping the transcription-initiation site. The Journal of general virology 90, 2402-2412.

Lacey, C.J., Lowndes, C.M., Shah, K.V., 2006. Chapter 4: Burden and management of non-cancerous HPV-related conditions: HPV-6/11 disease. Vaccine 24 Suppl 3, S3/35-41.

Lagunas-Martinez, A., Madrid-Marina, V., Gariglio, P., 2010. Modulation of apoptosis by early human papillomavirus proteins in cervical cancer. Biochimica et biophysica acta 1805, 6-16.

Lakin, N.D., Jackson, S.P., 1999. Regulation of p53 in response to DNA damage. Oncogene 18, 7644-7655.

Lambert, P.F., Ozbun, M.A., Collins, A., Holmgren, S., Lee, D., Nakahara, T., 2005. Using an immortalized cell line to study the HPV life cycle in organotypic "raft" cultures. Methods in molecular medicine 119, 141-155.

Laurson, J., Khan, S., Chung, R., Cross, K., Raj, K., 2010. Epigenetic repression of E-cadherin by human papillomavirus 16 E7 protein. Carcinogenesis 31, 918-926.

Lee, C., Chang, J.H., Lee, H.S., Cho, Y., 2002a. Structural basis for the recognition of the E2F transactivation domain by the retinoblastoma tumor suppressor. Genes & development 16, 3199-3212.

Lee, C.J., Suh, E.J., Kang, H.T., Im, J.S., Um, S.J., Park, J.S., Hwang, E.S., 2002b. Induction of senescence-like state and suppression of telomerase activity through inhibition of HPV E6/E7 gene expression in cells immortalized by HPV16 DNA. Experimental cell research 277, 173-182.

Liang CC, P.A., Guan JL., 2007. In vitro scratch assay: a convenient and inexpensive method for analysis of cell migration in vitro. Nat. Protoc. 2, 329-333.

Liu, X., Yuan, H., Fu, B., Disbrow, G.L., Apolinario, T., Tomaic, V., Kelley, M.L., Baker, C.C., Huibregtse, J., Schlegel, R., 2005. The E6AP ubiquitin ligase is required for transactivation of the hTERT promoter by the human papillomavirus E6 oncoprotein. The Journal of biological chemistry 280, 10807-10816.

Livak, K.J., Schmittgen, T.D., 2001. Analysis of relative gene expression data using real-time quantitative PCR and the 2(-Delta Delta C(T)) Method. Methods (San Diego, Calif.) 25, 402-408.

Lorenzon, L., Mazzetta, F., Venuti, A., Frega, A., Torrisi, M.R., French, D., 2011. In vivo HPV 16 E5 mRNA: expression pattern in patients with squamous intra-epithelial lesions of the cervix. Journal of clinical virology : the official publication of the Pan American Society for Clinical Virology 52, 79-83.

Maglennon, G.A., Doorbar, J., 2012. The biology of papillomavirus latency. The open virology journal 6, 190-197.

Maglennon, G.A., McIntosh, P., Doorbar, J., 2011. Persistence of viral DNA in the epithelial basal layer suggests a model for papillomavirus latency following immune regression. Virology 414, 153-163.

Major, T., Szarka, K., Sziklai, I., Gergely, L., Czegledy, J., 2005. The characteristics of human papillomavirus DNA in head and neck cancers and papillomas. Journal of clinical pathology 58, 51-55.

Martin, P., 1997. Wound healing--aiming for perfect skin regeneration. Science (New York, N.Y.) 276, 75-81.

Masterson, P.J., Stanley, M.A., Lewis, A.P., Romanos, M.A., 1998. A C-terminal helicase domain of the human papillomavirus E1 protein binds E2 and the DNA polymerase alpha-primase p68 subunit. Journal of virology 72, 7407-7419.

McIntosh, P.B., Laskey, P., Sullivan, K., Davy, C., Wang, Q., Jackson, D.J., Griffin, H.M., Doorbar, J., 2010. E1--E4-mediated keratin phosphorylation and ubiquitylation: a mechanism for keratin depletion in HPV16-infected epithelium. Journal of cell science 123, 2810-2822.

Middleton, K., Peh, W., Southern, S., Griffin, H., Sotlar, K., Nakahara, T., El-Sherif, A., Morris, L., Seth, R., Hibma, M., Jenkins, D., Lambert, P., Coleman, N., Doorbar, J., 2003. Organization of human papillomavirus productive cycle during neoplastic progression provides a basis for selection of diagnostic markers. Journal of virology 77, 10186-10201.

Milligan, S.G., Veerapraditsin, T., Ahamet, B., Mole, S., Graham, S.V., 2007. Analysis of novel human papillomavirus type 16 late mRNAs in differentiated W12 cervical epithelial cells. Virology 360, 172-181.

Moody, C.A., Laimins, L.A., 2009. Human papillomaviruses activate the ATM DNA damage pathway for viral genome amplification upon differentiation. PLoS pathogens 5, e1000605.

Munger, K., Werness, B.A., Dyson, N., Phelps, W.C., Harlow, E., Howley, P.M., 1989. Complex formation of human papillomavirus E7 proteins with the retinoblastoma tumor suppressor gene product. The EMBO journal 8, 4099-4105.

Nakahara, T., Peh, W.L., Doorbar, J., Lee, D., Lambert, P.F., 2005. Human papillomavirus type 16 E1circumflexE4 contributes to multiple facets of the papillomavirus life cycle. Journal of virology 79, 13150-13165.

Nanda, K., McCrory, D.C., Myers, E.R., Bastian, L.A., Hasselblad, V., Hickey, J.D., Matchar, D.B., 2000. Accuracy of the Papanicolaou test in screening for and follow-up of cervical cytologic abnormalities: a systematic review. Annals of internal medicine 132, 810-819.

Nanney, L.B., Magid, M., Stoscheck, C.M., King, L.E., Jr., 1984. Comparison of epidermal growth factor binding and receptor distribution in normal human epidermis and epidermal appendages. The Journal of investigative dermatology 83, 385-393.

Narayanan, R., Kim, H.N., Narayanan, N.K., Nargi, D., Narayanan, B., 2012. Epidermal growth factor-stimulated human cervical cancer cell growth is associated with EGFR and cyclin D1 activation, independent of COX-2 expression levels. International journal of oncology 40, 13-20.

Nickoloff, B.J., Qin, J.Z., Nestle, F.O., 2007. Immunopathogenesis of psoriasis. Clinical reviews in allergy & immunology 33, 45-56.

Nicol, C., Bunka, D.H., Blair, G.E., Stonehouse, N.J., 2011. Effects of single nucleotide changes on the binding and activity of RNA aptamers to human papillomavirus 16

E7 oncoprotein. Biochemical and biophysical research communications 405, 417-421.

Nicol, C., Cesur, O., Forrest, S., Belyaeva, T.A., Bunka, D.H., Blair, G.E., Stonehouse, N.J., 2013. An RNA aptamer provides a novel approach for the induction of apoptosis by targeting the HPV16 E7 oncoprotein. PloS one 8, e64781.

Nicolaides, L., Davy, C., Raj, K., Kranjec, C., Banks, L., Doorbar, J., 2011. Stabilization of HPV16 E6 protein by PDZ proteins, and potential implications for genome maintenance. Virology 414, 137-145.

Nowak, S.J., Corces, V.G., 2000. Phosphorylation of histone H3 correlates with transcriptionally active loci. Genes & development 14, 3003-3013.

Oh, S.T., Longworth, M.S., Laimins, L.A., 2004. Roles of the E6 and E7 proteins in the life cycle of low-risk human papillomavirus type 11. Journal of virology 78, 2620-2626.

Ozaki, T., Nakagawara, A., 2011. Role of p53 in Cell Death and Human Cancers. Cancers 3, 994-1013.

Ozbun, M.A., Meyers, C., 1997. Characterization of late gene transcripts expressed during vegetative replication of human papillomavirus type 31b. Journal of virology 71, 5161-5172.

Penn, I., 1986. The occurrence of malignant tumors in immunosuppressed states. Progress in allergy 37, 259-300.

Philipp, K., Riedel, F., Sauerbier, M., Hormann, K., Germann, G., 2004. Targeting TGF-beta in human keratinocytes and its potential role in wound healing. International journal of molecular medicine 14, 589-593.

Piccini, A., Storey, A., Romanos, M., Banks, L., 1997. Regulation of human papillomavirus type 16 DNA replication by E2, glucocorticoid hormone and epidermal growth factor. The Journal of general virology 78 (Pt 8), 1963-1970.

Pim, D., Banks, L., 2010. Interaction of viral oncoproteins with cellular target molecules: infection with high-risk vs low-risk human papillomaviruses. APMIS : acta pathologica, microbiologica, et immunologica Scandinavica 118, 471-493.

Pyeon, D., Pearce, S.M., Lank, S.M., Ahlquist, P., Lambert, P.F., 2009. Establishment of human papillomavirus infection requires cell cycle progression. PLoS pathogens 5, e1000318.

Remm, M., Remm, A., Ustav, M., 1999. Human papillomavirus type 18 E1 protein is translated from polycistronic mRNA by a discontinuous scanning mechanism. Journal of virology 73, 3062-3070.

Richart, R.M., 1973. Cervical intraepithelial neoplasia. Pathology annual 8, 301-328.

Roberts, J.N., Buck, C.B., Thompson, C.D., Kines, R., Bernardo, M., Choyke, P.L., Lowy, D.R., Schiller, J.T., 2007. Genital transmission of HPV in a mouse model is potentiated by nonoxynol-9 and inhibited by carrageenan. Nature medicine 13, 857-861.

Robles, A.I., Rodriguez-Puebla, M.L., Glick, A.B., Trempus, C., Hansen, L., Sicinski, P., Tennant, R.W., Weinberg, R.A., Yuspa, S.H., Conti, C.J., 1998. Reduced skin tumor development in cyclin D1-deficient mice highlights the oncogenic ras pathway in vivo. Genes & development 12, 2469-2474.

Rogers, L., Siu, S.S., Luesley, D., Bryant, A., Dickinson, H.O., 2012. Radiotherapy and chemoradiation after surgery for early cervical cancer. The Cochrane database of systematic reviews 5, CD007583.

Roman, A., 2006. The human papillomavirus E7 protein shines a spotlight on the pRB family member, p130. Cell cycle (Georgetown, Tex.) 5, 567-568.

Rosenberger, S., De-Castro Arce, J., Langbein, L., Steenbergen, R.D., Rosl, F., 2010. Alternative splicing of human papillomavirus type-16 E6/E6* early mRNA is coupled to EGF signaling via Erk1/2 activation. Proceedings of the National Academy of Sciences of the United States of America 107, 7006-7011.

Roy, M., King, T.W., 2013. Epidermal growth factor regulates NIKS keratinocyte proliferation through Notch signaling. The Journal of surgical research 185, 6-11.

Salunke, D.M., Caspar, D.L., Garcea, R.L., 1986. Self-assembly of purified polyomavirus capsid protein VP1. Cell 46, 895-904.

Santoro, M.M., Gaudino, G., 2005. Cellular and molecular facets of keratinocyte reepithelization during wound healing. Experimental cell research 304, 274-286.

Sasieni, P.D., Cuzick, J., Lynch-Farmery, E., 1996. Estimating the efficacy of screening by auditing smear histories of women with and without cervical cancer. The National Co-ordinating Network for Cervical Screening Working Group. British journal of cancer 73, 1001-1005.

Scheffner, M., Huibregtse, J.M., Vierstra, R.D., Howley, P.M., 1993. The HPV-16 E6 and E6-AP complex functions as a ubiquitin-protein ligase in the ubiquitination of p53. Cell 75, 495-505.

Schiller, J.T., Day, P.M., Kines, R.C., 2010. Current understanding of the mechanism of HPV infection. Gynecologic oncology 118, S12-17.

Schneider-Gadicke, A., Schwarz, E., 1986. Different human cervical carcinoma cell lines show similar transcription patterns of human papillomavirus type 18 early genes. The EMBO journal 5, 2285-2292.

Schultz, G., Rotatori, D.S., Clark, W., 1991. EGF and TGF-alpha in wound healing and repair. Journal of cellular biochemistry 45, 346-352.

Schultz, G.S., White, M., Mitchell, R., Brown, G., Lynch, J., Twardzik, D.R., Todaro, G.J., 1987. Epithelial wound healing enhanced by transforming growth factor-alpha and vaccinia growth factor. Science (New York, N.Y.) 235, 350-352.

Schurr, M.J., Foster, K.N., Centanni, J.M., Comer, A.R., Wicks, A., Gibson, A.L., Thomas-Virnig, C.L., Schlosser, S.J., Faucher, L.D., Lokuta, M.A., Allen-Hoffmann, B.L., 2009. Phase I/II clinical evaluation of StrataGraft: a consistent, pathogen-free human skin substitute. The Journal of trauma 66, 866-873; discussion 873-864.

Schwartz, S., 2008. HPV-16 RNA processing. Frontiers in bioscience : a journal and virtual library 13, 5880-5891.

Shai, A., Brake, T., Somoza, C., Lambert, P.F., 2007. The human papillomavirus E6 oncogene dysregulates the cell cycle and contributes to cervical carcinogenesis through two independent activities. Cancer research 67, 1626-1635.

Shaw TJ, M.P., 2009. Wound Repair at a Glance. J Cell Sci. 122, 3209-3213.

Sheardown, H., Cheng, Y.L., 1996. Tear EGF concentration following corneal epithelial wound creation. Journal of ocular pharmacology and therapeutics : the official journal of the Association for Ocular Pharmacology and Therapeutics 12, 239-243.

Sheetz, M.P., 1994. Cell migration by graded attachment to substrates and contraction. Seminars in cell biology 5, 149-155.

Shirakata, Y., 2010. Regulation of epidermal keratinocytes by growth factors. Journal of dermatological science 59, 73-80.

Sillman, F., Stanek, A., Sedlis, A., Rosenthal, J., Lanks, K.W., Buchhagen, D., Nicastri, A., Boyce, J., 1984. The relationship between human papillomavirus and lower genital intraepithelial neoplasia in immunosuppressed women. American journal of obstetrics and gynecology 150, 300-308.

Silva, R.J., Casseb, J., Andreoli, M.A., Villa, L.L., 2011. Persistence and clearance of HPV from the penis of men infected and non-infected with HIV. Journal of medical virology 83, 127-131.

Singer, A.J., Clark, R.A., 1999. Cutaneous wound healing. The New England journal of medicine 341, 738-746.

Smith, J.L., Campos, S.K., Wandinger-Ness, A., Ozbun, M.A., 2008. Caveolin-1-dependent infectious entry of human papillomavirus type 31 in human keratinocytes proceeds to the endosomal pathway for pH-dependent uncoating. Journal of virology 82, 9505-9512.

Smotkin, D., Wettstein, F.O., 1986. Transcription of human papillomavirus type 16 early genes in a cervical cancer and a cancer-derived cell line and identification of the E7 protein. Proceedings of the National Academy of Sciences of the United States of America 83, 4680-4684.

Solomon, D., 1990. The 1988 Bethesda System for reporting cervical/vaginal cytologic diagnoses: developed and approved at the National Cancer Institute Workshop in Bethesda, Maryland, December 12-13, 1988. Human pathology 21, 704-708.

Sousa, R., Dostatni, N., Yaniv, M., 1990. Control of papillomavirus gene expression. Biochimica et biophysica acta 1032, 19-37.

Spoden, G., Freitag, K., Husmann, M., Boller, K., Sapp, M., Lambert, C., Florin, L., 2008. Clathrin- and caveolin-independent entry of human papillomavirus type 16--involvement of tetraspanin-enriched microdomains (TEMs). PloS one 3, e3313.

Stacey, S.N., Jordan, D., Williamson, A.J., Brown, M., Coote, J.H., Arrand, J.R., 2000. Leaky scanning is the predominant mechanism for translation of human papillomavirus type 16 E7 oncoprotein from E6/E7 bicistronic mRNA. Journal of virology 74, 7284-7297.

Stanley, M., Pinto, L.A., Trimble, C., 2012. Human papillomavirus vaccines--immune responses. Vaccine 30 Suppl 5, F83-87.

Stanley, M.A., 2001. Human papillomavirus and cervical carcinogenesis. Best practice & research. Clinical obstetrics & gynaecology 15, 663-676.

Stanley, M.A., 2004. Human papillomavirus (HPV) vaccines: prospects for eradicating cervical cancer. The journal of family planning and reproductive health care / Faculty of Family Planning & Reproductive Health Care, Royal College of Obstetricians & Gynaecologists 30, 213-215.

Stanley, M.A., Pett, M.R., Coleman, N., 2007. HPV: from infection to cancer. Biochemical Society transactions 35, 1456-1460.

Steger, G., Schnabel, C., Schmidt, H.M., 2002. The hinge region of the human papillomavirus type 8 E2 protein activates the human p21(WAF1/CIP1) promoter via interaction with Sp1. The Journal of general virology 83, 503-510.

Stoler, M.H., Rhodes, C.R., Whitbeck, A., Wolinsky, S.M., Chow, L.T., Broker, T.R., 1992. Human papillomavirus type 16 and 18 gene expression in cervical neoplasias. Human pathology 23, 117-128.

Straight, S.W., Hinkle, P.M., Jewers, R.J., McCance, D.J., 1993. The E5 oncoprotein of human papillomavirus type 16 transforms fibroblasts and effects the downregulation of the epidermal growth factor receptor in keratinocytes. Journal of virology 67, 4521-4532.

Stubenrauch, F., Hummel, M., Iftner, T., Laimins, L.A., 2000. The E8E2C protein, a negative regulator of viral transcription and replication, is required for extrachromosomal maintenance of human papillomavirus type 31 in keratinocytes. Journal of virology 74, 1178-1186.

Studzinski, G.O., 2007. Cell differentiaion in vitro: model systems. New Jersey Medical School, Newark, New Jersey, USA.

Surviladze, Z., Dziduszko, A., Ozbun, M.A., 2012. Essential roles for soluble virion-associated heparan sulfonated proteoglycans and growth factors in human papillomavirus infections. PLoS pathogens 8, e1002519.

Syrjanen, S., Lodi, G., von Bultzingslowen, I., Aliko, A., Arduino, P., Campisi, G., Challacombe, S., Ficarra, G., Flaitz, C., Zhou, H.M., Maeda, H., Miller, C., Jontell, M., 2011. Human papillomaviruses in oral carcinoma and oral potentially malignant disorders: a systematic review. Oral diseases 17 Suppl 1, 58-72.

Szarewski, A., 2007. Prophylactic HPV vaccines. European journal of gynaecological oncology 28, 165-169.

Szentirmay, Z., Polus, K., Tamas, L., Szentkuti, G., Kurcsics, J., Csernak, E., Toth, E., Kasler, M., 2005. Human papillomavirus in head and neck cancer: molecular biology and clinicopathological correlations. Cancer metastasis reviews 24, 19-34.

Tang, S., Tao, M., McCoy, J.P., Jr., Zheng, Z.M., 2006. The E7 oncoprotein is translated from spliced E6*I transcripts in high-risk human papillomavirus type 16- or type 18-positive cervical cancer cell lines via translation reinitiation. Journal of virology 80, 4249-4263.

Theelen, W., Speel, E.J., Herfs, M., Reijans, M., Simons, G., Meulemans, E.V., Baldewijns, M.M., Ramaekers, F.C., Somja, J., Delvenne, P., Hopman, A.H., 2010. Increase in viral load, viral integration, and gain of telomerase genes during uterine cervical carcinogenesis can be simultaneously assessed by the HPV 16/18 MLPA-assay. The American journal of pathology 177, 2022-2033.

Thomson, S., Mahadevan, L.C., Clayton, A.L., 1999. MAP kinase-mediated signalling to nucleosomes and immediate-early gene induction. Seminars in cell & developmental biology 10, 205-214.

Todaro, G.J., Green, H., 1963. Quantitative studies of the growth of mouse embryo cells in culture and their development into established lines. The Journal of cell biology 17, 299-313.

Tomaic, V., Pim, D., Banks, L., 2009. The stability of the human papillomavirus E6 oncoprotein is E6AP dependent. Virology 393, 7-10.

Tomasz, M., 1995. Mitomicyn C: small, fast and deadly (but very selective). Chem Biol 2, 575-579.

Valencia, C., Bonilla-Delgado, J., Oktaba, K., Ocadiz-Delgado, R., Gariglio, P., Covarrubias, L., 2008. Human papillomavirus E6/E7 oncogenes promote mouse ear regeneration by increasing the rate of wound re-epithelization and epidermal growth. The Journal of investigative dermatology 128, 2894-2903.

Veldman, T., Liu, X., Yuan, H., Schlegel, R., 2003. Human papillomavirus E6 and Myc proteins associate in vivo and bind to and cooperatively activate the telomerase reverse transcriptase promoter. Proceedings of the National Academy of Sciences of the United States of America 100, 8211-8216.

Venuti, A., Paolini, F., Nasir, L., Corteggio, A., Roperto, S., Campo, M.S., Borzacchiello, G., 2011. Papillomavirus E5: the smallest oncoprotein with many functions. Molecular cancer 10, 140.

Vizcaino, A.P., Moreno, V., Bosch, F.X., Munoz, N., Barros-Dios, X.M., Borras, J., Parkin, D.M., 2000. International trends in incidence of cervical cancer: II. Squamous-cell carcinoma. International journal of cancer. Journal international du cancer 86, 429-435.

Walboomers, J.M., Jacobs, M.V., Manos, M.M., Bosch, F.X., Kummer, J.A., Shah, K.V., Snijders, P.J., Peto, J., Meijer, C.J., Munoz, N., 1999. Human papillomavirus is a necessary cause of invasive cervical cancer worldwide. The Journal of pathology 189, 12-19.

Weltman, J.K., 1987. The 1986 Nobel Prize for Physiology or Medicine awarded for discovery of growth factors: Rita Levi-Montalcini, M.D., and Stanley Cohen, Ph.D. New England and regional allergy proceedings 8, 47-48.

Wentzensen, N., Ridder, R., Klaes, R., Vinokurova, S., Schaefer, U., Doeberitz, M., 2002. Characterization of viral-cellular fusion transcripts in a large series of HPV16 and 18 positive anogenital lesions. Oncogene 21, 419-426.

Werner, S., Grose, R., 2003. Regulation of wound healing by growth factors and cytokines. Physiological reviews 83, 835-870.

Werner, S., Krieg, T., Smola, H., 2007. Keratinocyte-fibroblast interactions in wound healing. The Journal of investigative dermatology 127, 998-1008.

Wetherill, L.F., Holmes, K.K., Verow, M., Muller, M., Howell, G., Harris, M., Fishwick, C., Stonehouse, N., Foster, R., Blair, G.E., Griffin, S., Macdonald, A., 2012. High-risk human papillomavirus E5 oncoprotein displays channel-forming activity sensitive to small-molecule inhibitors. Journal of virology 86, 5341-5351.

White, E.A., Kramer, R.E., Tan, M.J., Hayes, S.D., Harper, J.W., Howley, P.M., 2012. Comprehensive analysis of host cellular interactions with human papillomavirus E6 proteins identifies new E6 binding partners and reflects viral diversity. Journal of virology 86, 13174-13186.

Wikstrom, A., Hedblad, M.A., Syrjanen, S., 2012. Penile intraepithelial neoplasia: histopathological evaluation, HPV typing, clinical presentation and treatment. Journal of the European Academy of Dermatology and Venereology : JEADV 26, 325-330.

Wilson, R., Laimins, L.A., 2005. Differentiation of HPV-containing cells using organotypic "raft" culture or methylcellulose. Methods in molecular medicine 119, 157-169.

Wilson, S.E., Liang, Q., Kim, W.J., 1999. Lacrimal gland HGF, KGF, and EGF mRNA levels increase after corneal epithelial wounding. Investigative ophthalmology & visual science 40, 2185-2190.

Wojcik, S.M., Bundman, D.S., Roop, D.R., 2000. Delayed wound healing in keratin 6a knockout mice. Molecular and cellular biology 20, 5248-5255.

Woodworth, C.D., Doniger, J., DiPaolo, J.A., 1989. Immortalization of human foreskin keratinocytes by various human papillomavirus DNAs corresponds to their association with cervical carcinoma. Journal of virology 63, 159-164.

Woolhouse, M., Gaunt, E., 2007. Ecological origins of novel human pathogens. Critical reviews in microbiology 33, 231-242.

Xu, M., Luo, W., Elzi, D.J., Grandori, C., Galloway, D.A., 2008. NFX1 interacts with mSin3A/histone deacetylase to repress hTERT transcription in keratinocytes. Molecular and cellular biology 28, 4819-4828.

Yarden, Y., 2001. The EGFR family and its ligands in human cancer. signalling mechanisms and therapeutic opportunities. European journal of cancer (Oxford, England : 1990) 37 Suppl 4, S3-8.

Yasumoto, S., Taniguchi, A., Sohma, K., 1991. Epidermal growth factor (EGF) elicits down-regulation of human papillomavirus type 16 (HPV-16) E6/E7 mRNA at the transcriptional level in an EGF-stimulated human keratinocyte cell line: functional role of EGF-responsive silencer in the HPV-16 long control region. Journal of virology 65, 2000-2009.

Yokota, K., Kusaka, M., Ohshima, T., Yamamoto, S., Kurihara, N., Yoshino, T., Kumegawa, M., 1986. Stimulation of prostaglandin E2 synthesis in cloned osteoblastic cells of mouse (MC3T3-E1) by epidermal growth factor. The Journal of biological chemistry 261, 15410-15415.

You, J., Croyle, J.L., Nishimura, A., Ozato, K., Howley, P.M., 2004. Interaction of the bovine papillomavirus E2 protein with Brd4 tethers the viral DNA to host mitotic chromosomes. Cell 117, 349-360.

Yu, W., Naim, J.O., Lanzafame, R.J., 1994. Expression of growth factors in early wound healing in rat skin. Lasers in surgery and medicine 15, 281-289.

Yugawa, T., Kiyono, T., 2009. Molecular mechanisms of cervical carcinogenesis by high-risk human papillomaviruses: novel functions of E6 and E7 oncoproteins. Reviews in medical virology 19, 97-113.

Zerfass, K., Levy, L.M., Cremonesi, C., Ciccolini, F., Jansen-Durr, P., Crawford, L., Ralston, R., Tommasino, M., 1995. Cell cycle-dependent disruption of E2F-p107 complexes by human papillomavirus type 16 E7. The Journal of general virology 76 (Pt 7), 1815-1820.

Zhang, Y., Liou, G.I., Gulati, A.K., Akhtar, R.A., 1999. Expression of phosphatidylinositol 3-kinase during EGF-stimulated wound repair in rabbit corneal epithelium. Invest Ophthalmol Vis Sci 40, 2819-2826.

Zhao, K.N., Chen, J., 2011. Codon usage roles in human papillomavirus. Reviews in medical virology 21, 397-411.

Zheng, Z.M., Baker, C.C., 2006. Papillomavirus genome structure, expression, and post-transcriptional regulation. Frontiers in bioscience : a journal and virtual library 11, 2286-2302.

zur Hausen, H., 2002. Papillomaviruses and cancer: from basic studies to clinical application. Nature reviews. Cancer 2, 342-350.

zur Hausen, H., 2009. Human papillomavirus & cervical cancer. The Indian journal of medical research 130, 209.